A NOVEL MOUSE MODEL TO ELUCIDATE THE ORIGINS AND THERAPEUTIC SENSITIVITY OF TESTICULAR GERM CELL TUMORS

A Dissertation
Presented to the Faculty of the Graduate School
of Cornell University
In Partial Fulfillment of the Requirements for the Degree of
Doctor of Philosophy

By
Timothy M. Pierpont
January 2017

ABSTRACT

A NOVEL MOUSE MODEL TO ELUCIDATE THE ORIGINS AND THERAPEUTIC SENSITIVITY OF TESTICULAR GERM CELL TUMORS

Timothy M. Pierpont, Ph.D.

Cornell University 2017

Testicular germ cell tumors (TGCTs) are the most common malignancy among young men. These cancers are exquisitely sensitive to genotoxic chemotherapies, even after distant metastasis. A better understanding of the mechanisms underlying this chemosensitivity could improve treatments for more chemoresistant cancers. Because TGCTs arise from germ cells and contain cells with prominent pluripotent stem cell features, we hypothesized that specialized DNA damage response (DDR) properties associated with pluripotent stem cells might underlie their exquisite chemosensitivity. To test this hypothesis and to further elucidate the biology of these cancers, we generated a novel mouse model of malignant TGCTs. Tumorigenesis was induced by simultaneous cre mediated *Pten* inactivation and $Kras^{G12D}$ activation controlled by *Stra8-cre*, a germ cell-specific cre recombinase. Approximately 75% of mice with both *Pten* and *Kras* alterations developed grossly apparent teratocarcinoma by five weeks of age. These tumors harbored both a teratoma component and malignant embryonal carcinoma (EC), a totipotent cancer stem cell (CSC) identified diagnostically by expression of OCT4, NANOG, and SOX2. Early neoplasms were also detected in testes as early as postnatal-day 3, and only 1-2 tumor initiation sites were

observed per testis, suggesting that tumor induction occurred prenatally. Indeed, lineage tracing analyses identified Cre-mediated excision in rare, isolated clusters of germ cells as early as 12.5 post fertilization. Treatment of TGCT bearing mice with genotoxic chemotherapeutics resulted in significantly increased survival and reduced tumor burden. Most significantly, the EC cells were selectively depleted from the primary tumors of treated mice. These findings suggested these CSCs were uniquely sensitive to genotoxic chemotherapy, which may help explain why genotoxic drugs are so efficacious in treating this disease. To better understand how the CSCs were responding to chemotherapeutics, we established two EC cell lines from our mouse model. Both EC cell lines retained their ability to reproduce teratocarcinomas and exhibited increased chemosensitivity compared to differentiated cells derived from the same cell lines. Using these *in vivo* and *in vitro* models, ongoing research will continue to identify more specific mechanisms underlying the chemosensitivity in these cancers.

BIOGRAPHICAL SKETCH

Timothy M. Pierpont was born in Waterbury CT in 1983 and grew up in Delaware, where he graduated from Polytech High School in 2001. He began a bachelor's of science degree in biology at Delaware State University in 2007, quickly choosing to pursue a career in research. In 2011 he was accepted into the biochemistry, molecular, and cellular biology (BMCB) Ph.D. program at Cornell University where he joined the laboratory of Dr. Robert Weiss to do the thesis research presented on the following pages.

DEDICATION

I dedicate this thesis to Mr. Richard Driskill, who's dedication to education and love of biology lead me towards starting my own scientific career.

ACKNOWLEDGMENTS

To my wife Rebecca, my family, and my friends, thank you all for your love and support, without which this achievement would not have been possible. I also want to acknowledge Dr. Harbinder Singh Dhillon, who mentored me for most of my time as an undergraduate researcher. Without his mentoring, or the support from many great faculty at Delaware State University, I would not have been prepared to begin my graduate level research 5 years ago. Thanks to Dr. Robert Weiss for being an amazing thesis mentor, who challenged me to grow and hone skills necessary for the many facets of independent research. I'd also like to express great appreciation to my thesis committee, Dr. Tudorita Tumbar, and Dr. John Schimenti, who helped develop several scientific concepts for my work throughout the years. The work described in this thesis were financially supported by NYSTEM contract #C026421 and NIH grant R21 CA185256.

TABLE OF CONTENTS

CHAPTER 1

INTRODUCTION

Testicular germ cell tumors (TGCTs) represent a rare success in the ongoing battle against cancer, as this highly aggressive solid cancer can be effectively treated in most patients. The drugs used to treat TGCTs work by damaging DNA to induce cell death, yet those same drugs are much less efficacious against most other forms of cancer. Understanding the basis for the impressive chemosensitivity of TGCTs requires a thorough understanding of germ cell development, germ cell and somatic cancers, DNA damage response (DDR) to treatment, and the role of stem cell-like cells in tumor development and treatment response. Chapter 1 is a review of historically relevant and current knowledge in these areas which supports the importance of the findings unveiled in the chapters that follow.

1.1 GERM CELL DEVELOPMENT

With very few exceptions, all cells of the body harbor identical genetic information. Despite this, the cells of a multicellular organism display an immense phenotypic variation. In all mammals, development begins as a fertilized totipotent zygote, capable of differentiating into any of the unique and specialized cells necessary to maintain the maturing organism and its extraembryonic tissues. The phenotypic variation among cells is created through relatively small changes in gene expression, mostly regulated by transcription factors and other regulatory proteins and RNAs, as well as more global changes in gene expression facilitated by chromatin remodeling and changes in DNA methylation[1]. These changes in gene expression which are heritable by daughter cells are

known as epigenetic modifications. After a few rounds of division as a totipotent stem cell, the majority of cells of the early embryo lose their totipotent potential through these epigenetic modifications, and nearly all cells commit to increasingly specific and limited cell fates. Somatic differentiation is rarely reversed during development and is necessary to produce stable somatic cell lineages that ensure homeostasis of the mature organism. Germ cells, however, undergo a distinct, highly specialized maturation process which leaves these unique cells able to revert to a totipotent state such that they retain the potential to form an entirely new individual. The work described in this dissertation revolves around cancers arising from these particular cells. Thus it is important to begin where these cancers begin, within normal germ cell development, and where it goes awry.

Figure 1.1 Model of murine primordial germ cell specification and migration (Illustrations adapted from Saitou et al., 2012)[2]**.** PGC specification initiates around E6.25. Migration from the initial site of specification to the genital ridge begins around E7.5 with germ cells arriving at the genital ridge around E10.5, finally completing migration around E11.5.

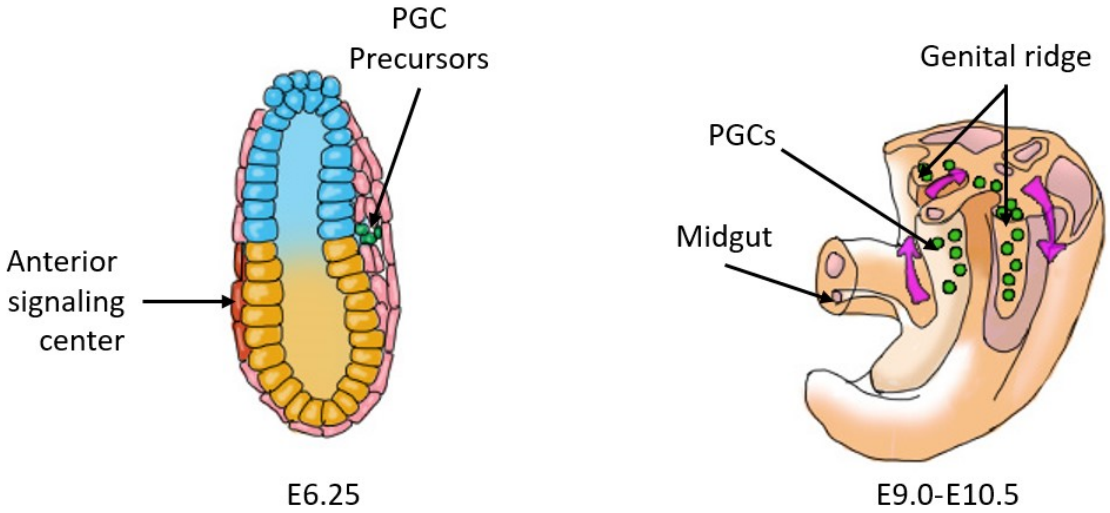

1.1.1 Primordial Germ Cell Specification

Development technically begins following oocyte fertilization by a single mature spermatozoon. After initial fertilization; the zygote divides four times to form a tight ball of totipotent cells called a morula. With the 5th morula division, the cells begin to lose totipotency, and the outer morula cells commit to trophoblastic lineages, while the inner cells commit to embryonic lineages[3]. At approximately three days after fertilization, tight junctions have formed which seal the outer morula while Na^+/K^+ pumps and aquaporins work to form a lumen at the center of the morula, thus signaling the transition to the blastocyst phase[4]. At this phase, the inner cell mass (ICM) forms within the lumen and contains the precursor cells for all of the embryonic cell lineages, while the outer cells contain the trophoblastic extraembryonic precursor cells.

Mouse primordial germ cell (mPGC) specification initiates around 6.25 days post fertilization, after a substantial increase in cell number and blastocyst implantation. At this time, the cells of the extraembryonic ectoderm begin producing BMP4, an important signaling protein for several stages of development[1,5]. Surprisingly, although all cells of the epiblast have the potential to undergo PGC specification in response to BMP4 exposure, only a few hundred cells in the proximal posterior epiblast undergo this transformation[6]. The exact mechanisms controlling cell number are still unknown, however, the anterior signaling center, an area of the developing embryo located on the opposite side from PGC precursors, actively inhibits BMP4 signal induction, and is likely the main mechanism preventing the majority of epiblast cells from undergoing germ cell specification[6].

Expression of Wnt3 from the epiblast is also required to sensitize the epiblast cells to the BMP4 produced from the extraembryonic ectoderm, the combination of WNT3/BMP4 activation

drives the expression of three key transcription factors which facilitate susceptible cells' commitment to the primordial germ cell fate. Mesodermal transcription factor T is expressed downstream of *Wnt3*, which in turn upregulates expression *Prdm1*(BLIMP1) and *Prdm14*[7]. BLIMP1 then upregulates expression of *Tfap2c* (also known as *Ap2y*) and these three factors together bring about the transcriptional changes that drive primordial germ cell fate[7,8]. While this pathway is well characterized in mice, ethical concerns prevent similar studies being carried out to elucidate human germ cell specification. However, recent *in vitro* models have highlighted some of the key regulatory pathways in human PGC (hPGC) specification.

Murine *in vitro* models of PGCs have been successfully generated using a stepwise differentiation process; the resulting cells are labeled mouse primordial germ cell-like cells (mPGCLC)[9]. These models faithfully recapitulate many of the germ cell transcriptional networks that have been verified using *in vivo* mouse studies, supporting the biological relevance of carefully interpreted data from such models[7,8]. Recently, a conceptually similar stepwise differentiation process was established for creation of human PGCLCs (hPGCLs)[10]. Based on the findings of the study, expression of mesodermal transcription factor SOX17, rather than T, appears to play a vital role in the hPGC specification as a master regulator of BLIMP1[10]. This difference between hPGC and mPGC may help explain the complete lack of seminoma formation in mouse TGCT models which will be discussed later in this chapter[10,11].

1.1.2 Primordial Germ Cell Migration

In vertebrates, PGCs do not continue to proliferate immediately after specification but instead migrate from the initial site, in mammals, these early germ cells migrate to a somatic structure known as the genital ridge. The molecular underpinnings of germ cell migration in *Drosophila* and zebrafish are well established but comparatively little is known about what initiates and regulates germ cell migration in mice or humans[5]. In mice, germ cells initiate migration around E7.5, leaving the primitive hindgut and entering the endoderm. From there, they travel through the hindgut and mesentery, finally reaching the genital ridge by E11.5. KIT and its ligand are necessary for germ cell survival during migration and function as a mechanism for eliminating germ cells that do not properly migrate through the midline[12]. During and immediately after their migration, PGCs undergo significant epigenetic reprogramming, clearing histone markers and DNA methylation to remove imprinting and restore a totipotent state[13]. Much less is known about the molecular control of human PGC migration and reprogramming, but it appears to happen at similar developmental milestones as murine PGC migration and occurs between the fourth and tenth weeks in human fetal development[13]. After arriving at the genital ridge and completing epigenetic reprogramming, male germ cells undergo a mitotic arrest until after birth, while meiosis begins in females.

1.1.3 Gonadal Sex Differentiation

Before germ cells arrive at the genital ridge starting around day E10.5, the somatic portion of the gonad is just a thickening of the intermediate mesoderm with no sexual differentiation. As germ

cells arrive at the genital ridge, they infiltrate this tissue, transition from primordial germ cell into gonocyte, and begin to facilitate the development of either testes or ovaries[14,15]. Development of the testis is set in motion by expression of SRY from around day 10.5 to 12.5 in mice (week 4-5 in humans), with its main function being to up-regulate SOX9 in the pre-sertoli cells[16]. SOX9 then upregulates pathways which induce endothelial cell migration into the developing testis which is followed by vascularization and ultimately the formation of the sex cords[16]. Formation of the sex cords of the testis occurs around E12.5 in the fetal mouse, or in the 2nd month of human development, and marks the first appearance of sexual differentiation[14,15].

After an initial burst of proliferation at the genital ridge, male germ cells are quiescent until postnatal day 2, where they remain in the center of the sex cords surrounded by sertoli cells. At postnatal day 1, the gonocytes begin a short second migration from the center of the sex cords, through the sertoli cells, and flatten out against the basement membrane of the seminiferous tubule. Here, these germ cells differentiate into spermatogonial stem cells (SSC) and establish the polarization of the seminiferous tubule. In females, ovaries are characterized by a lack of sex cord formation, and less dramatic early morphological changes compared to the testis[15].

Development of the ovary was thought to be the default passive gonadal progression in the absence of SRY. However, RSPO1 and WNT4 are now known to be vital regulators of ovarian development through upregulation of the *Wnt/β-Catenin* pathway in mice and humans[17,18]. In part, this discovery came from studies aimed at understanding why, in rare cases, XX humans developed as phenotypic males. This rare event was eventually attributed to loss of function mutations for RSPO1 (Figure 2). While RSPO1 actively drives ovarian gonadal differentiation, earlier expression of SRY usually leads to repression of *Rspo1* and *β-Catenin* through SOX9, to facilitate testicular development. In the absence of SRY, expression of RSPO1 is required to repress *Sox9*

and avoid testicular gonadal differentiation[19]. Despite active repression of the alternative pathway, incomplete gonadal development or development not matching genetic sex occurs with some frequency. This developmental aberration is associated with infertility as well as the development of TGCT in males (discussed more under etiology). Although current work and prior literature presented in this dissertation suggest that malignant TGCTs initiate before SSC specification, the protective mechanisms that prevent malignant transformation in later germ cells make it a relevant process to explain.

Figure 1.2 Crosstalk between ovarian and testis developmental pathways. (Figure adapted from Knarston et al., 2016[20]). The diagram indicates that expression of SRY locks in male sex development by inhibition of the *B-catenin* pathway necessary for ovarian development. Later, SRY leads to SOX9 expression which inhibits RSPO1. Failure to inhibit these pathways result in ovarian development. Loss of RSPO1, however, allows testis development without SRY expression. The diagram shows current understanding of gonadal sex development choice at this stage and how both pathways are mutually exclusive, active processes.

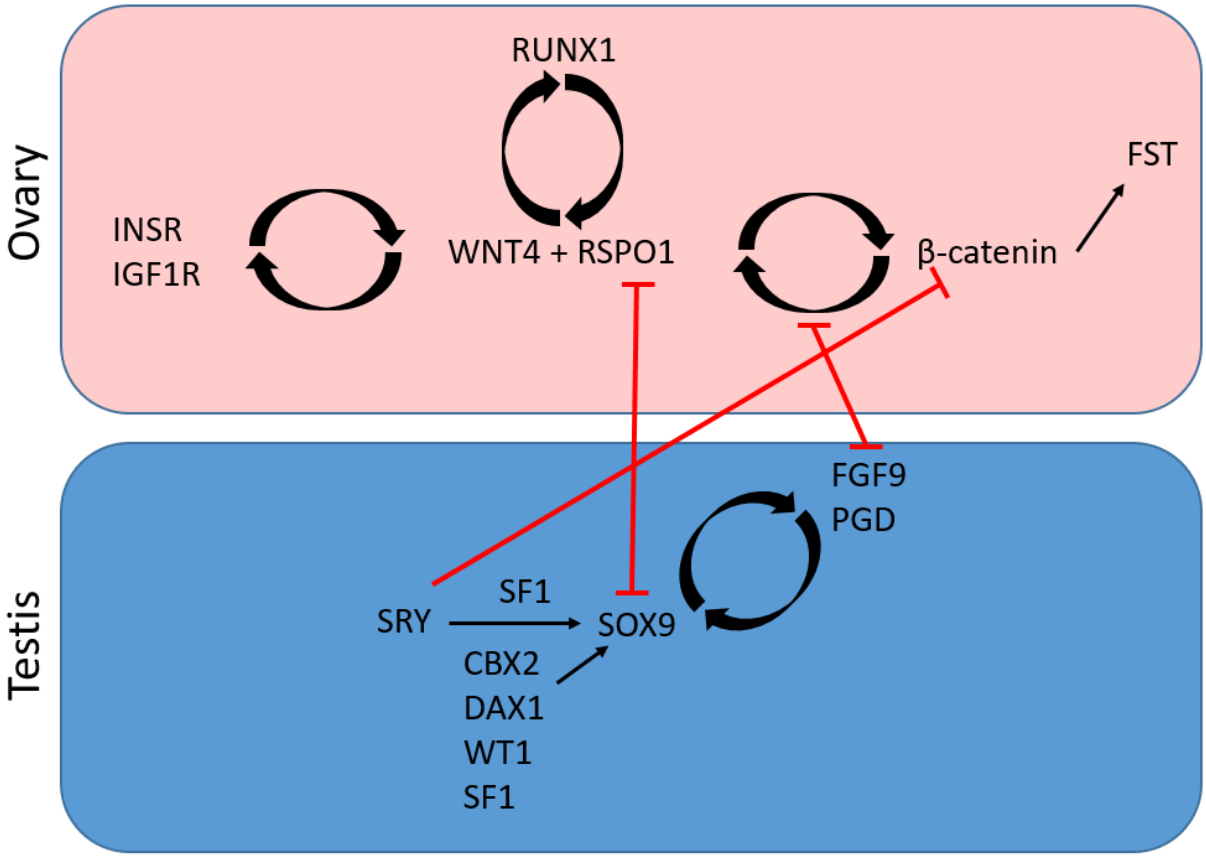

1.1.4 Spermatogenesis

Retinoic acid (RA) is a metabolite of vitamin A, also known as retinol, and is an important signaling molecule during development. In mice, during gonadal development, RA is produced from the mesonephroi, an early embryonic structure adjacent to the developing gonad[21]. RA synthesis initiates around E13.5 and diffuses into the gonads of both sexes[21]. In female mice, the presence of RA at E13.5 leads to expression of *Stra8*[21,22]. *Stra8* (Stimulated by Retinoic Acid 8) is a cytoplasmic factor whose expression is necessary for entrance into meiosis of both oogenesis and spermatogenesis[23].

In male mice, on the other hand, RA is actively degraded by increased expression of CYP26 in the sertoli cells. During this time, the male germ cells undergo mitotic arrest until birth. This CYP26 activity prevents RA from initiating meiosis until postnatal day three or four, at which point RA degradation ceases due to downregulation of CYP26[21]. After downregulation of CYP26, RA stimulates postnatal expression of *Stra8* and drives the transformation of pro-spermatogonia to spermatogonia. Interestingly, it is still not entirely clear which spermatogonial cells function as SSC. Based on experiments using an SSC-specific luciferase reporter, which expresses luciferase under the control of a 400bp portion of the *Stra8* promoter, it was found that only a small population of *Stra8* expressing spermatogonia had a high capacity to restore spermatogenesis upon transplantation into germ cell-depleted testes[21,22]. Proficient restoration of spermatogenesis reflects an ability to repopulate the SSC population and suggests that the 400bp marker is unique to SSCs. However, it is not yet known if those cells isolated by *Stra8* expression, are SSCs, or spermatogonia from cysts (described below) which retained the ability to dedifferentiate to SSCs.

After gonocytes migrate to the basal lamina of the seminiferous tubule, they remain there throughout the life of the male, dividing asymmetrically as spermatogonial stem cells (SSC) and differentiating spermatogonia. However, despite their important role as the progenitors of all sperm, SSCs comprise a mere estimated 0.03% of all germ cells in the rodent testis[24]. Due to their extreme rarity, SSC properties have proven difficult to study. However, through a combination of *in vivo*, *ex vivo*, and *in vitro* analyses, there is a growing understanding of the molecular underpinnings for self-renewal, differentiation, and dedifferentiation of spermatoga[25]. SSC are a subset of spermatogonia type A (A_{Single}) cells, which undergo the first stages of differentiation by dividing four times with incomplete cytokinesis and are collectively referred to as a cyst[25]. Although it was believed that SSCs were limited to a portion of asymmetrically divided spermatogonial A_{Single} cells, it is now clear that many spermatogonia A cyst cells have the ability to disassociate and dedifferentiate back into individual SSCs rather than be committed to obligatory development towards meiosis[25,26].

After their first mitotic division with incomplete cytokinesis, spermatogonia A cells are referred to as A_{paired} rather than A_{single}, and during the subsequent divisions, they are referred to as $A_{Aligned}$. After four mitotic divisions, at which point the matured cyst is comprised of 16 spermatogonia $A_{Aligned}$ with connected cytoplasm[25,26]. During this progression, one notable change in gene expression is a loss of GFRA1 and gain of NGNA. These markers were used to help demonstrate the plasticity of $A_{aligned}$ spermatogonia by showing that late stage, $NGNa^{+}/GFRA1^{-}$ can still contribute to the SCS population[27]. Furthermore, re-expression of *Kit* seems to initiate a key step in differentiation, and Kit^{+} spermatogonia cells from any stage show an impaired ability to regain the SSC phenotype[27]. These Kit expressing spermatogonia continue to differentiate as spermatogonial intermediates, and then spermatogonial B cells, as they enter pre-leptotene phase

of meiosis and transition to spermatocytes[25]. Spermatocytes undergo two rounds of meiosis, resulting in up to 64 mature gametes from the original spermatogonia A_{single}[25]. After the last stages of meiosis, spermatocytes begin a dramatic genomic remodel and morphological change to become mature spermatids and ultimately, mature spermatozoa, by way of a process whose details are beyond the scope of this dissertation.

1.2 TESTICULAR GERM CELL TUMORS

1.2.1 Germ Cell Neoplasia *in situ*

Germ cell tumors comprise a heterogeneous array of well-characterized solid neoplasms that arise from germ cells[28–30]. TGCTs comprise the vast majority of germ cell tumors, and 98% of all testicular cancers, although ovarian and ectopic germ cell tumors are well documented[28–30]. While TGCTs are rare compared to other cancers, they are the most common malignancy among men 15 to 44 years of age[28,31]. The majority of TGCTs arise from the same precursor lesion, germ cell neoplasia in situ (GCNIS), also known as intratubular germ cell neoplasia, undefined/carcinoma in situ (IGCNU/CIS)[29]. There is a fascinating and relevant history behind the discovery GCNIS as the precursor lesion of malignant TGCTs.

In a historic paper, pathologist Dr. Skakkebæk proposed that GCNIS is the precursor lesion to TGCTs after he identified the pre-malignancy in the biopsies of two male infertility patients, both of whom later developed TGCTs[32]. Because of this connection, he initially termed the lesion carcinoma in situ (CIS), indicating a very early neoplasm growing “in its place.” The field initially dismissed the connection, but Skakkebæk went on to publish two landmark studies further

establishing this connection. The first of which analyzed biopsies of 555 male infertility patients, finding the precursor lesion in six[33]. Four of those six later developed invasive germ cell tumors within five years[33]. None of the patients without the precursor lesion developed TGCTs[33]. The second study analyzed the contralateral testis of 500 patients with TGCTs, in which 27 of them were found to have the precursor lesion[34]. Of these, eight were treated with aggressive chemotherapy for their initial malignancy, and none of those eight suffered a relapse[34]. Of the 19 who did not receive aggressive treatment, seven later developed invasive TGCTs while all 473 without contralateral GCNIS remained disease free for the 19 to 96 months following the biopsy[34].

GCNIS is morphologically distinguishable from normal germ cell tubules by a thickened seminiferous tubule wall and abnormally large tetraploid germ cells[32]. The transformed germ cells are further characterized by increased expression of OCT4, NANOG, LIN28, TFAP2C, PLAP, PDPN, and KIT, and may have expression of SALL4 or DMRT1[35]. These lesions have a hypomethylated genome with histone modifications (lack of repressive markers H3K9me2 and H3K27me3 and overrepresentation of activating markers H3K4me, H3K9ac, and H2A.Z) that make them more permissive to gene expression than the untransformed germ cells of normal tubules[36]. Importantly, GCNIS also expresses BLIMP1 and have similar permissive histone modification levels of H2K3me2s and H4K3me2s compared to PGCs, and seminomas (The most common TGCT, discussed below)[37]. These data support the idea of GCNIS as having a PGC or gonocyte origin, and its status as a precursor to mature TGCTs.

While Skakkebæk and others have helped solidify GCNIS as the precursor to all malignant post-pubescent TGCTs, the original name, CIS, has continued to be controversial. Carcinoma *in situ* (CIS) implies an epithelial cell of origin, while the name intratubular germ cell neoplasia,

unclassified (IGCNU) implied a lack of knowledge about the lesion and the U is often misinterpreted as undifferentiated, undefined or unknown. After nearly a year of correspondence among experts in the field on the issue, the World Health Organization (WHO) consensus meeting in 2016 ultimately reclassified the lesion as germ cell neoplasia *in situ* (GCNIS)[38]. Along with the nomenclature change came a recommendation to change the broad classification of type I, II, or III TGCTs to the simplified and more descriptive categorization of TGCTs originating from GCNIS and TGCTs that do not[29].

1.2.2 Germ cell tumors derived from germ cell neoplasia *in situ*

Based on WHO guidelines, germ cell tumors derived from GCNIS is the recommended category for TGCTs previously classified as type II. These germ cell tumors are the most commonly occurring germ cell malignancies, and occur in adolescent and young adult males (rates of incidence discussed more in depth in section 2.3.1). Amazingly, it is considered pathognomonic for all lesions in this category to harbor an extra copy of the short arm of chromosome 12, often as an isochromosome, i(12p). Because of the near-invariable presence of this chromosomal aberration, it is a useful diagnostic tool to identify germ cell tumors in this category as well as strong evidence for them sharing the GCNIS precursor lesion and similar pathogenesis. Germ cell tumors derived from GCNIS are highly aggressive metastatic malignancies that can be further subdivided into two categories, seminomas, and non-seminomas[29,30].

Seminomas

Seminomas, also known as pure seminoma or classical seminoma, are comprised of a mostly uniform cancer cell which resembles primordial germ cell morphology and has diagnostic expression profiles that are nearly identical to PGCs and GCNIS (Fig. 1.1). Importantly, these tumors are distinguishable from GCNIS and embryonal carcinoma (EC) by SOX17 expression[10]. The fact that SOX17 is implicated as a key regulator for specification of hPGCs supports the theory that these malignancies initiate during early embryogenesis[10,11]. Approximately 45-55% of all TGCTs are pure seminoma, while nearly all others are mixed nonseminomas[39]. These cancers tend to present as an enlarged testis or lump which is usually painless. From the initial site, they often metastasize through the lymphatics to nearby lymph nodes as well as the liver, lung, bones and other organs at later stages.

Nonseminomas

Comprising approximately 45% of TGCTs, these tumors tend to be very heterogeneous and more aggressive than seminomas[39,40]. They also tend to justify more aggressive treatments at advanced stages compared to seminomas[41]. Nonseminomas are divided into the four most commonly occurring subtypes: EC, teratoma, yolk sac or trophoblastic choriocarcinoma. Unlike seminomas, nonseminomas rarely occur in a pure form and are instead usually a mixed germ cell tumor, which is comprised of multiple GCNIS derived germ cell cancers types[39].

Embryonal Carcinoma

Embryonal carcinoma (EC) is a malignant totipotent cancer cell capable of differentiating into embryonic tissues, as well as extraembryonic yolk sac and trophoblastic tissues[42,43]. It tends to metastasize through the lymphatic system and to the lungs and is frequently more aggressive than seminomas[40]. Only 2-10% of all nonseminomas are a pure EC, but it occurs in 80% of all mixed germ cell tumors making it the second most commonly present germ cell cancer[30]. EC frequently occurs with teratoma components, which together form a malignant mixed nonseminoma, teratocarcinoma[42,43]. The discovery and early experiments of EC in mice played a critical role in advancing stem cell biology, the history, and implications of EC research are discussed in depth later.

Postpubertal-Teratoma

All teratomas are defined by the presence of cells resembling at least two of the three germ layers, mesoderm, ectoderm, and endoderm[30]. These tissues can occur as predominantly mature-like, or predominantly immature fetal-like in phenotype[30]. Postpubertal-teratomas arise from GCNIS and are frequently malignant, showing metastasis in 22-37% of all cases[30]. Although histologically identical, prepubertal-teratomas are benign, lack of i(12p), and are not believed to derive from GCNIS[29,30].

Postpubertal-Yolk Sac Tumor

Yolk sac tumors originate from extraembryonic trophoblast tissues. These tumors rarely occur in pure form and are present as a component in 40% of all non-seminomas. Both postpubertal and prepubertal-yolk sac tumors have identical histology comprised of a wide range of patterns that resemble normal yolk sac, allantois, and extra-embryonic mesenchyme. Postpubertal-yolk sac tumors, like postpubertal-teratomas, originate from the GCNIS precursor lesion, while Prepubertal-yolk sac tumors do not[29,30].

Choriocarcinoma

Like yolk sac tumors, choriocarcinoma originates from extraembryonic trophoblast tissues. These tumors are a rare but highly malignant neoplasm. In pure form, it represents a mere 0.19% of all TGCTs but occurs as a portion of mixed germ cell tumors in about 8%[29,30]. Because this cancer spreads relatively early during tumorigenesis, often before discovery, most patients present with an advanced stage of this disease, and it, therefore, carries the worst prognosis[10].

1.2.3 Germ cell tumors unrelated to germ cell neoplasia *in situ*

Following the revised WHO guidelines established at the 2016 consensus meeting, Type I and Type III germ cell tumors are now classified as germ cell tumors unrelated to GCNIS [29,30,38]. Type

I consisted of TGCTs that arose during fetal and prepubescent life and offered no distinction between pre and postpubertal-yolk sac tumors or teratomas which, despite being histologically similar, have different genomic aberrations and very different progressions[29,30]. Germ cell tumors unrelated to GCNIS germ cell tumors unrelated to GCNIS have no known precursor lesion, and the initiation is believed to happen earlier in development than GCNIS, but the specific progression of the disease remains unknown[44]. These occur very rarely, at a rate of about 0.5 to 2.0 per 1,000,000 in children, but are worth mentioning because most mouse models of TGCTs are more representative of prepubertal-teratomas (models discussed later)[45]. Spermatocytic tumors (also known as type III or spermatocyte seminoma) are a benign TGCT that occurs much later in life, around 52 years of age, and has no analogous lesion in women[45]. These neoplasms are believed to originate from spermatogonial stem cells in older men, likely initiated by gain of function mutations in FGFR3 or HRAS, followed by clonal expansion[35,46,47].

1.2.4 Epidemiology and Etiology of GCNIS Derived TGCTs

The incidence of TGCTs has steadily increased for the past 30 to 40 years, especially in developed countries[39]. Importantly, the rate of increasing incidence is not equal across ethnic groups, which suggests there is not only a strong environmental component but also a genetic component to susceptibility as well[31]. In a study looking at changes in cancer incidence among people who immigrated to Sweden, it was discovered that the rate of TGCTs decreased after immigration, suggesting important environmental risk factors[48]. Other studies looking at familial risk factors found that TGCT risk comes from both environmental and genetic factors[49]. While an environmental influence on risk factor seems almost certain, no solid exogenous risk factors have

yet been identified. However, several diseases and genetic aberrations have been associated with increased risk of TGCT.

1.2.5 Potential genetic risk factors and driver mutations

Although it is clear that there exist important environmental risk factors for TGCTs, discovering them has proven elusive. Genetic risk factors and alterations have proven more amenable to elucidation. Interestingly, while prepubertal TGCTs are diploid, GCNIS derived TGCTs are aneuploid and tend to have reoccurring chromosomal rearrangements[50]. Furthermore, largely thanks to genome-wide association studies (GWAS), many genetic risk factors and potential driver mutations have also been identified. The combination of these findings is helping us unravel the molecular details of TGCT pathogenesis, the exact mechanisms, and timing of which remain unknown.

Genomic instability in TGCTs

All GCNIS associated TGCTs are aneuploid. Interestingly, as mentioned above, nearly all TGCTs that derive from GCNIS harbor a duplication of the short arm of chromosome 12, usually as an isochromosome (i(12p)), which is present in approximately 80 percent of seminoma and nonseminoma[51]. Most GCNIS are hypertetraploid, as are most seminomas, yet cells of GCNIS rarely contain an isochromosome of 12p[35,51,52]. This finding has led to the hypothesis that acquisition of i(12p) plays a key role in the transition from pre-malignant GCNIS to invasive

seminoma and nonseminomas. The most likely explanation of how an extra copy of 12p facilitates this step in the progression is that extra copies of genes contained on the chromosome fragment are sufficient to facilitate sertoli cell independence[52]. Supporting this idea, several genes on 12p, such *Nanog, Stellar, Kitlg, and Kras2* facilitate maintenance of stemness, cell proliferation, and cell survival, some of which have been implicated as susceptibility genes of TGCTs in independent studies[53]. Importantly, these genes not only have copy number increased due to i(12p), but their expression is upregulated in invasive TGCTs compared to pre-invasive GCNIS[54,55]. Increased expression of these control genes could make it more permissive for transformed germ cells to survive outside of the tubule niche, thus implicating the underlying mechanisms for transition to invasive TGCT and explaining the near ubiquitous presence of i(12p) among invasive germ cell tumors. Although many gene mutations have been found in TGCTs, I will elaborate on only *Kitlg*, because of its high incidence of mutation in TGCTs, as well as *Kras* and *Pten* due to their high prevalence of the disease as well as their relevance to the work presented in this thesis.

Kit

The KIT protein is a receptor tyrosine kinase (also known as CD117) which dimerizes to activate its downstream cascade upon extracellular binding of its ligand, KITLG (Also known as STEEL or Stem Cell Factor, SCF)[56]. KIT is critical for a variety of stem cell development, including germ cells (See section 2.1). Kemmer et al. was the first to screen a cohort 54 seminomas for expression, sequence mutation, and constitutive kinase activity of KIT, discovering that 24.1% harbored activating point mutations in KIT[57]. Additional studies found that 21% of seminomas had increased copy number and expression of KIT, but it was rarely overexpressed in nonseminomas

or GCNIS[58]. Mutations affecting KITLG have also been associated with the development of seminomas through GWA studies[59]. The prevalence of KIT and KITLG mutations in seminomas suggests that having over-activation of its downstream pathways facilitate survival and invasiveness in transformed germ cell tumors similar to its effects on normal PGC survival and migration during development.

Kras

Kras is a GTPase, generally tethered to the plasma membrane. It is part of the RAS superfamily of proteins which interacts with c-Raf, stimulating the MEK/ERK pathway, and PI3K, stimulating the AKT pathway, along with other interactors, activation of these pathways play key roles in regulating cell proliferation, survival[60]. Importantly, RAS is a downstream target of KIT activation, as well as other RTKs[61,62]. KIT and RAS signaling are implicated as an important mechanism for transition into an invasive TGCT[62]. As mentioned above, this connection comes in part due to the extra copies of the *Kras2* gene present in nearly all GCNIS derived TGCTs by way of i(12p). Aside from increased copy number of *Kras* in nearly all tumors, activating mutations of *Kras* and *Nras* have been found in TGCTs, mainly seminomas[63]. *Kras* was also found to be overexpressed in several different studies[64]. To induce tumors in our model (described in more depth below), a conditional transgene coding for a constitutively active G12D mutation was used.

Pten

Aside from overexpression, or overactivation of genes that drive tumorigenesis, tumor suppressor genes are also reported to be mutated in TGCTs. *Pten* is a phosphatase that dephosphorylates phosphatidylinositol (3,4,5)-trisphosphate, helping to regulate the AKT pathway and serving as a tumor suppressor by negatively regulating cell survival and proliferation. Notably, it is one of the most commonly mutated tumor suppressor genes in cancers, and some SNPs are a risk factor for TGCT development[65]. Loss of *Pten* expression is also associated with the transition from GCNIS to invasive TGCT[66]. Along with the conditional activation of constitutively active *Kras* within the mouse model used in the presented studies, *Pten* is conditionally inactivated in the male germ cells of these mice. These alterations together drive tumorigenesis in the model.

1.2.6 Disorders of Sex Development and Developmental Urogenital Abnormalities

Disorders of sex development (DSD) are defined when a person's phenotypic sex does not match their chromosomal sex, and usually resulting in infertility[67]. DSD often results from an inability to activate the canonical genetic gonad sex differentiation pathways, or a failure to repress the opposing pathways[67]. 66 genes involved in the regulation of gonadal sex differentiation appear to play a role in this disease[68]. Although most genes associated with DSD are not associated with TGCT formation, it has been proposed that TGCTs result from similar defects which also lead to

impaired spermatogenesis (infertility), cryptorchidism, hypospadias and inguinal hernias[44,69]. Testicular dysgenesis syndrome (TSD) is a notable model proposed as a unifying syndrome, which places more mild sex development abnormalities on a spectrum with DSD, and indicates an increasing risk of TGCT among more severe TSD cases[44,70]. This theory suggests that aberrant gonadal sex developmental may lead to malignant transformation of germ cells into TGCTs. This concept is important to understanding why malignant TGCT initiation is limited to early development.

1.2.7 The high cure rate of TGCTs after platinum-based chemotherapy

Before the use of cisplatin, TGCTs carried a terrible prognosis similar to aggressive somatic cancers with only 5% of patients surviving beyond five years after diagnosis with late-stage disease[71]. At that time, germ cell tumors were treated with dactinomycin, vinblastine, and bleomycin, the last of which is still part of the current treatment regimen[71]. In a 1980s landmark study, in which 50 metastatic TGCT patients received a novel combination therapy of vinblastine, bleomycin, and cisplatin, there was an astounding 85% survival rate and is now considered the cure for this formerly incurable disease[72]. Today, cisplatin, etoposide, and bleomycin (BEP protocol) remain the standard of care for TGCTs, and this treatment results in up to 80% survival for advanced metastatic disease, with a 96% rate survival at all stages[71].

The key facilitator of this revolution in treatment came with the discovery of cisplatin. The platinum-based drug originated from a 1967 screen of electrolysis generated compounds that were tested for their ability to inhibit the growth of *E. coli*[73]. Cisplatin causes inter and intra-DNA-strand

crosslinks as its main mechanism of inducing double strand breaks and apoptosis[74]. Because cisplatin causes renal and neurotoxicity, alternative platinum-based drugs carboplatin, and oxaliplatin are increasingly used, which tend to be equally effective for treating most somatic cancers and can be given at higher doses due to lower side effects[75]. Surprisingly, cisplatin is still the most efficacious platinum-based drugs against TGCTs, despite its greater toxicity, and is therefore still used in nearly all TGCT chemotherapy protocols[76].

Cisplatin is given with both etoposide and bleomycin as the standard of care treatment for TGCTs. Etoposide is a topoisomerase II inhibitor, which also induces double strand DNA breaks leading to DNA damage and apoptosis. The topoisomerase II enzyme is necessary to release the tension of the supercoiled DNA caused by the helicase-mediated unwinding of DNA during replication. To do this, it first cuts and then uncoils double stranded DNA, before ligating both strands of DNA back together. Etoposide was first synthesized in 1967 from a class of toxins known as podophyllotoxins, derived from *Podophyllum* or wild mandrake plant[77]. Etoposide binds to topoisomerase II, and does not interfere with endonuclease activity of the enzyme, allowing the cuts to be made, but the drug does prevent the ligation step, thus facilitating the double strand break[77]. Bleomycin was isolated from *Streptomyces verticillus* in 1966 as a complex glycopeptide that had antibiotic properties[78]. Surprisingly, the exact mechanism by which the drug acts is still unknown. It is known that the drug acts directly on DNA, and utilizes a redox-active metal ion of iron or copper to induce the double strand breaks[79].

1.2.8 Current mouse models of TGCTs

The TGCT mouse model used to generate the data presented in Chapters 2 and 3 relies on two oncogenic events, mediated by Stra8-cre recombinase activity, which induces teratocarcinoma formation. Malignant transformation is driven by inactivation of tumor suppressor *Pten*, and simultaneous expression of constitutively active $Kras^{G12D}$. This model is described in more depth within the data chapters. However, it is worth noting the alternative mouse models of TGCTs as they produce teratomas, rather than the more malignant teratocarcinoma, and are less characteristic of GCNIS derived TGCTs.

The original mouse model of TGCTs is the spontaneous formation of teratomas in 129 inbred mice. Discussed in other portions of this dissertation, these tumors also rarely contained EC which was used in the early experiments of the disease[80]. Additionally, inbred 129 mice that are $P53^{-/-}$ develop teratomas at an increased rate[81]. Primordial germ cell-specific inactivation of PTEN starting from E9.5, facilitated by TNAP/Cre, leads to germ cell depletion and increased teratoma formation[82,83]. The Ter mutation in DND ($DND^{Ter/Ter}$) also increases the rate of teratoma formation, as does consomic substitution of Chr19 from MOLF strain mice and genes on Chr19 appear to enhance tumor formation in normal 129 strain mice, as well as DNDTer/Ter[84,85]. Importantly, both of these mutations are only known to enhance tumor formation in 129 strain mice[84,85].

1.3 THE DNA DAMAGE RESPONSE, CHEMORESISTANCE, AND CHEMOSENSITIVITY

Genome integrity is necessary for the survival of all cellular life and ensures that genetic material is reliably passed to daughter cells, and from one organism to its offspring. DNA, however, encounters a continuous assault of potentially mutagenic DNA damage from both normal cellular function, as well as exogenous sources. The initial DNA damage response (DDR) is the detection of a break or adduct in the DNA, usually resulting in activation of kinases ATM (which responds to double strand breaks) or ATR (which responds to single stranded DNA)[86]. The activation of ATM and ATR leads to cell cycle checkpoint activation, thus halting or slowing the cell cycle while also signaling to downstream effectors to repair the damage, or if the damage is too extensive, to enter senescence or undergo apoptosis. While DDR pathways are critical for maintaining homeostasis and preventing genomic instability which can lead to cancer, these pathways are also a pivotal determinant of genotoxic chemotherapeutic sensitivity of all forms of cancers.

1.3.1 Mutations in DNA damage response pathways lead to chemoresistance

P53 is one of the most commonly mutated genes in cancers, and loss of P53 function is associated with increased chemoresistance[87]. Gains and losses of other genes that perturb DDR pathways are also associated with tumorigenesis, and because many modern chemotherapeutics work by damaging DNA to facilitate cancer cell death, disruption of DDR pathways often leads to chemoresistance[88,89]. Genotoxin induced cell death in cancer can be circumvented if cancer cells obtain increased DNA repair, or can avoid cell cycle arrest and apoptosis.

DDR as tumorigenesis barrier

The DDR not only protects our genome from the constant barrage of DNA-damaging insults, but it also plays an important role as a barrier to tumorigenesis. Oncogene activation drives tumorigenesis and also rapidly increases DNA damage through double strand breaks and increased ROS[88]. In response to this damage, even during early tumorigenesis, somatic cancers exhibit constitutively active DDR as evidenced by phosphorylated CHK2, ATM, and yH2AX which often persist at late stages[90]. The exact source of the damage is still unknown but is likely aberrant replication structures and DNA damage caused by unscheduled replication brought about by the oncogenic activation. This hypothesis is supported by the observed activation of phosphorylated P53, CHK1, and y-H2AX, in U-2-OS cell lines after oncogenic activation of either *E2F1*, *Cdc25a*, or *Cyclin E*[90].

While DDR activation in response to aberrant proliferation acts as a barrier to tumorigenesis, it also causes selective pressure to mutate genes responsible for maintaining

checkpoint activation and senescence. Indeed, cell cycle progression despite persistent DNA damage occurs in many cancers, suggesting failed checkpoint activation[88,91]. Importantly, P53 is necessary for maintaining cellular senescence and would, therefore, often be subjected to these selective pressures which may explain why it is the most commonly mutated gene in somatic cancers[88,91]. Loss of proper DDR leads to increased genomic instability, observable by the increase in mutations and genomic abnormalities in later stage cancers[90]. Importantly, GCNIS, the early stage TGCT lesions described earlier, do not show the constitutive activation of the DDR that is seen in most somatic cancers[92,93]. This lack of DDR activation in TGCTs avoids selective pressures to mutate genes that control proper DDR and checkpoint signaling, and it is a likely explanation for the comparatively low mutation rate of DDR genes including P53 in TGCTs.

Chemoresistance due to disruptions in apoptotic pathways

P53 is the master regulator of cell cycle arrest and cell death, acting as a barrier to tumorigenesis and an important determinant of therapeutic responses to genotoxic chemotherapies after tumorigenesis. Unfortunately, P53 mutations range as high 50% frequency among certain cancers and are the most common gene mutations in cancers overall[94]. While P53 mutations can cause defects in signaling for cell senescence and apoptosis, downstream players in these pathways are also commonly mutated in chemoresistant cancers.

Mitochondrial-dependent apoptosis is one of the main pathways of DNA damage-induced cell death, also known as the BCL-2 regulated apoptotic pathway. This pathway is regulated by anti-apoptotic BCL-2 like proteins, and pro-apoptotic BH3-only proteins (so named for the

presence of conserved BH3 domain) which include PUMA, and NOXA. PUMA and NOXA are p53 regulated BH3 family proteins which induce apoptosis in response to DNA damage by interacting with BCL-2 family proteins and inhibiting their ability to negatively regulate pro-apoptotic factors BAK and BAX. Without inhibition, BAK and BAX can localize to the mitochondria and permeabilize the membrane allowing the release of cytochrome c[95]. Once released, cytochrome c activates the caspase cascade and thus initiates apoptosis.

Many cancers hijack the proteins that regulate apoptosis, allowing them to evade programmed cell death and thus conveying chemoresistance. Overexpression of BCL-2 family proteins correlates with chemoresistance and is a potential target for combination therapies[96–98]. Pushing the apoptosis pathway in the other direction can have beneficial therapeutic outcomes, further emphasizing the importance of these pathways in chemoresistance. For instance, expression of BH3-only proteins PUMA, NOXA, and BIM confer sensitivity to chemotherapeutics resulting in a better prognosis in chronic lymphocytic leukima[99]. Caspases can be divided into two main groups, initiator capsases-2, -8, and -9, which help regulate the choice of apoptosis, and effector caspases-3, -6, and -7 which drive apoptosis after the cell fate has been chosen[100]. Mutations in caspase proteins are also associated with chemoresistance. Nonsense mutations in caspase-8 and loss of its expression are associated with increased chemoresistance in a variety of cancers, which can be at least partially re-sensitized by re-expression of the protein[101]. Reduced or absent caspase-3 expression was found also found in 75% of breast cancer cell lines and freshly isolated samples, suggesting a loss of caspase-3 expression contributes to breast cancer cell survival and resistance to apoptosis[102]. Taken together, it is clear that loss of canonical apoptotic pathways can, and do, play a role in the loss of chemosensitivity of many cancers.

Chemoresistance due to increased DNA damage repair

A cell's ability to repair damage caused by genotoxic chemotherapies directly impacts its response to those drugs. Cisplatin, carboplatin, and oxaliplatin are platinum-based therapeutics that are used against a wide range of cancers. They work primarily by forming DNA intra- and interstrand crosslinks. Several key repair pathways play a role in resolving the damage caused by these drugs: Homologous recombination (HR), nucleotide excision repair (NER) and DNA mismatch repair (MMR)[103]. Defects and reduced expression of MMR genes MLH1 and MLH2 are associated with increased chemoresistance, likely due reduced ability to detect, and respond appropriately to, the DNA lesions caused by platinum-based chemotheraputics[104,105]. NER, on the other hand, is the primary pathway responsible for removing the crosslinks formed by platinum-based drugs. ERCC1 and XPF form a nuclease complex which, along with ERCC4, facilitates the excision of the crosslink, which is followed by complete repair of the break. ERCC1 and XPF expression levels are prognostic for chemosensitivity[103]. In a study of 60 patients with locally invasive cervical squamous cell cancer, 86.21% patients with low mRNA levels of ERCC1 had a complete response to cisplatin-based therapy, while only 19.36% of patients with high mRNA levels showed complete response[106]. In a separate study, ERCC1 expression was evaluated immunohistochemically in paraffin-embedded tumors[107]. Samples were collected from 101 patients diagnosed with epithelial ovarian cancer before treatment. These patients were then treated with carboplatin-paclitaxel combination therapy. ERCC1 expression positively correlated with resistance to treatment, and 75% of tumors expressing ERCC1 were resistant while only 27% of tumors which did not show ERCC1 expression were resistant[107]. HR is a pivotal player in repairing interstrand crosslinks mediated by Fanconi Anemia and BRCA proteins. Epithelial ovarian cancers have a high incidence

of platinum drug sensitivity which has been linked to the high frequency of HR defects of the cancers[108].

1.3.2 Other mechanisms of chemoresistance

Aside from alterations in the DDR, drug resistance in somatic cancers often occurs from three other well-characterized mechanisms. These include increased cellular export of the drug, an increase in molecules that can render the drug less reactive, and alterations to the cellular components targeted by the drug.

Drug Efflux

The ability to clear a drug from a cell, or prevent its accumulation, is a cause of both primary or acquired multi-drug resistance. The major mechanism for this type of resistance is a family of multidrug exporters named ATP-Binding Cassette (ABC) transporters[109]. These are a tissue specific set of active transporters that can pump a variety of molecules, including chemotherapeutics, out of the cell against its concentration gradient[109]. A recent study of osteosarcoma cell line OS-65 found increased resistance to a variety of chemotherapeutics within a subpopulation of the cultured cells[110]. This subpopulation was found to harbor increased expression of ABCG2, ABCB1/MDR1, and ABCB5 transporters[110]. ABCC1 and ABCC3 are also overexpressed in many breast cancer cell lines, the knockdown of which can cause increased

chemosensitivity[111]. Similar findings of increased chemoresistance associated with increased expression of ABC transporters were found in glioblastoma, pancreatic, and colorectal cancers[112–114]. Targeting these pathways has become an area of intense clinical interest in hopes of using combination therapy to sensitize certain resistant cancers[115].

Drug Detoxification

The increase in two different proteins accounts for the majority of drug detoxification induced chemoresistance, glutathione S-transferase (GST), and dihydropyrimidine dehydrogenase (DPD). GST catalyzes the joining of glutathione with a variety of exogenous sources, including many platinum-based chemotherapeutics, which makes them accessible to ABC transporters. Some studies suggest that the conjugation activity of GST may not be the primary mechanism of resistance, but those, and others find that increased GST expression does contribute to chemoresistance[116]. One study took biopsies before treatment from 61 patients with primary ovarian cancer. 10 out of 11 tumors from cancers that were positive for GST-π were later found to be resistant to cisplatin-based treatment, while only 6 out of 17 GST-π negative tumors were resistant[117]. In a separate study of 107 patients with colorectal cancer treated with oxaliplatin, three common polymorphisms of GST known to decrease the proteins' function were associated with increased patient survival. Higher expression of DPD, on the other hand, plays a key role in the catabolism of fluorouracil (5-FU) and is highly associated with resistance to the drug[118].

Alteration of drug target

Another mechanism of chemoresistance occurs when cancer cells have altered variants of the cellular component that the therapeutic drug targets. The most relevant examples to this dissertation are alterations of topoisomerase-II, is the known target of etoposide, described in Section 1.2.7. Etoposide inhibits topoisomerase-II, allowing the endonuclease activity of the enzyme, but blocking the ligation step, ultimately leading to the DNA damage which induces apoptosis as an effective chemotherapy for many cancers. Altered expression of topoisomerase-II isoforms is associated with altered sensitivity to etoposide and other topoisomerase inhibitors[119]. For instance, in several melanoma cell lines, increased topoisomerase II activity directly correlated with increase etoposide resistance[120].

1.3.3 Uncommon occurrences of TGCT chemoresistance mechanisms

Although TGCTs are considered curable, even after distant metastasis, rare chemoresistant variants of the disease do occur. These mechanisms of resistance are often similar to resistance in somatic cancers, but at a much lower frequency. Most notable is the comparably low rate of P53 and other DDR gene mutation in TGCTs[121]. Although almost non-occurring in random panels of TGCTs, P53 mutations were found in 5 out of 28 chemoresistant TGCTs[122]. Higher levels of P21, an important cell cycle regulator, were more highly expressed in chemoresistant EC cell lines and tumors, compared to their chemosensitive counterparts[123]. Within a panel of 35 chemoresistant TGCTs, MMR deficiencies, BRAF mutation (V600E), and microsatellite instabilities were all

increased compared to 100 chemosensitive controls[124]. The fact that DDR mutations are rare in TGCTs, yet do cause chemoresistance when they occur, further supports the idea that the lack of DDR during early tumorigenesis of TGCTs avoids a key step in selecting for the DDR mutations that regularly occur in somatic cancers. The avoidance of chemoresistance inducing mutations is likely to play an important role in keeping TGCTs sensitive to genotoxic chemotherapy drugs. However, there is also evidence that germ cells, and other pluripotent cell types, have a unique DDR that makes the hypersensitive to genotoxic DNA damage as detailed below. Because TGCTs arise from germ cells and have many similar phenotypes to other pluripotent cells, they likely share some of the same hypersensitivity mechanisms.

1.3.4 The hypersensitive DDR of pluripotent stem cells

Germ cells protect the genome that is to be passed to future generations and utilize a proficient DDR to avoid deleterious mutations from entering the germline. Other pluripotent cells, such as cells of the inner cell mass, or pluripotent cells that only exist *in vitro*, like embryonic stem (ES) cells and induced pluripotent stem (iPS) cells, all share certain similar properties. All of these cell groups have a unique DDR compared to somatic cells and tend to apoptosis at a lower threshold of DNA damage, likely to limit the chance of passing on deleterious mutations to a larger number of daughter cells, or offspring in the case of germ cells[125,126]. Less evidence exists regarding TGCTs DDR. However, sharing these the same mechanisms would help explain why TGCTs have such a positive response to genotoxic chemotherapies.

Apoptosis, senescence, and differentiation are all DDR mechanisms employed to prevent or limit pluripotent cell proliferation. Although ES cells and iPS cells have increased DNA damage repair which leads to a more robust resolution of DNA damage compared to their differentiated counterparts, they also trigger apoptosis at lower thresholds of damage[125,126]. One aspect of this hypersensitive response is the fast induction of P53-dependent apoptosis in ES cells after DNA damage. In most cells not committed to apoptosis, BAX is cytosolic, and only after sufficient DNA damage is it activated to induce oligomerization and localization to the mitochondrial membrane where it facilitates the release of cytochrome c and induces apoptosis[95]. In human ES cells, however, BAX is already activated and primed at the golgi where it remains ready to relocate to the mitochondria at all times[127]. Importantly, this primed BAX phenotype does not remain after ES cells differentiate[127]. An additional mediator of hypersensitivity in ES cells is a reduced or absent G1 checkpoint. The G1 checkpoint is critical to ensure DNA replication does not begin if unrepaired DNA damage is present, thus preventing additional damage and genomic instability. Human ES and iPS cells, however, do not activate the CHK1 kinase after induction of replication stress and tend to induce apoptosis instead[128]. Human ES and iPS cells also fail to activate proper G1 checkpoints following irradiation and instead commit to apoptosis at a higher rate at compared to their differentiated counterparts[125]. Mouse ES cells appear to lack a G1 checkpoint which, similar to hESCs, results in elevated levels of DNA damage induced apoptosis compared to somatic counterparts[129].

Differentiation in response to DNA damage is another unique response of pluripotent cells. *Nanog* is a necessary transcription factor required to maintain the pluripotency state of a cell[130]. In mouse ES cells, P53 binds to the *Nanog* promoter, in a DNA damage-dependent manner, and the resulting loss of *Nanog* expression induces differentiation[131]. Loss of *Oct4* expression, another key

pluripotency transcription factor, also induces P53 mediated differentiation of embryonic stem cells[132]. These findings not only show a mechanism to limit pluripotent stem cell proliferative capacity after damage but demonstrate tightly woven DNA damage and pluripotency networks within these cells. This evolved interplay of these two complex cellular pathways likely helps ensure that cells attaining potentially harmful mutations will lose the indefinite proliferative capacity normally associated with pluripotent stem cells.

1.4 CANCER STEM CELLS

The CSC theory is rooted as far back as the mid-1800s. During this period, German pathologists Rudolf Virchow and Julius Cohnheim first postulated the embryonic rest theory which postulated that cancer might arise from embryonic remnants, or cells left over from embryogenesis, which retained embryonic properties[133]. Over the decades, the theory had many key contributions, most relevant to this dissertations was the discovery that single EC cells from mice could regrow entire teratocarcinoma[43]. Since those experiments, a steady trickle of findings has become a flood of evidence which supports the existence and importance of CSCs in a variety of cancers. From this growing field, a well-defined yet still controversial model of CSCs has emerged.

1.4.1 Clonal vs. cancer stem cell model of cancer

The most widely accepted theories of cancer growth and heterogeneity are depicted in a key 2001 Nature review (Fig. 1.4)[134]. In the stochastic model of cancer, most cancer cells can divide extensively and create new tumors while mutating to form tumor heterogeneity. In the CSC theory of cancer, while the tumor cells also have mutations and are heterogeneous, only a small population of cells can divide extensively and form new tumors. This limited population of cells is referred to as cancer stem cells, (also called tumor-propagating cells or tumor initiating cells) which fit the definition of normal stem cells in that they can self-renew and differentiate but in within the context of continued tumor progression rather than homeostasis. There is evidence to support both models,

but realistically both apply to different extents, in a variety of cancers. The first clear support for the modern CSC theory can be traced back to one defining study in leukemia.

Figure 1.4 Graphical depiction of classical and cancer stem cell models of cancer. (Figure adapted from Reya et al., 2001[134])Graphical representation of the classical model of cancer (Left), in which all cancer cells have the ability to divide indefinitely *versus* the CSC model of cancer (Right) in which only a very small population of cells have the ability to divide indefinitely.

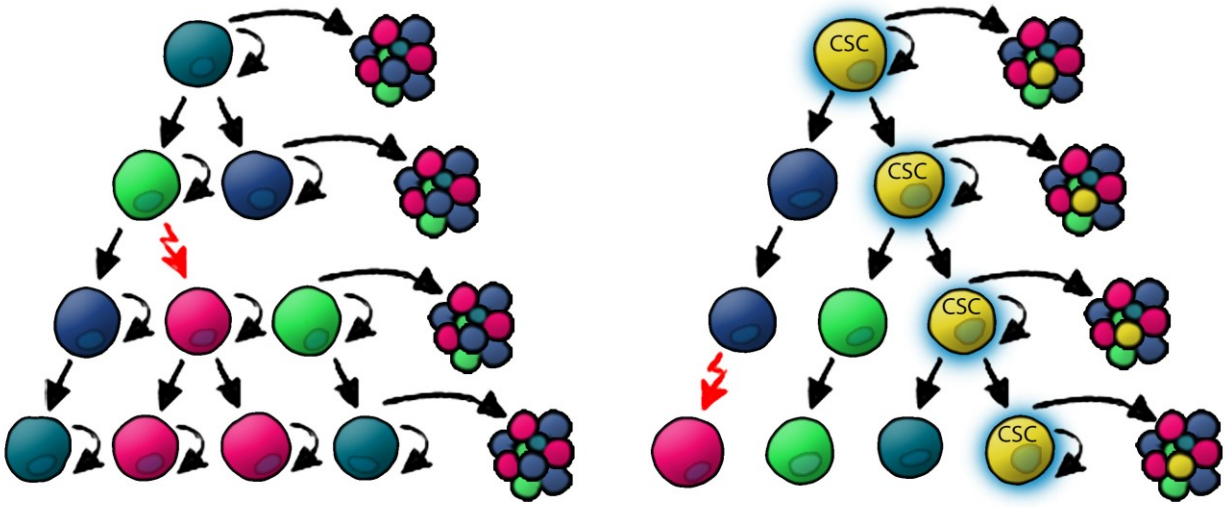

It has been known since the 1960s that only a subpopulation of leukemic cells would grow and form colonies, but it was not known from these studies if all cells had a rare chance to begin proliferation, or if only a subset of cells had this potential[134]. These two undetermined possibilities highlighted the key distinction between the classical and CSC model of cancer respectively. A study was done in 1997 which determined that acute myeloid leukemia stem cells could be isolated as CD34+ CD38- using FACS, thus confirming the idea that only a small population can divide extensively, rather than all cancer cells having a chance of doing so[135]. Since then, many studies have identified CSC populations in many solid cancers, contributing to the growing excitement that CSC-targeted treatments could lead to higher cure rates in a variety of cancers.

1.4.2 The hope and controversy of CSC-targeted therapy

The CSC theory of cancer is intensely alluring due to advances in treatment prospects as well as a valuable model for recurrence and metastasis. After treatment, there is often an initial response measured by reduction of bulk tumor, yet many patients relapse months or years later, ultimately succumbing to the disease. The CSC theory offers a potential explanation for relapse if CSCs are more resistant to canonical treatment. Even if a small number CSCs evade chemotherapy, it still leaves the malignancy able to regrow and metastasize (Fig. 1.5). Most importantly, targeting those CSCs specifically, in combination with broader treatments, would reduce the risk of relapse and perhaps make the disease curable. Indeed, several studies discussed in the next section have found that the percentage of CSCs often increases following conventional treatment, suggesting those cells are evading those therapies.

Figure 1.5 Cancer stem cell model and treatment response. (Figure adapted from Das et al., 2008[136]). Graphical depiction of the possible role of CSCs in tumor recurrence following conventional cancer therapies. Alternatively, depicted on the lower pathway, a therapy directly targeting CSCs may cause loss of tumor malignancy and ultimately higher cure rates.

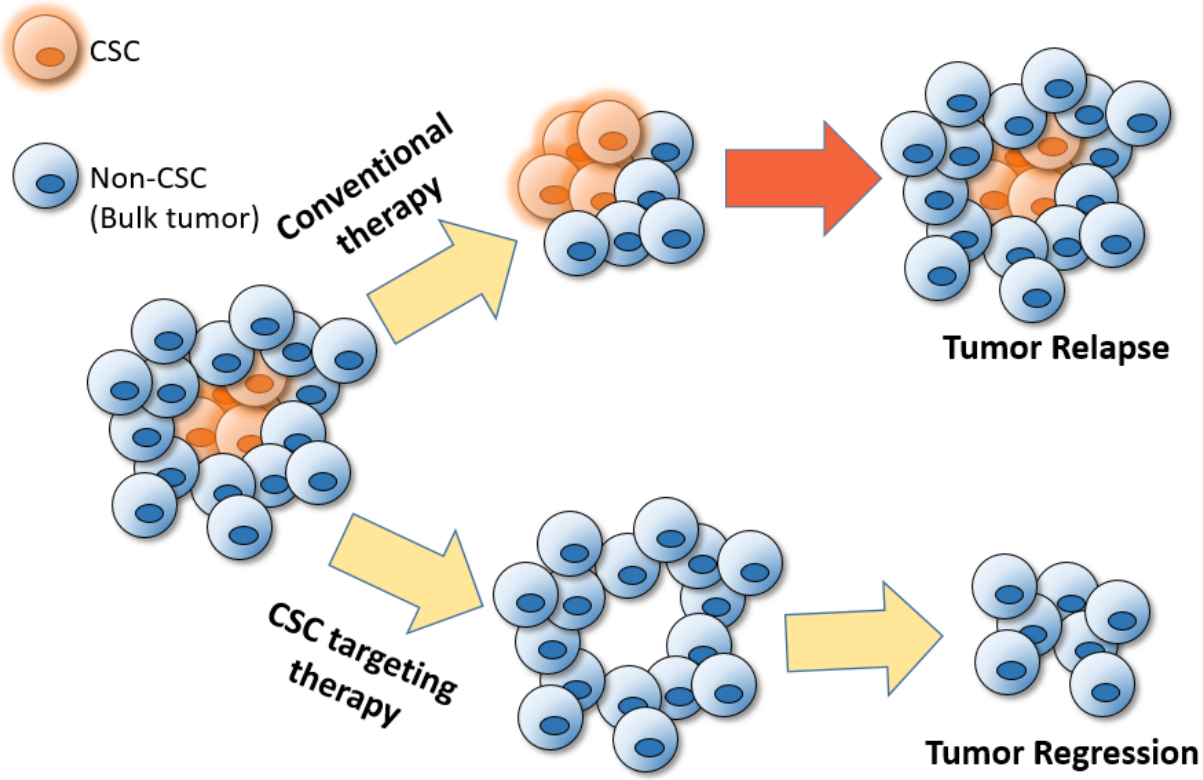

Despite the hope of better cancer treatments, there are some important caveats to the CSC theory of cancer. A portion of the controversy revolves around the nomenclature itself. The term CSC describes any cancer cell that can self-renew as well as differentiate into the other cellular phenotypes of that cancer. However, it is often mistakenly thought that the term implies that CSCs arise from a stem cell origin, or that the CSC is expected to possess similar phenotypes as normal stem cells, such as similar population sizes or consistency of markers. While CSCs certainly might arise from stem cells, and often have phenotypes comparable to stem cells from their tissue of origin, this is not necessarily the case and should not be implied by the term CSC. While clarification of nomenclature is necessary to avoid confusion, they do not pose concerns for the validity of CSC-targeted therapies[137].

More relevant are concerns regarding the prevalence of CSCs and whether they are a sufficiently stable population of cells to be irradicated by targeted drugs. It is clear that some cancers have a high population of cells that can propagate tumors, rather than a small population of CSCs. One study found that 28% of melanoma cells obtained from patients' cancer were able to propagate tumors and divide indefinitely[138]. Furthermore, the researchers sorted tumor cells based on 22 different cell markers but were unable to distinguish any subpopulation of cells without a tumor-propagating phenotype, which provides evidence against the CSC model. Other studies find that the CSC population is not necessarily well defined, suggesting that targeted therapies may work for a more limited range of cancers than hoped. Boiko et al. found that CD271+ tumor cells isolated from melanoma patients were able to form tumors in immunocompromised mice, while CD271- cells rarely did (70% vs. 7% engraftment success respectively)[139]. However, they concluded that the CSC population ranged from 2.5% to 41%, suggesting extreme variation in the population depending on the disease stage and the individual. Despite this conflicting

evidence, the CSC field of cancer research has rapidly increased over the recent decade, unveiling an overwhelming amount of evidence that CSCs exist in many cancers and that they appear to play a role in chemoresistance and disease progression.

1.4.3 Somatic cancer stem cells and their therapeutic impact

Acute Myelogenous Leukemia (AML) and Chronic Myelogenous Leukemia (CML)

Leukemia is the uncontrolled proliferation of hematopoietic cells, generally arising from the aberrant self-renewal of hematopoietic stem cells. AML and CML are two well-characterized types of leukemia. As the name suggest, AML progresses rapidly as cells of the hematopoietic system fail to differentiate. The cure rate is approximately 35% to 40% in patients under 60, but only 5% to 15% survival for patients over 60, with older patients having a median survival of just 5 to 10 months[140]. In part, the poor survival among older patients is due to lack of efficacious treatments with a low enough toxicity to use safely. CML, on the other hand, has poorly differentiated hematopoietic cells which may appear normal, and be somewhat functional which allows the disease progress considerably slower. Bone marrow transplant is often a curative treatment for CML, although Imatinib, an inhibitor of the constitutively active tyrosine kinase fusion protein BCR-ABL which that is frequently expressed after a chromosomal translocation between 9 and 22 that occurs in most CML patients, produced exceptional 89% five-year survival rates[141]. Aside from Imatinib and bone marrow transplants, both AML and CML are also treated with genotoxic chemotherapy drugs.

As mentioned above, CSCs of AML were convincingly identified in 1997 as a population of CD34+ CD38- cells[135]. Similarly, hematopoietic stem cells (HCS), and CML CSCs, can also be identified based on CD34+ CD38- CD90+. This population was initially demonstrated by only those cells having the ability to repopulate nonobese diabetic–scid/scid mice in a lympho/myeloid assay[142,143]. It suggests that HCS are the CSC progenitor cell, or that at least two cell types share some phenotypes. Indeed, AML and CML CSCs have similar mechanisms of surviving genotoxic chemotherapies as compared to HCS, including quiescence which avoids induction of damage that usually occurs in proliferative cells[143]. An additional study utilized a NOD/SCID/IL2rγ^{null} mouse model of human AML to demonstrate that not only does quiescence offer a protective mechanism for AML CSCs, but the cells can also be re-sensitized to chemotherapy by inducing proliferation using granulocyte-colony stimulating factor[144]. Currently, work to generate targeted therapy against leukemia stem cells includes targeting unique membrane proteins, disrupting the CSC niche, and differentiation therapies[145–147].

Breast Cancer

Unlike leukemia cancer stem, the majority of solid CSCs have yet to be confidently characterized and are often not easily isolated by cell surface markers. Breast CSCs were the first solid somatic CSC to be identified, although the populations also have a great deal of heterogeneity. Initial CSC identification came from a comparison of nine human breast cancers grown as patient-derived xenografts. After isolating and transplanting many different cell populations from these nine samples, researchers found that only CD44^{+} CD24$^{-/low}$ ESA^{+} cells were able to form tumors in NOD/SCID mice even with as few as 100 cells transplanted[148]. While all identified breast CSCs

have been $CD44^+$ $CD24^{-/low}$, ALDH1, EpCAM, and CD48f have all been shown to identify additional sub-populations[149].

Like most somatic CSCs, breast CSCs appear to be more resistant to conventional treatments compared to the bulk tumor. The best evidence of CSC chemoresistance comes from studies finding increased CSC populations in tumor biopsies from breast cancer patients after receiving platinum-based treatments compared to their pretreatment biopsies[150,151]. Although many chemotherapeutics and targeted treatments exist, radiation therapy remains an important component of breast cancer treatment, especially at earlier stages[152]. However, like untransformed mammary stem cells, breast CSCs have lower levels of ROS compared to the bulk tumor cells, which gives them an increased resistance to radiotherapy[153].

Glioblastoma

Although a relatively rare cancer, glioblastoma is the most common brain cancer with a dismal median survival of 12 to 16 months, and only a 4-5% five-year survival rate[154]. The standard of care is surgery, radiation, and treatment with chemotherapeutic temozolomide, but is rarely curative[155]. While glioblastoma has a well-characterized CSC population, the markers to identify the CSC population remains somewhat elusive. The presence of CSCs in gliomas has been recognized for over a decade, as discovered by the presence of a small population of tumor-propagating cells expressing markers of neuronal stem cells[156]. Although $CD133^+$ glioblastoma cells have been identified as CSCs, a major limitation remains in that most studies of this cancer rely on cell lines and rare cultured primary tumors, almost certainly perturbing the natural CSC population[157]. Key studies utilizing *in vitro* strategies have identified that forced expression of

transcription factors RCOR2, OCT1, SOX2, and SALL2 are sufficient to dedifferentiate non-tumorigenic glioblastoma cells into CSCs[158]. The forced expression of these four transcription factors restored the tumor-propagating potential of the differentiated cell and gained gene expression similar to neural stem cells. The findings also provided tools to identify a more meaningful and specific population of CSCs in human glioblastoma tissue samples for future studies.

Similar to breast CSCs, CD133+ glioblastoma cells were found to have a stronger DDR activation in response to radiotherapy compared to the bulk tumor cells[159]. CSC resistance to radiotherapy, despite an initial reduction of bulk tumor, was also shown by increased percentages of CD133+ in glioblastomas following radiotherapy, which was reversed with CHK1 and CHK2 inhibitors in xenograft models[159]. Temozolomide is the main chemotherapeutic used to treat glioblastomas, and it induces DNA damage by alkylating base pairs of the DNA, thus inducing apoptosis. Importantly, this type of damage is rapidly repaired by increased expression of methylguanine DNA methyltransferase (MGMT). Conflicting findings suggest that some glioblastoma CSCs overexpress MGMT, making them more resistant than the bulk tumor, while others have lower expression compared to the bulk tumor[160,161].

1.4.4 Embryonal carcinoma, a model of curable cancer

Although there are obvious differences between cancer cells and the normal stem cells from which they arise, there are often relevant similarities. Many of the mechanisms of CSC chemoresistance mentioned above, quiescence, increased checkpoint signaling after damage, and increased MGMT expression, are also phenotypes of the stem cells found in their respective tissue of origin. For this

reason, the first portion of the introduction was devoted to normal germ cell biology because they are the cells from which TGCTs arise. Also as mentioned above, germ cells and other pluripotent cells have an increased DDR, making them extremely sensitive to genotoxic chemotherapies. The significant risk to fertility among young cancer patients most clearly emphasizes this germ cell hypersensitivity[162]. Based on transcriptional regulators used as diagnostic markers, EC shares many of the same pluripotent transcriptional networks as primordial germ cells, or embryonic stem cells, which demonstrate hypersensitivity to genotoxic stress compared to most somatic cells[35]. Importantly, EC exists as the CSC component for many mixed TGCTs. As described above, many somatic CSCs tend to be resistant to standard of care therapy which may explain why many somatic cancers relapse and are not curable, even after a good initial response. However, if TGCT CSCs are hypersensitive to the standard of care therapies; then it would help explain their overall high cure rate. Demonstrating this would emphasize the potential of CSC-targeted therapies, and place importance on gaining a better understanding of the mechanisms behind the *in vivo* chemosensitivity of EC cells.

History of embryonal carcinoma

Leroy Stevens is credited with initiating research of EC. While studying the effects of tobacco on mice at Jackson labs in 1953, he discovered that inbred line 129 mice had a high rate of teratoma formation[163]. A year later, he published a study demonstrating that disaggregated cells from a small percentage of these teratomas continued to grow when transplanted into syngeneic mice[80]. Follow-up experiments by Pierce et al. identified that these teratomas had tissue from all three germ layers like all teratomas, but they also harbored a fourth undifferentiated tissue type known as EC[164].

From this work, these rare tumors were categorized as malignant teratocarcinoma[164]. A key study from the same group in 1964 demonstrated unequivocal evidence that EC is the functional CSC of teratocarcinoma[43].

In those studies, Kleinsmith et al. observed that when teratocarcinoma was transplanted intraperitoneally, the mouse would develop ascites with free floating clusters of cells which appeared similar to very early embryos. These clusters were aptly called embryoid bodies. Within these embryoid bodies, a small percentage of cells were observed to contain EC cells, and when single embryoid bodies were transplanted into syngeneic mice, that same small percentage of engraftments were successful. To determine if the entire embryoid body was necessary to regrow a teratocarcinoma, or if a single EC cell held the unlimited growth and differentiation capacity, single cells were engrafted into syngeneic mice. Single cells were carefully isolated from embryoid bodies collected from ascites. Using glass capillary tubes, researchers first confirmed the isolation of single cells, and then transplanted those cells into 1790 mice, resulting in 43 successful engraftments of teratocarcinoma. This set of experiments provided some of the earliest evidence that single cells can function as CSCs and demonstrated that EC is functionally the CSC of teratocarcinoma[43].

Continued work with EC laid the groundwork for isolation of embryonic stem cells as well as their culture conditions[165]. Characterization of embryoid bodies morphologically linked EC to the inner cell mass (ICM) of early blastocysts outlined in section 2.1[166]. Finally, in 1981, ICM cells were explanted from early stage embryos into teratocarcinoma conditioned media, thus facilitating the first embryonic stem cell cultures[167]. While embryonic stem cells have become a superior system for many research applications, EC remains a valuable model of CSCs. Importantly, the two cell types share key phenotypes and often respond similarly to a given stimulus. Possibly the

most important and well-established similarities are that both cell types express pluripotency markers NANOG, OCT4, and SOX2, which are vital transcription factors of pluripotency. Substantial differences also exist, such as a unique crosstalk between OCT4 and AKT promotes self-renewal in human EC cells but is absent from human ES cells[168]. Upon *in vivo* transplantation of EC cells form teratocarcinoma; ES cells, on the other hand, only form the teratoma component, and fail to maintain their pluripotent stem cell population within the resulting tumor.

Much more is known about the unique DDR of ES and iPS cells, but there is evidence to suggest EC cells share a similar hypersensitivity to DNA damage. One study found that rather than a robust P53 mediated transient cell cycle arrest, which can cause chemoresistance in some somatic CSCs, EC cells can have a robust P53 mediated senescence response to the same level of damage[169]. Other studies found EC cells have a preferential apoptotic pathway over P21 induced cell cycle arrest after damage[170]. P53 in EC cells appears to be regulated by MDMX and MDM2. However, in somatic cancers, activation of P53 by disruption of MDM2-P53 association usually leads to P21 induced cell cycle arrest while the same disruption triggers an apoptotic response in EC[171]. All of these data suggest EC cells have a preferential apoptotic response to DNA damage similar to other pluripotent cells. Importantly, all of that evidence has been gathered from *in vitro* work using long-term cultured EC cell lines. A lack of a robust TGCT animal model has limited the *in vivo* validation of these findings. However, direct comparison of teratocarcinoma patient tumors before and after treatment found that EC cells tend to be eliminated by chemotherapy, leaving only the teratoma component, which rarely continues to grow[172,173]. This depletion following treatment is contrary to chemoresistant somatic CSCs, highlighting the functional *in vivo* hypersensitivity of EC under real world conditions.

The remaining chapters of this dissertation address important questions about germ cell susceptibility to oncogene-induced malignant transformation and provide evidence that malignant TGCTs arise from insults during a specific window of embryonic development. I show that EC functions as a CSC within our mouse model. The data presented based on this model shows it as a relevant system to study malignant TGCTs as well as highly chemosensitive CSCs. This work helps us understand why TGCTs respond so well to genotoxic chemotherapies. Furthermore, the evidence that an effective therapy against CSCs can dramatically increase survival also serves to emphasize that targeting CSCs could be a valuable part of combination therapy. Targeting CSCs within chemoresistant somatic cancers may lead to increased cure rates similar to those obtained following the introduction of cisplatin and other genotoxic drugs used to treat TGCTs.

CHAPTER 2

CHEMOTHERAPY-INDUCED DEPLETION OF OCT4-POSITIVE CANCER STEM CELLS IN A NOVEL MOUSE MODEL OF MALIGNANT TESTICULAR CANCER

2.1 ABSTRACT

TGCTs are among the most responsive solid cancers to conventional chemotherapy. To elucidate the underlying mechanisms, we developed a mouse testicular germ cell tumor model in which germ cell-specific oncogenic *Kras* activation and tumor suppressor *Pten* inactivation were driven by CRE-mediated recombination. The resulting mice rapidly developed malignant, metastatic testicular cancers composed of both teratoma and embryonal carcinoma, the latter of which exhibited stem cell characteristics, including expression of the pluripotency factor OCT4. Several lines of evidence suggested that germ cell susceptibility to malignant transformation was restricted to embryogenesis, with the same oncogenic events triggering apoptosis in adult germ cells. Treatment of tumor-bearing mice with genotoxic chemotherapy not only prolonged survival and reduced tumor size, but selectively eliminated the OCT4-positive cancer stem cells. We conclude that the chemosensitivity of testicular cancers derives from the sensitivity of their cancer stem cells to DNA-damaging chemotherapy.

This chapter represents a manuscript that is currently under review.

Amy M. Lyndaker*, Timothy M. Pierpont*, Claire M. Anderson, Jamie L. Roden, Alicia Braxton, Lina Bagepalli, Nandita Kataria, Hilary Zhaoxu Hu, Jason Garness, Matthew S. Cook, Blanche Capel, Donald H. Schlafer, Teresa Southard, and Robert S. Weiss, Chemotherapy-Induced Depletion Of Oct4-Positive Cancer Stem Cells In A Novel Mouse Model Of Malignant Testicular Cancer. *Cell Reports*, Submitted

* These authors contributed equally to the manuscript.

I, Timothy M. Pierpont, generated all or partial data for the following figures of Chapter 2:

Figure 2.1
Figure 2.2
Figure 2.3
Figure 2.4
Figure 2.5
Figure 2.6
Figure 2.7

Figure 2.S1
Figure 2.S2
Figure 2.S3
Figure 2.S6
Figure 2.S7

Table 2.S1
Table 2.S4

2.2 STATEMENT OF SIGNIFICANCE

TGCTs are among the most curable solid cancers in humans, yet the mechanisms underlying their sensitivity to conventional DNA-damaging chemotherapies remain unclear. Here we demonstrate in a novel mouse model of malignant, metastatic testicular cancer that genotoxic chemotherapy prolongs survival and reduces testicular germ cell tumor size by preferentially depleting the cancer stem cells.

2.3 INTRODUCTION

Testicular germ cell tumors (TGCTs) are the most commonly diagnosed cancers in young men in the U.S. and Europe and are increasing in incidence[174]. Intriguingly, testicular cancers are among the most responsive cancers to chemotherapy. In the 1970s, prior to the advent of modern genotoxic chemotherapy drugs, the five-year survival rate for patients diagnosed with metastatic testicular germ cell cancer was only 5%. Remarkably, with conventional chemotherapeutics and surgery, 99% of patients with early-stage disease and 74% of patients with late-stage disease now live at least 5 years[175].As the name implies, TGCTs arise from transformed germ cells, most likely prenatal germ cells, such as primordial germ cells or spermatogonial precursors. In the latest classification scheme, TGCTs are categorized by whether or not they originate from a precursor lesion termed germ cell neoplasia in situ (GCNIS) of the testis[176]. Seminomas and nonseminomas are malignancies that do originate from GCNIS and were referred to as type II TGCTs in earlier classifications. These are the most common TGCTs, and they typically occur in adult males and frequently metastasize to abdominal lymph nodes, distant lymph nodes, and lung[177]. TGCTs that do not originate from GCNIS include infantile teratomas and yolk sac tumors as well as spermatocytic seminomas (previously referred to as type I and type III TGCTs, respectively). To date, mouse TGCT models have featured primarily benign teratomas rather than the more common malignancies originating from GCNIS.

Men presenting with TGCTs often have mixed TGCTs comprised of both seminoma and nonseminoma components, most notably containing highly malignant embryonal carcinoma (EC) tissue. EC cells are totipotent, and are the well-characterized stem cells of TGCTs. Indeed, a single EC cell is sufficient to recapitulate an entire tumor[43]. EC cells share many characteristics with

embryonic stem (ES) cells, and are similarly identified by expression of the pluripotency factor OCT4[178]. OCT4 is used clinically as the diagnostic marker for EC and seminoma as well as for early pre-invasive GCNIS lesions[179]. EC cells also express other pluripotency markers, including SOX2 and NANOG[180,181], and either differentiate, giving rise to teratoma tissue, or remain undifferentiated and highly malignant, as they do in metastatic TGCTs such as teratocarcinoma, a mixed germ cell tumor composed of EC and teratoma.

Cancer stem cells (CSCs), also referred to as tumor-initiating cells or tumor-propagating cells, are cancer cells with the capacity to self-renew as well as differentiate into the myriad of cells found within a malignancy[182]. Such cell populations have been characterized in several cancers, including glioblastomas, breast cancers, and germ cell tumors. Many somatic CSCs have been linked with chemoresistance, making them particularly interesting clinically because failure to target and eliminate CSCs would leave a patient susceptible to relapse. In contrast to CSCs in somatic cancers, EC cells cultured *in vitro* are sensitive to DNA-damaging chemotherapeutics[183]. We propose that this unique chemosensitivity of germ cell-derived CSCs plays an important role in the overall curability of testicular cancer and highlights the potential benefit of developing combination therapies that successfully target CSCs in cancers that are refractory to current treatments.

The molecular basis for the chemosensitivity of TGCTs remains elusive. One explanation for why somatic cancers are resistant to genotoxic chemotherapy is that they accumulate mutations in their DDR pathways, most notoriously in the *p53* gene[92]. p53, MDC1, 53BP1, and other DDR signals, like the early double-strand break marker γH2AX, are often constitutively active in early-stage somatic cancers[90,93]. This DDR activation can act as a tumorigenesis barrier by slowing or halting cell cycle progression in the presence of oncogene-induced DNA damage, but may also

create selective pressure to mutate the genes involved in maintaining that barrier, thus facilitating continued tumorigenesis despite genomic instability[90,92,93]. Once DDR genes have been mutated, cells no longer respond appropriately to DNA damage, including damage induced by chemotherapy drugs like cisplatin, ultimately allowing avoidance of DNA damage-induced apoptotic signals. Unlike solid tumors of somatic origin, human TGCTs do not exhibit constitutive DDR activation during early tumorigenesis[93]. This lack of DDR signaling in TGCTs may alleviate the selective pressure to mutate DDR genes, such as *Atm* and *p53*, which are mutated at unusually low frequency in TGCTs compared to somatically derived solid tumors.[92,93].

Previous studies of malignant TGCTs have focused primarily on analysis of cultured tumor cells and histological sections of human tumors, since genetically engineered mouse models of TGCT have been limited to those that develop well-differentiated teratomas with little EC and low rates of metastasis, thus being representative of the less-common pediatric TGCTs. These mouse teratoma models include a conditional knockout of the *Pten* tumor suppressor targeted to primordial germ cells[83] as well as *129-Dnd1*$^{Ter/Ter}$ mice[184], which are homozygous for a mutation in the *Dead end* gene[85]. Interestingly, these mouse models of testicular teratoma are limited to the 129 strain background; the *Dnd1*$^{Ter/Ter}$ mutation leads to BAX-mediated germ cell apoptosis rather than tumorigenesis on other strain backgrounds[185].

Susceptibility genes have been identified for mouse testicular teratomas, including the *Steel* locus, which encodes Kit ligand[186], as well as additional genes on Chromosome 19 (MOLF-Chr. 19 strain[84]); and the X chromosome[187]. Genome-wide association studies have identified similar susceptibility factors in human TGCTs, including *PTEN* and *KITLG*[188]. Inactivating *Pten* mutations in humans specifically mark the transition from TGCT precursor lesions to invasive germ cell tumors[66]. The emerging links between TGCT susceptibility and *Kitlg* and *Pten*

alterations are particularly interesting, since both are functionally related to the RAS signaling pathways that normally promote cellular proliferation. Activating mutations in the *Kras* (*K-Ras*) oncogene are very common in a variety of cancers. The most common chromosomal aberration in human TGCTs is isochromosome 12p[188], an additional copy of a region from the small arm of Chromosome 12 which contains the *Kras* gene (*Kras2*) as well as several stem cell-related genes (*Nanog, Stella*, *Cyclin D2*, *Cd9, Gdf3, Edr1*).

In order to develop a genetically engineered TGCT mouse model representative of malignant TGCTs in men, we targeted both *Kras* activation and *Pten* tumor suppressor inactivation to pre-meiotic germ cells, which led to rapid development of metastatic mixed testicular germ cell tumors in young male mice. These malignancies contained substantial populations of pluripotent EC cells with tumor-propagating activity, and these cancer stem cells were selectively depleted following chemotherapy, defining a key determinant of the remarkable chemosensitivity of TGCTs.

2.4 RESULTS

Generation of germ cell-specific Pten and Kras (gPAK) mutant mice. In order to study the remarkable responsiveness of TGCTs to DNA-damaging chemotherapeutics, we developed the first genetically engineered mouse model of malignant, metastatic TGCT by conditionally activating the *Kras* oncogene and inactivating the *Pten* tumor suppressor gene specifically in germ cells. This was accomplished using mice carrying a G12D activating mutation in the first exon of the endogenous *Kras* gene, preceded by a conditional *LoxP-Stop-LoxP* cassette (*LSL-Kras*^{G12D};[189]), as well as a conditional allele of *Pten* (*Pten*$^{flox/flox}$) in which the critical exon 5 is flanked by *LoxP* sites[190]. Recombination between adjacent *LoxP* sites, which enables *Kras*^{G12D} expression and inactivates *Pten*, was mediated by the CRE recombinase under control of a portion of the *Stra8* (stimulated by retinoic acid 8) promoter (*Stra8-Cre*[191]), which is active primarily in mitotic spermatogonia in early postnatal life and continuing throughout adulthood. Double mutant experimental animals, which we refer to as gPAK mice for germ cell-specific *Pten* and *Kras* mutant mice, harbored one conditional and one null allele of *Pten Pten*$^{flox/-}$*),* one copy of the conditional *LSL-Kras*^{G12D} allele (*Kras*$^{+/LSL}$), and the *Stra8-Cre* transgene (*Stra8-Cre*^{Tg}) on a mixed strain background. Single and double mutant mice were obtained at expected frequencies, indicating that these manipulations did not cause embryonic lethality or severe developmental abnormalities.

Figure 2.1. Combined *Pten* inactivation and oncogenic *Kras*^{G12D} activation in early germ cells results in rapid testicular tumorigenesis. A. Kaplan-Meier tumor-free survival curve depicting that 75% of *Stra8-Cre*^{Tg} *Pten*$^{flox/-}$ *Kras*$^{+/LSL}$ (*Pten/Kras* double mutant, or gPAK) mice and 17% of *Stra8-Cre*^{Tg} *Pten*$^{flox/-}$ *Kras*$^{+/+}$ (*Pten* single mutant) mice developed palpable testicular cancers by approximately 4 weeks of age. No tumors developed in *Stra8-Cre*^{Tg} *Pten*$^{+/flox}$ *Kras*$^{+/LSL}$ (*Kras* single mutant) or control mice (including Cre-negative as well as *Stra8-Cre*^{Tg} *Pten*$^{+/flox}$ *Kras*$^{+/+}$ animals). Tumor-free survival was significantly reduced in gPAK mice relative to controls (log rank test; $p=1.56 \times 10^{-6}$), but not in *Pten* single mutants despite low incidence tumor formation (log rank test; p=0.0713). B-D. High magnification images of differentiated tissues from all three germ layers within gPAK TGCTs indicative of teratomatous components, including: respiratory epithelium (B; endoderm), neural cells (C; ectoderm), and skeletal muscle (D; mesoderm). E. Low magnification image of EC within a teratocarcinoma. F. Higher magnification of EC from panel E. G. EC present in a lumbar lymph node metastasis. Scale bars represent 100 µm.

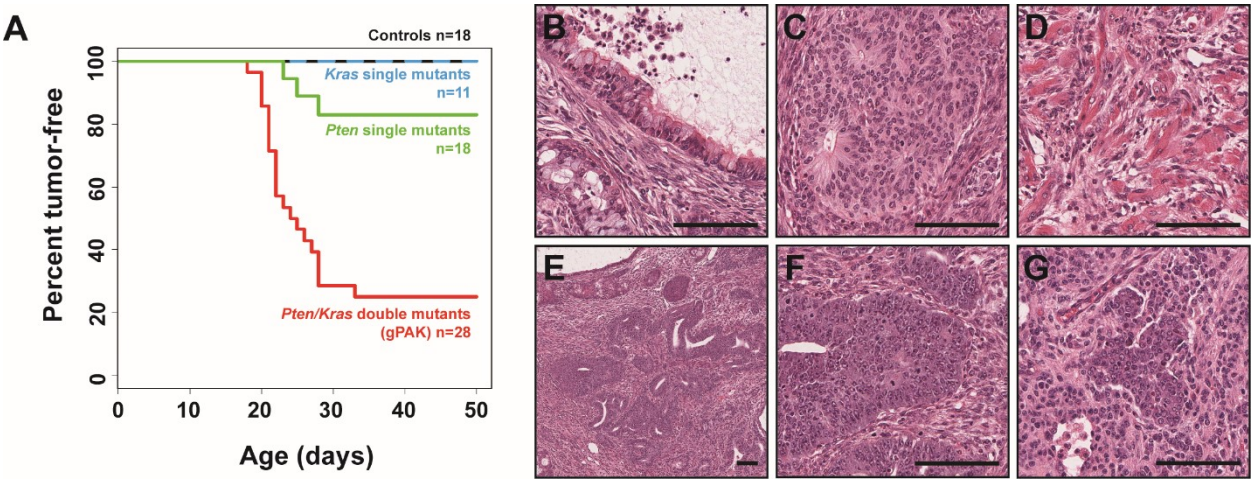

Simultaneous Stra8-Cre-driven Kras activation and Pten inactivation result in testicular germ cell tumorigenesis. While *Kras* activation or *Pten* inactivation individually rarely resulted in TGCT formation, combined *Kras* activation and *Pten* inactivation in gPAK mice led to rapid germ cell tumorigenesis, with 75% of gPAK mice succumbing to large bilateral or unilateral TGCTs with a median tumor-free survival of 24.5 days (Fig. 2.1A). Although rare spontaneous TGCTs can develop in mice, pairwise log-rank tests between gPAK mice and control animals revealed a highly significant reduction in tumor-free survival ($p=1.56x10^{-6}$), with no control mice developing tumors within the same time period.

TGCTs in these mice were characterized histologically as teratocarcinomas, which are mixed germ cell tumors (nonseminoma) containing teratomatous components, including tissues derived from all three germ layers, such as respiratory epithelium (endoderm; Fig. 2.1B), neural rosettes (ectoderm; Fig. 2.1C), and skeletal muscle (mesoderm; Fig. 2.1D), as well as highly malignant EC tissue (Fig. 2.1E,F). Metastases that histopathologically resembled the primary neoplasms were detected in at least 37% of TGCT-bearing gPAK mice at various sites, including spleen, liver, pancreas, and abdominal lymph nodes (Fig. 2.1G).

Figure 2.2. gPAK testicular germ cell tumors contain OCT4-positive cell clusters that express pluripotency markers but not SOX17 or γH2AX. Immunohistochemical staining for stem cell and proliferation markers of gPAK tumors (A-F) and *129-Dnd1*$^{Ter/Ter}$ tumors (G). A. OCT4-positive cells in gPAK TGCTs are also positive for NANOG, SSEA1, and SOX2. B. OCT4-positive regions of gPAK TGCTs are distinct from those expressing SOX17 and include proliferating, Ki67-positive cells. C. Low magnification view of OCT4-positive cell distribution in a primary gPAK TGCT. D. OCT4-positive EC within a proximal lymph node metastasis (see Fig. 1G for H&E image of a serial section from this tumor). E,F. Serial-sectioned TGCTs from 10-day old (E) or 14-day old (F) gPAK mice indicating that the DNA damage marker γH2AX is not present in early-stage gPAK TGCT cells expressing OCT4. Meiotic germ cells surrounding the neoplasm exhibit expected levels of γH2AX. G. Lack of OCT4 expression in *129-Dnd*$^{Ter/Ter}$ teratomas, which express SOX2 and SOX17. Scale bars represent 200 μm.

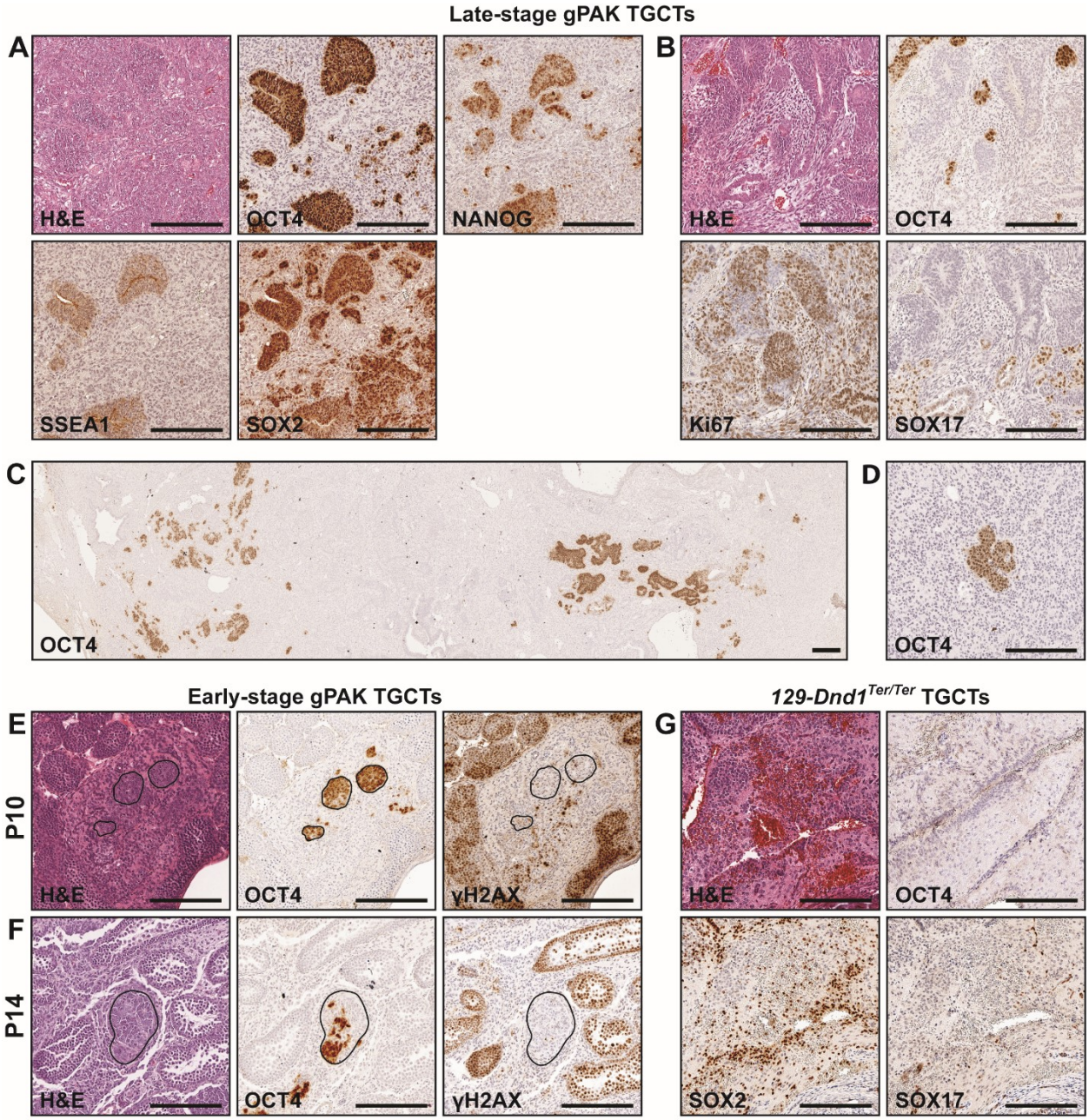
Late-stage gPAK TGCTs
A
H&E
OCT4
NANOG
SSEA1
SOX2
B
H&E
OCT4
Ki67
SOX17
C
OCT4
D
OCT4
Early-stage gPAK TGCTs
E
P10
H&E
OCT4
γH2AX
F
P14
H&E
OCT4
γH2AX
129-Dnd1Ter/Ter TGCTs
G
H&E
OCT4
SOX2
SOX17

Supplemental Figure 2.S1. OCT4 positive cells are retained in multiple sequential transplantations. H&E staining (left column) revealed similar morphology of primary gPAK TGCT (top row) compared to tumors arising from transplanted tumor cells (bottom two rows). OCT4 positive embryonal carcinoma is also present in the primary TGCT and retained in the transplanted tumors (right column).

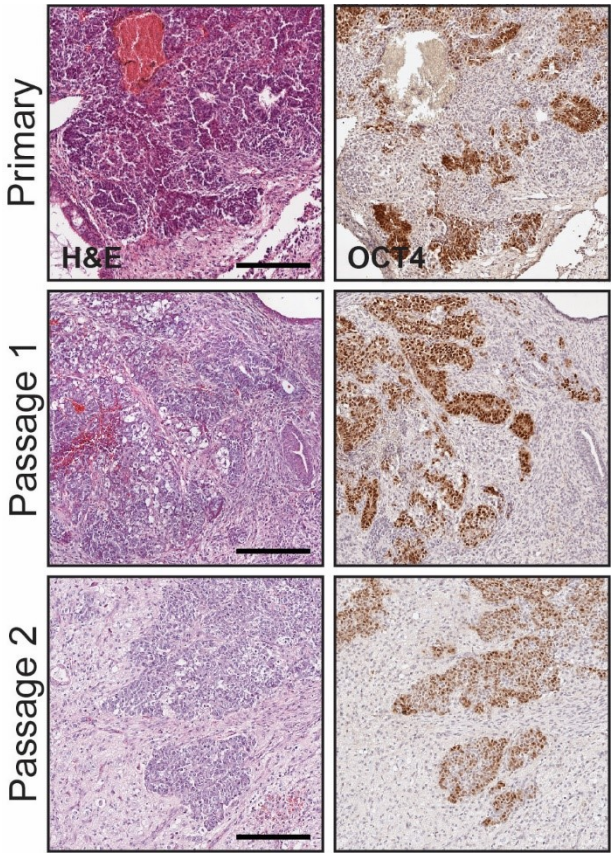

Supplemental Table 2.S1. Serial transplantation of primary tumors into immunocompromised mice. Tumors were disaggregated to single cell suspension, and 500k cells per flank were transplanted into immunocompromised mice. Cells for the primary transplant came from disaggregated primary gPAK TGCTs; cells for the secondary transplant came from a primary transplant tumor; cells for the tertiary transplant came from a secondary transplant tumor. N/D: Not done.

	Primary Transplant		Secondary Transplant		Tertiary Transplant	
	Sites Injected	Tumors formed	Sites Injected	Tumors formed	Sites Injected	Tumors formed
primary tumor 1	3	3	2	2	2	2
primary tumor 2	2	2	2	2	2	0
primary tumor 3	2	2	2	2	N/D	N/D
primary tumor 4	2	2	N/D	N/D	N/D	N/D
primary tumor 5	2	2	N/D	N/D	N/D	N/D

Supplemental Figure 2.S2. OCT4-GFP expressing gPAK cells have higher tumor propagating potential compared to OCT4-GFP negative gPAK cells. Gross images of gPAK TGCTs from mice harboring OCT4-GFP transgene (A), as well as serial sections stained for H&E, OCT4, and GFP from the same tumor (B). Tumors were disaggregated into single cells and sorted using FACS into OCT4-GFP positive and negative cell populations in (C). Both populations were injected into the flanks of immune compromised mice. OCT4-GFP positive cells were able to propagate the tumor when 20,000 cells were injected, while 40,000 – 100,000 negative cells were not sufficient for tumor propagation.

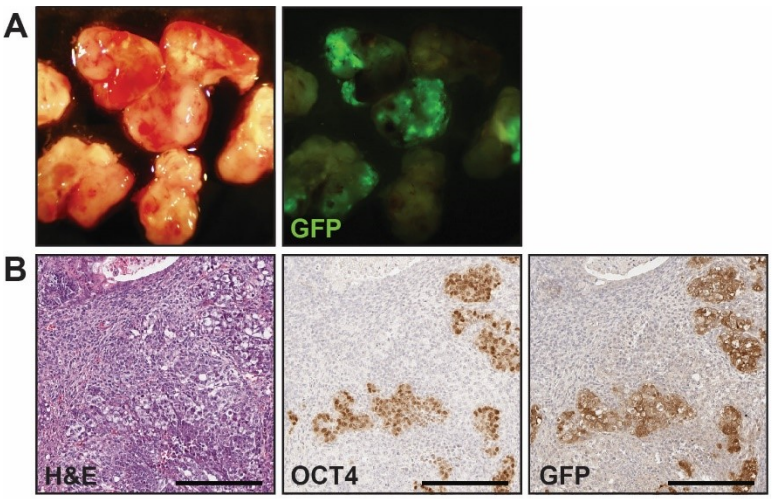

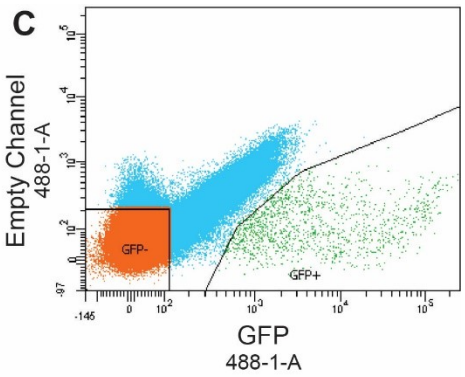

D

	Primary TGCT	Number of cells injected	Injection sites	Tumors formed	Mean Latency
GFP+	1	2×10^4	2	2	54.5
	2	2×10^4	1	1	31
GFP–	1	1×10^5	2	0	-
	2	4×10^4	1	0	-

gPAK TGCTs express OCT4 and other pluripotency markers. The OCT4 (POU5F1) transcription factor is a key regulator of pluripotency, and is one of the four Yamanaka factors that together can induce pluripotency in differentiated cells. OCT4 expression is used in human patients as a diagnostic marker for EC as well as for TGCT precursor lesions (ITGCNU/CIS)[179]. The presence of EC is the main histological feature that distinguishes teratocarcinoma from benign teratoma. To assess OCT4 expression in gPAK TGCTs, we performed OCT4 immunohistochemistry on serial sections from early- and late-stage gPAK teratocarcinomas and metastases, as well as on benign *129-Dnd1*$^{Ter/Ter}$ teratomas for comparative purposes. All gPAK tumors from adult mice contained prominent clusters of OCT4-positive cells distributed in a multifocal pattern throughout the primary tumors (Fig. 2.2A-C), as did 50% of metastases (Fig. 2.2D; proximal lymph node metastasis). Distinct clusters of OCT4-positive cells were also prominent in early-stage gPAK tumors at P10 (Fig. 2.2E) and P14 (Fig. 2.2F). In contrast, 3 out of 3 *129-Dnd1*$^{Ter/Ter}$ teratoma samples were OCT4-negative (Fig. 2.2G). In addition to the use of OCT4 in human TGCT diagnostics, an array of stem cell markers has been established for distinguishing between subtypes of TGCTs. For example, NANOG is a specific marker of EC and seminoma as well as the precursor lesion GCNIS, and is not expressed in teratomas[181], and SOX2 is expressed in EC but not in GCNIS or seminoma[180]. SOX17 is present in GCNIS, seminoma, and teratoma, but not in EC[180,192]. Similar to what has been reported for human specimens[192], *129-Dnd1*$^{Ter/Ter}$ teratomas did contain cells expressing SOX2 and SOX17, whereas EC clusters within gPAK teratocarcinomas were positive for the stem cell markers OCT4, NANOG, SSEA1, and SOX2, but were devoid of SOX17 (Fig. 2.2A,B,G). gPAK TGCTs were also highly proliferative, as indicated by Ki67 staining (Fig. 2.2B). Thus, gPAK TGCTs express the same stem cell-associated markers as human malignant TGCTs. To determine whether gPAK EC were CSCs, we first tested for tumor

propagation by transplantation into secondary recipient mice. Whereas teratomas fail to form secondary tumors upon transplantation[193], gPAK TGCTs could readily be transplanted into secondary recipient mice and serially propagated (Table 2.S1), and the resulting tumors contained $OCT4^+$ EC cells (Fig. 2.S1). These results suggested that EC, the malignant component of teratocarcinoma that is lacking in teratoma, had tumor-propagating activity, in agreement with previous studies[43]. To confirm this, we bred an OCT4-GFP transgene into the gPAK model, isolated $OCT4^+$ and $OCT4^-$ cells from the resulting tumors, and tested tumor-propagating activity by transplantation (Fig. 2.S2). The $OCT4^+$ population formed teratocarcinoma in secondary hosts whereas $OCT4^-$ cells did not, confirming that the $OCT4^+$ EC cells have tumor-propagating activity and function as CSCs.

Most pre-invasive somatic cancers express markers of DNA damage response (DDR) activation, including γH2AX, but human TGCTs interestingly lack such activation[90,92,93]. It has been proposed that a lack of constitutive DDR activation in TGCTs may reduce selective pressure to mutate key DDR genes that enforce the anti-cancer barrier, explaining why TGCTs have a much lower frequency of mutations in DDR genes like *p53* compared to somatic cancers. To test whether gPAK mouse TGCTs similarly share this property, we assessed the presence of γH2AX, one of the earliest DDR signals at DNA damage sites, in gPAK TGCTs collected at P10 and P14. Similar to what has been reported for early-stage human TGCTs[92], we found that gPAK TGCTs were devoid of γH2AX-positive cells. γH2AX expression was instead confined to the meiotic cells of the seminiferous epithelium, which are known to mount a developmentally appropriate DDR associated with meiotic events (Fig. 2.2E,F). These results provide further parallels between the gPAK TGCT model and human disease, establishing the utility of gPAK mice for investigating the link between DDR activation status and chemosensitivity in these uniquely treatable cancers.

gPAK TGCTs originate during embryonic development. The rapid development of TGCTs in gPAK mice prompted us to examine the precise timing of tumor initiation in this model. *Stra8* is a developmentally regulated gene that is expressed in early germ cells just prior to their entry into the meiotic program[194]. In mice, *Stra8* is typically expressed in spermatogonia beginning at P3. The *Stra8-Cre* transgene, used here to generate gPAK mice, contains a fragment of the *Stra8* promoter that is reported to be expressed in spermatogonial stem cells[191]. While *Stra8-Cre* has been shown to be expressed at P3 in the pre-meiotic spermatogonial cells[191], we observed substantial tumors, sometimes occupying the majority of the testis, in 3 out of 4 gPAK mice at P10, 1 out of 1 gPAK mouse at P6, and 3 out of 7 gPAK mice at P3, as well as 2 out of 5 *Pten* single mutant mice at P3, suggesting that the neoplasms originate prior to P3 (Fig. 2.3A). Furthermore, all gPAK mice that developed TGCTs did so by 33 days. Thus, in order to determine the developmental timing of *Pten/Kras* manipulation in our model, we used a CRE-responsive fluorescent reporter (B6;129S6-*Gt(ROSA)26Sor*$^{tm9(CAG\text{-}tdTomato)Hze}$/J) and assessed the precise timing of *Stra8-Cre* activity. While *Stra8-Cre* was broadly expressed in spermatogonia beginning at P3 (Fig. 2.3B), a few small clusters of *tdTomato*-positive cells (indicative of *Stra8-Cre* expression) were identifiable within the seminiferous tubules beginning at E12.5 and observed in 6 out of 6 embryos (Fig. 2.3B). No *tdTomato*-positive cells were detected prior to E12.5. From E13.5 to E18.5 the number and approximate size of the clusters remained unchanged. Beginning at P0, additional individual cells throughout the testes became *tdTomato*-positive and the clusters also expanded, resulting in staining throughout the testes by P3. Similar results were observed with a *LacZ* reporter (Fig. 2.S3). The presence of these infrequent clusters of *Cre*-expressing cells in the embryonic testis, together with our observations of only one or two tumor initiation sites per

testis in gPAK mice, is consistent with the notion that germ cell tumorigenesis in the gPAK model arises from rare, early *Stra8-Cre* expression in only a few germ cells during embryogenesis.

Figure 2.3. gPAK testicular tumors initiate during embryonic development. A. H&E staining and OCT4 IHC on serial sections from gPAK TGCTs at postnatal day 3 and 6 indicating substantial tumor growth at these early developmental stages. B. *tdTomato* expression (top) indicating *Stra8-Cre* activity in embryonic germ cells at E12.5 and E18.5 with an absence of expression at E11.5. Postnatal expression at P0 with increasingly widespread expression shown at P3. Counter stained with DAPI or tissue shown in brightfield (bottom). Scale bars represent 100 µm (A) or 75 µm (B).

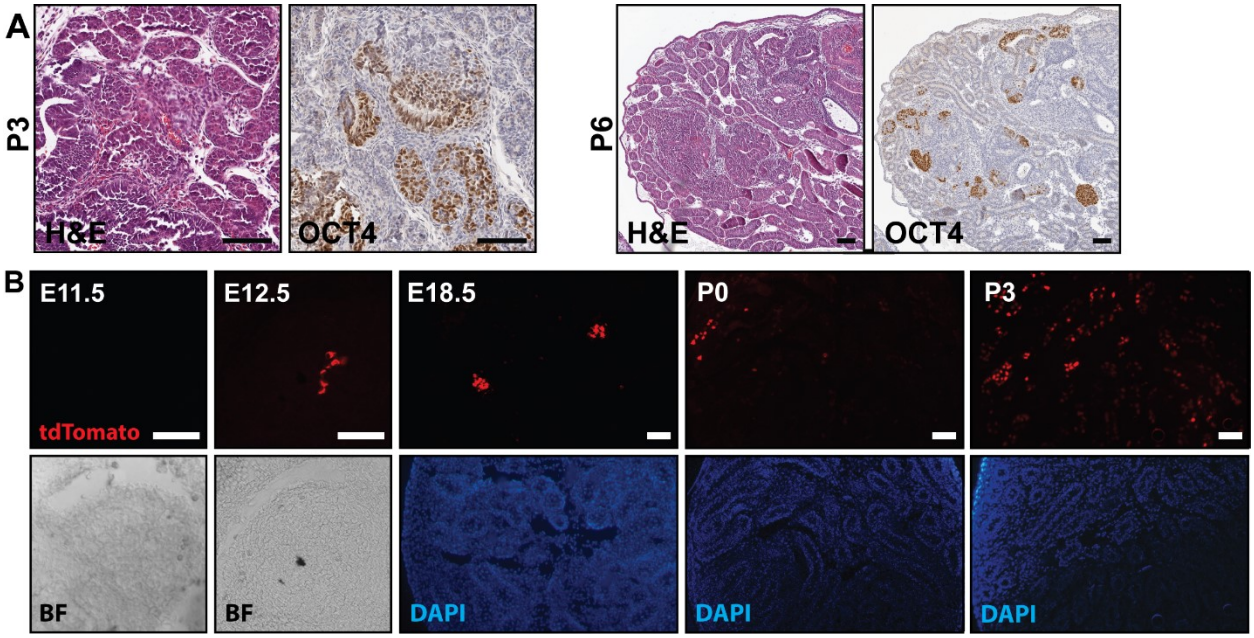

Supplemental Figure 2.S3. Lineage tracing analysis of Stra8-Cre expression in testes using a lacZ reporter. X-gal staining of fixed tissue sections highlights cells that have experienced *Stra8-Cre*-mediated excision, at postnatal day 6 (A), 3 (B), 0 (C), and embryonic day E16.5 (D) in animals of the indicated genotypes, counterstained with nuclear fast red. B-G, middle and right images. High and low magnification images of disaggregated whole-mount testes show X-gal staining in isolated clusters of cells, indicating *Stra8-Cre* activity in embryonic germ cells.

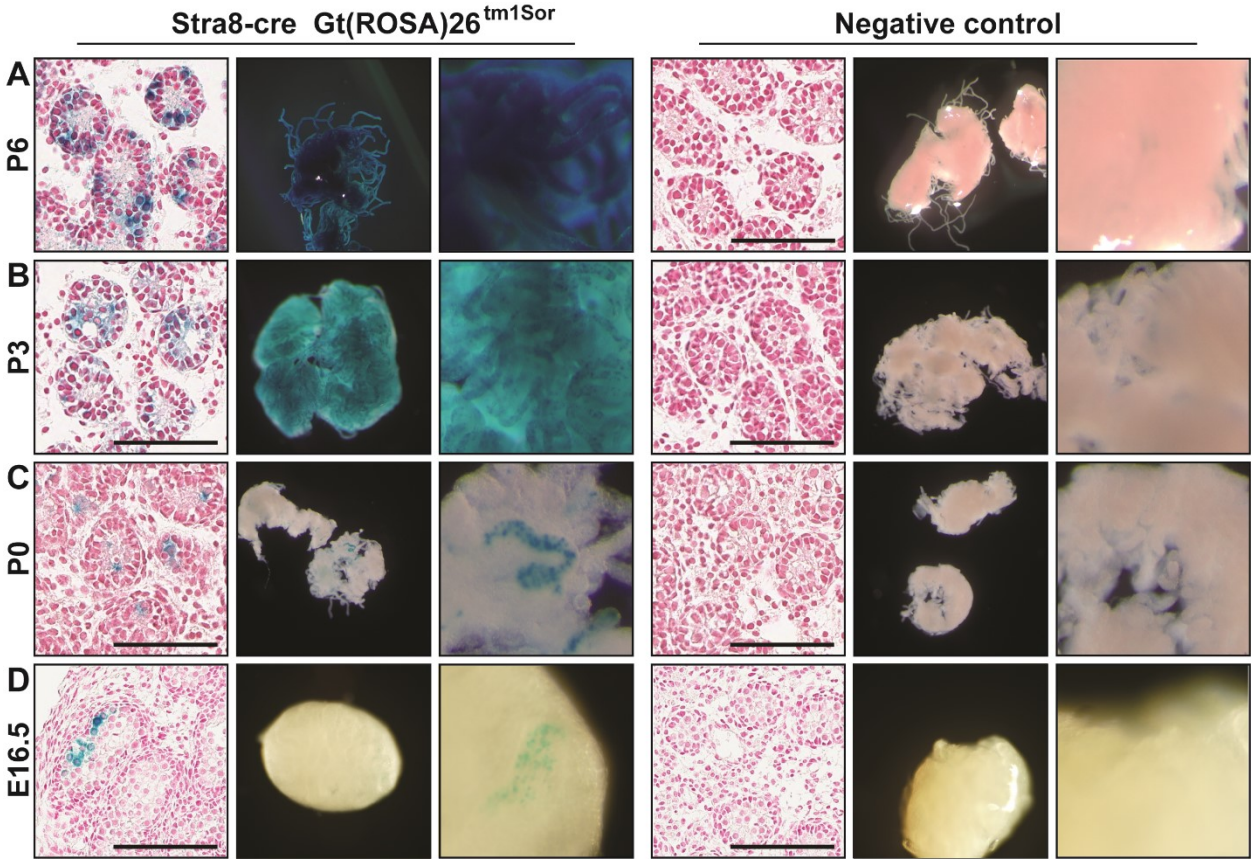

Testicular germ cells exhibit a restricted developmental window of susceptibility to oncogenic transformation. Since *Stra8-Cre* expression occurs early in embryonic testis, and gPAK tumor formation appears to initiate from rare CRE-expressing embryonic germ cells, we were interested in understanding the impact of oncogenic events occurring at higher frequency with the onset of broader CRE expression at P3. Germ cell proliferation and germ cell numbers were therefore quantified in post-natal gPAK mice without apparent neoplasms. We first assessed the cellularity of P3 gPAK testes (Fig. 2.4A) and performed IHC staining for mouse VASA homolog (MVH/Ddx4; Fig. 2.4B), which marks early germ cells[195]. No significant differences in germ cell numbers were detected at P3 in any of the tumor-free single or double mutants (Fig. 2.4C). There was, however, increased cellularity in the seminiferous epithelium of gPAK testes relative to controls at P10 and P17 (Fig. 2.4D). To measure proliferating germ cells, we performed IHC staining for the proliferation marker phospho-histone H3 (pH3). Tumor-free gPAK testes had significantly increased numbers of pH3-positive cells at P10 relative to controls ($p=0.045$), but not at P3 (Fig. 2.4E, F). Interestingly proliferation returned to normal levels by P17 in tumor-free gPAK testes and was followed by dysplastic changes in the testis as early as P30 and P40, accompanied by significantly increased germ cell death ($p<0.005$) (Fig. 2.5A, B).

By P180 the seminiferous tubules of tumor-free gPAK mice exhibited prominent degenerative changes including vacuolization, pyknotic nuclei, and multinucleate spermatid giant cells as well as increased numbers of TUNEL-positive apoptotic cells (Fig. 2.5C-E; $p=0.002$). 25% of gPAK mice never developed tumors, and these tumor-free adult gPAK mice had decreased testis size and significantly decreased numbers of epididymal sperm ($p<0.005$ and $p<0.001$, respectively; Fig. 2.5F,G). *Pten* single mutants showed increased vacuolization and degenerative changes at P180 (Fig. 2.5C), as well as increased germ cell apoptosis (Fig. 2.5D,E; $p=0.01$) and significantly

reduced sperm counts (Fig. 2.5G; $p<0.001$). That some gPAK mice experience testicular degeneration rather than tumorigenesis suggests that germ cell transformation in this model is a relatively rare cellular event, likely occurring during a restricted development window during embryogenesis when male germ cells are susceptible to malignant transformation. Subsequent widespread oncogenic events in post-natal germ cells (P3 and beyond) initially promote germ cell hyperproliferation in the postnatal testis but ultimately lead to germ cell death and impaired fertility rather than malignant transformation and tumorigenesis.

Figure 2.4. gPAK testes exhibit increased cellularity and phospho-histone H3-positive cells in early postnatal life. A-C. Comparable numbers of germ cells are detected in gPAK and control testes at P3 as shown in representative H&E staining (A) and IHC for the germ cell marker MVH (B; quantified in C). D-E. H&E (D) and phospho-histone H3 IHC staining (E) of P10 and P17 control and gPAK testes indicating increased cellularity in the seminiferous tubules of gPAK mice compared to controls at both time points. Increased numbers of mitotic cells, shown by phospho-histone H3 staining, were detected in gPAK mice relative to controls at P10 (mean +/- SD; Student's T-Test; p=0.045), but not P17. Scale bars represent 100 µm.

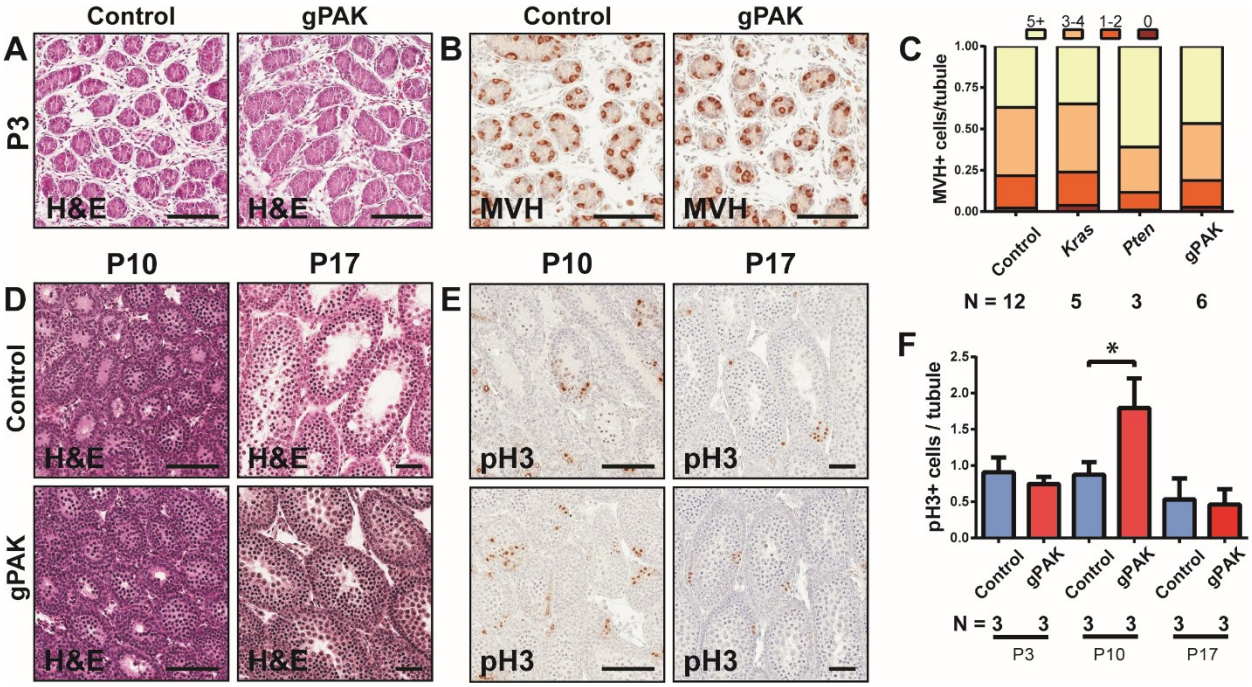

Figure 2.5. Combined *Pten* inactivation and *Kras* activation in postnatal germ cells is associated with dysplastic histological changes in the testis, reduced testis size, and reduced sperm counts in non-tumor-bearing mice. A. H&E staining of P30 and P40 gPAK testes indicates increased germ cell abnormalities compared to controls. B. gPAK testes exhibit significantly more tubules with apoptotic germ cells as measured by TUNEL staining (mean +/- SD; n=3, Student's T-test; $p<0.005$) compared to controls (n=3). C-E. 6-month old gPAK mice exhibit significant dysplastic changes in the testis and loss of sperm production. C,D. H&E and TUNEL staining 6-month old male mice indicating significant vacuolization, increased presence of multinucleate spermatid giant cells and pyknotic nuclei, decreased tubule diameter, and increased apoptosis in gPAK and *Pten* mutants (quantified in E; mean +/- SD; Student's T-Test; $p=0.002$; $p=0.01$ respectively). F,G. Graphical representations of testis weights (F) and sperm counts (G) from six-month old mice (mean +/- SEM; *$p<0.005$, Student's T-test; **$p<0.001$, Tukey-Kramer HSD test). Scale bars represent 200 μm.

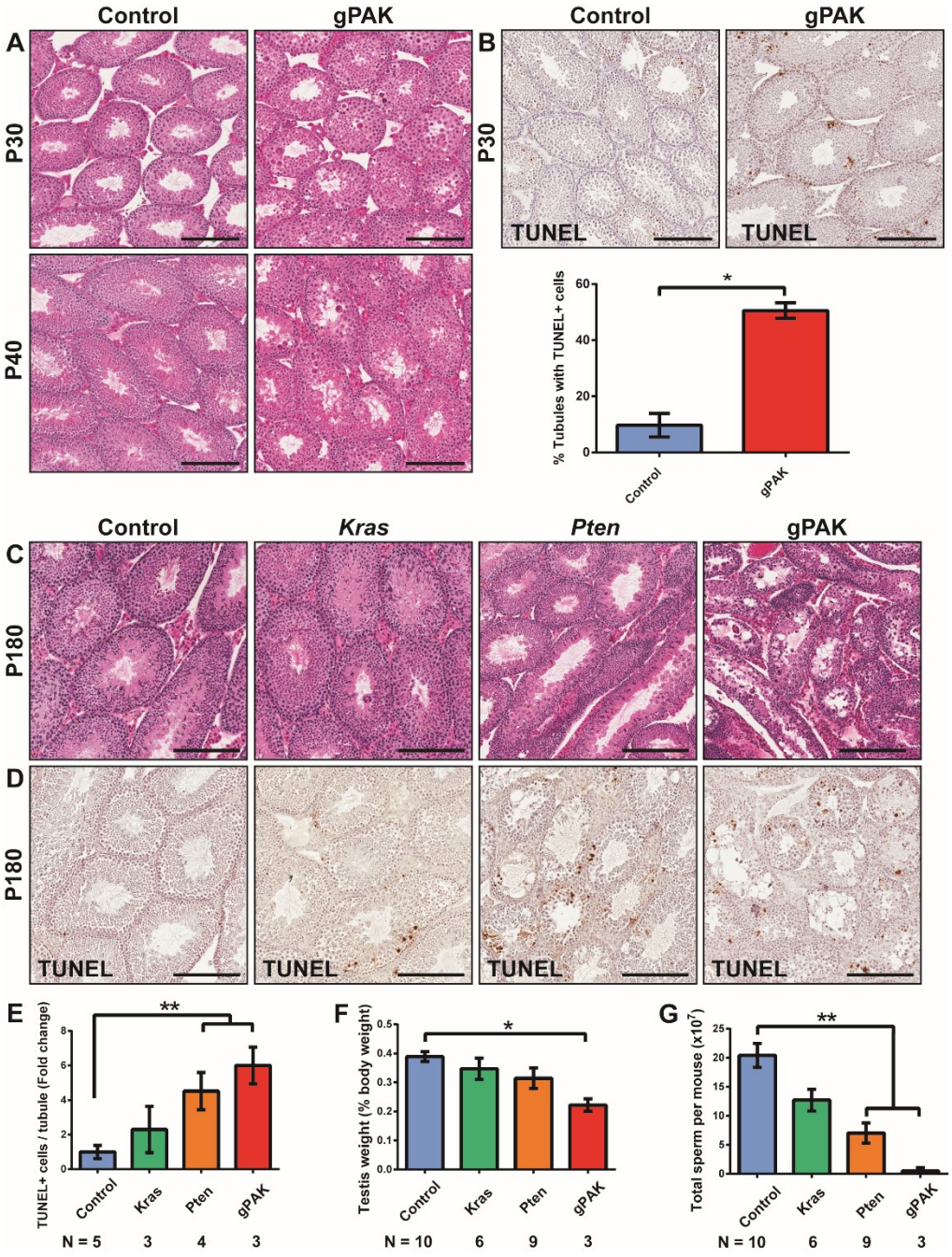
Control
gPAK
A
P30
P40
B
TUNEL
% Tubules with TUNEL+ cells
Control
gPAK
Kras
Pten
C
P180
D
E
TUNEL+ cells / tubule (Fold change)
N = 5 3 4 3
F
Testis weight (% body weight)
N = 10 6 9 3
G
Total sperm per mouse (x10^7)
N = 10 6 9 3

gPAK tumor cells are predominantly diploid and harbor recurrent DNA copy number aberrations. Aneuploidy is a distinguishing characteristic of most cancers, with karyotypes ranging from gain or loss of single chromosomes to whole-genome duplication, most often with additional chromosome rearrangements as well as copy number aberrations. Interestingly, teratomas have been reported to have normal diploid chromosome numbers[50]. To test this, and also to determine whether an absence of oncogene-induced DNA damage might underlie the lack of DNA damage response activation seen in human TGCTs[93], we performed metaphase chromosome analysis of gPAK teratocarcinoma cells as well as cells from benign 129-*Dnd1*$^{Ter/Ter}$ mouse teratomas. As shown in Fig. 2.S4, cells from both tumor types were primarily diploid, with a mean metaphase chromosome number between 38 and 42, indicating that the increased malignancy of germ cell-derived tumors in the gPAK mouse model *versus* the 129-*Dnd1*$^{Ter/Ter}$ model is not associated with gross chromosomal instability. These results are consistent with previous studies of cultured mouse teratocarcinoma cells, which found that the tumorigenic cells had near-diploid chromosome numbers[196]. Thus, if tumorigenesis is associated with oncogene-induced DNA damage in this model, the damage must be comprised of smaller-scale aberrations rather than gross changes in chromosome number or structure.

To further assess oncogene-induced genomic alterations in gPAK tumors, we analyzed copy number aberrations via array comparative genome hybridization (aCGH). As depicted in Fig. 2.S5A and summarized in Table 2.S2, gPAK tumors harbored recurrent gains and losses of copy number across the six tumors analyzed, including events on Chromosomes 1, 7, 9, 12, 14, 17, and X. A subset of the regions recurrently altered in gPAK tumors were also altered in *129-Dnd1*$^{Ter/Ter}$ tumors (Table 2.S2, right), such as loss of Chr. 7qA3 (Fig. 2.S5B), which was confirmed in both tumor types by qPCR (Fig. 2.S5C). *129-Dnd1*$^{Ter/Ter}$ teratomas additionally harbored recurrent copy

number changes on Chromosomes 4, 6, 11, and 20 that were not identified in gPAK tumors (Table 2.S3). Analysis of the altered gPAK chromosomal regions via Panther and Enrichr gene list analysis tools revealed enrichment for G-protein-coupled receptors ($p=3.45x10^{-21}$) and receptors ($p=1.79x10^{-11}$) as well as for genes regulated by particular transcription factors, most notably SOX2 (33/188 genes, $p=4.97x10^{-18}$; Table 2.S4). SOX2 is highly expressed in gPAK neoplasms, likely reflecting the cell of origin and consistent with the idea that regions of the genome containing highly expressed gene clusters are prone to replication-associated chromosome breakage[197].

Supplemental Figure 2.S4. Cells isolated from gPAK teratocarcinomas and *129-Dnd1*$^{Ter/Ter}$ teratomas contain predominantly diploid cells. A,C. Representative Giemsa-stained diploid metaphase chromosome spreads from early-passage cultured gPAK (A) and *129-Dnd1*$^{Ter/Ter}$ (C) tumor cells. B,D. Chromosome counts from gPAK (B) or *129-Dnd1*$^{Ter/Ter}$ (D) tumors, with results for three independent cultured tumors per genotype shown (N>100 per genotype). The majority of cells contained a diploid genome, while a small percentage of cells exhibited aneuploidy.

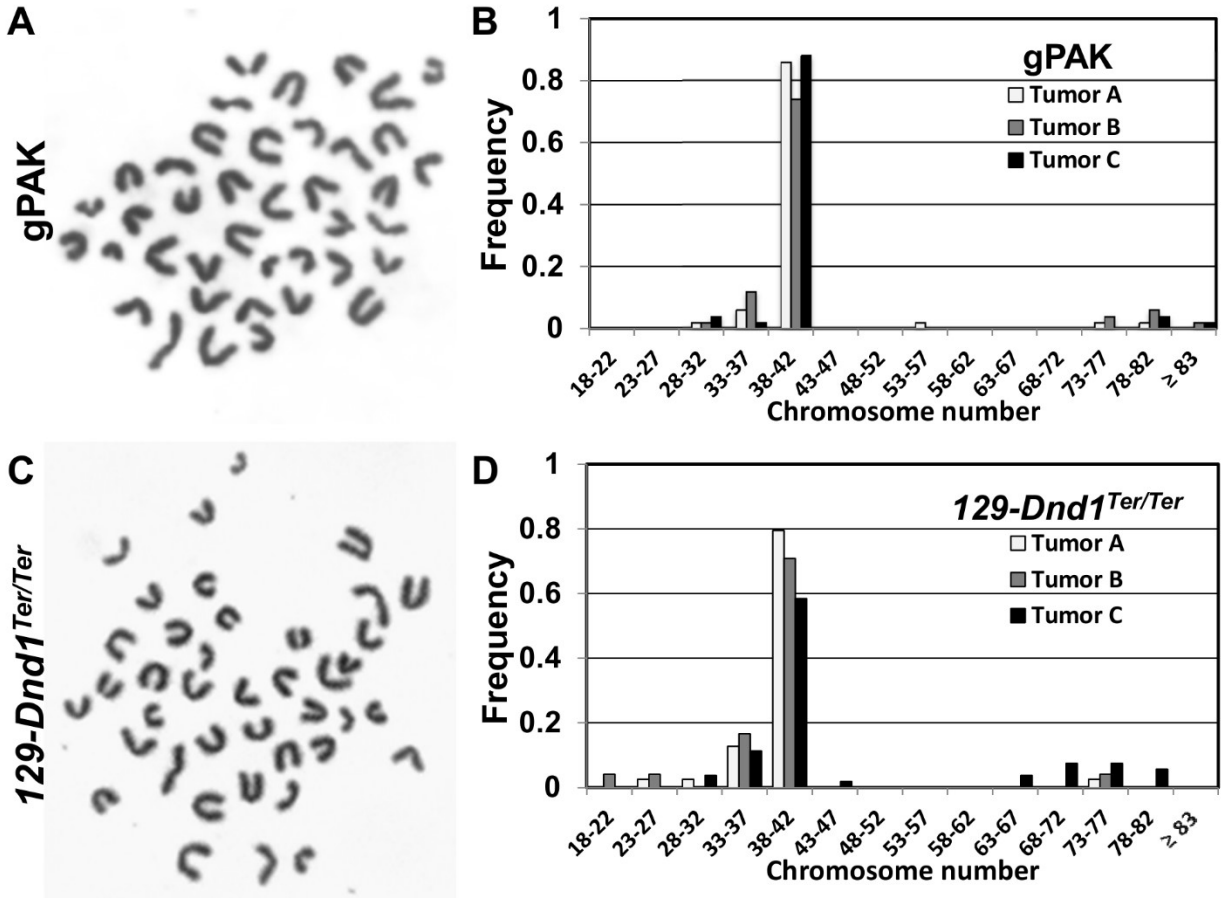

Supplemental Table 2.S2. Minimal common regions (MCRs) of high frequency DNA copy number aberration in *gPAK* tumors as identified via array CGH. Summary of minimal common regions (greater than 100kb) of copy number aberrations found in at least 50% of gPAK tumors, including chromosome band, genomic coordinates, frequency, and included genes. Regions also altered in *129-Dnd1*$^{Ter/Ter}$ tumors are indicated at the right.

		MCR coordinates							Also altered in 129-*Dnd1*$^{Ter/Ter}$			
Chromosome	Band	Start	End	Length (bases)	Frequency	Gain(+)/loss(-)	Protein-coding genes	Non-coding RNAs	Coordinates	Length (bases)	Frequency	Gain(+)/loss(-)
1	D	95,743,880	95,867,335	123,455	0.667	-		Gm22360 snRNA				
7	C	67,543,082	67,930,349	387,267	0.5	-	Lrrc28, Synm, Ttc23	Gm23233 snoRNA, Gm23844 miRNA, 4833412C05Rik lincRNA	67,819,999-68,139,999	320,000	0.5	+
7	A3	26,771,203	26,981,472	210,269	0.5	-	Cyp2g1, Cyp2a5, Cyp2a22		26,699,999-26,939,999	240,000	0.333	-
7	A3	23,982,568	24,083,728	101,160	0.5	-	Vmn1r181, V1rd19, Vmn1r183		20,659,999-24,099,999	3,440,000	0.333	-
7	A3	23,624,249	23,868,726	244,477	0.5	-	Vmn1r171, Vmn1r172, Vmn1r173, Vmn1r174, Vmn1r175, Vmn1r176, Vmn1r177		20,659,999-24,099,999	3,440,000	0.333	-
7	A3	23,426,948	23,556,303	129,355	0.5	-	Nlrp5, Vmn1r168		20,659,999-24,099,999	3,440,000	0.333	-
7	A3	22,044,359	22,231,130	186,771	0.5	-	Gm6176, Vmn1r139, Gm16451, Gm10666, Vmn1r142, Vmn1r143, Gm8653, Gm8453		20,659,999-24,099,999	3,440,000	0.333	-
7	A3	21,847,461	21,972,216	124,755	0.5	-	Gm5891		20,659,999-24,099,999	3,440,000	0.333	-
7	A3	21,173,972	21,598,501	424,529	0.5	-	Vmn1r124, Vmn1r125, Vmn1r126, Vmn1r127, Vmn1r128, Vmn1r129, Vmn1r130, Gm4172		20,659,999-24,099,999	3,440,000	0.333	-
7	A1	10,512,821	10,635,131	122,310	0.5	+	Vmn1r68, Vmn1r69, Vmn1r70					
7	A1	10,139,634	10,344,422	204,788	0.5	+	Vmn2r52, Vmn2r66					
7	A1	9,611,531	10,046,377	434,846	0.5	+	Vmn2r46, Vmn2r47, Vmn2r48, Vmn2r49					
7	A1	9,108,827	9,320,666	211,839	0.5	+	Vmn2r37					
7	A1	8,826,724	9,092,223	265,499	0.5	+	Vmn2r40, Vmn2r39					
7	A1	8,328,453	8,805,401	476,948	0.5	+	Vmn2r44, Vmn2r45					
7	A1	7,787,897	7,949,658	161,761	0.5	+	Vmn2r35, Vmn2r36					
7	A1	7,260,763	7,565,119	304,356	0.5	+	Vmn2r30, Vmn2r31, Vmn2r32, Vmn2r33	Gm3912 unclassified				
9	A5.3	46,679,538	46,966,815	287,277	0.5	+						
12	D3	89,294,409	89,406,696	112,287	0.5	-	Nrxn3	AC171335 miRNA				
14	C2	53,413,811	53,531,288	117,477	0.833	-	Trav4-2, Trav6-3, Trav7-3, Trav6-4, Trav7-4, Trav8-1, Trav6-5, Trav9-1, Trav10, Trav6-6, Trav11		50,019,999-54,459,999	4,440,000	0.333	+
14	D2	69,873,924	69,984,940	111,016	0.5	-	Pebp4					
14	C2	53,727,564	53,842,263	114,699	0.5	-	Trav16, Trav13-4-dv7, Trav14-3, Trav3-4, B230359F08Rik, Trav17, Trav18		50,019,999-54,459,999	4,440,000	0.333	+
14	A1	8,195,205	8,372,762	177,557	0.5	-	Kctd6, Acox2, Fam107a, Oit1					
14	A1	7,823,764	8,164,652	340,888	0.5	-	Flnb, Dnase1l3, Abhd6, Rpp14, Pxk					
14	A1	7,404,011	7,589,842	185,831	0.5	-	Gm3755, Gm3752, Gm3558, Gm10338	4933406F09Rik unclassified				
14	A1	6,671,865	7,230,851	558,986	0.5	-	Gm8050, Gm3636, Gm3642, Gm3667, Gm6356, Gm10406, Gm3685, Gm3696, Gm6676, Gm3512, Gm16434	Gm26680 unclassified				
14	A1	6,358,639	6,583,765	225,126	0.5	-	Gm16440, Gm3591, Gm3594, Gm8356					
14	A1	5,893,387	6,215,520	322,133	0.5	-	Gm3248, Gm3453, Gm8206, Gm3468, Gm6337, Gm3411, Gm3476, Gm21560					
14	A1	5,611,953	5,768,034	156,081	0.5	-	Gm8265, Gm9603, Gm3373					
14	A1	5,240,585	5,373,218	132,633	0.5	-	Gm3526, Gm3542					
14	A1	4,958,987	5,109,957	150,970	0.5	-	Gm8297, Gm3298, 4930555G01Rik, Gm8281					
14	A1	4,543,128	4,804,004	260,876	0.5	-	Gm26655, Gm3047, Gm8159, Gm3239, Gm7876, Gm3252, Gm9602	Gm26655 unclassified				
14	A1	3,921,002	4,275,370	354,368	0.5	-	Gm3029, Gm3095, Gm3099, Gm5796, Gm3115, Gm8108, Gm3127, Gm2974, Gm3138					
14	A1	3,316,290	3,856,591	540,301	0.5	-	Gm2956, Gm10413, Gm10409, Gm3005, Gm10408, Gm3012, Gm3020, Gm3043, Gm3002, Gm3033					
14	A1	3,004,892	3,270,616	265,724	0.5	-	Gm2888, Gm2897, Gm10340, Gm17188, Gm5795, D830030K20Rik					
17	A1	6,228,664	6,886,236	657,572	0.667	-	Tulp4, Tmem181a, Dynlt1a, Dynlt1b, Dynlt1c, Dynlt1f, Sytl3, Ezr	Gm2885 lincRNA	6,259,999-6,779,999	520,000	0.333	-
X	A3.1	31,685,457	32,185,861	500,404	0.5	-	Gm21608, Gm21637, Gm21645		28,699,999-32,899,999; 4,419,999-28,659,999	4,200,000; 24,240,000	0.333; 0.333	-; +
X	A3.1	31,291,210	31,609,280	318,070	0.5	-	Gm2784, Gm2777, Gm21883		28,699,999-32,899,999; 4,419,999-28,659,999	4,200,000; 24,240,000	0.333; 0.333	-; +
X	A3.1	30,212,689	31,243,243	1,030,554	0.5	-	Gm14632, Gm10487, Gm21447	Gm7437 lincRNA, Gm14974 lincRNA	28,699,999-32,899,999; 4,419,999-28,659,999	4,200,000; 24,240,000	0.333; 0.333	-; +
X	A1.1	4,668,783	4,940,406	271,623	0.5	-	Gm3750		3,019,999-4,899,999	1,880,000	0.5	-
X	A1.1	3,030,592	4,235,784	1,205,192	0.5	-	Gm21950, Gm21364, Gm14346, Gm14345, Gm14351, Gm3701, Gm3706, Gm14347		3,019,999-4,899,999	1,880,000	0.5	-

Supplemental Figure 2.S5. Array comparative genome hybridization (aCGH) analysis of gPAK and *129-Dnd1*$^{Ter/Ter}$ tumors reveals recurrent copy number aberrations (CNAs). A. Karyotype depiction of copy number aberrations in six gPAK teratocarcinomas compared to control spleen tissue via aCGH using Roche Nimblegen mouse 3x720k whole-genome tiling arrays, with amplifications shown as green lines to the right of each chromosome and deletions shown as red lines to the left. B. Segment of mouse Chromosome 7 (7qA3) with copy number aberrations in both gPAK and *129-Dnd1*$^{Ter/Ter}$ tumors. C. qPCR validation of Chr. 7qA3 deletion in both gPAK and *129-Dnd1*$^{Ter/Ter}$ tumors.

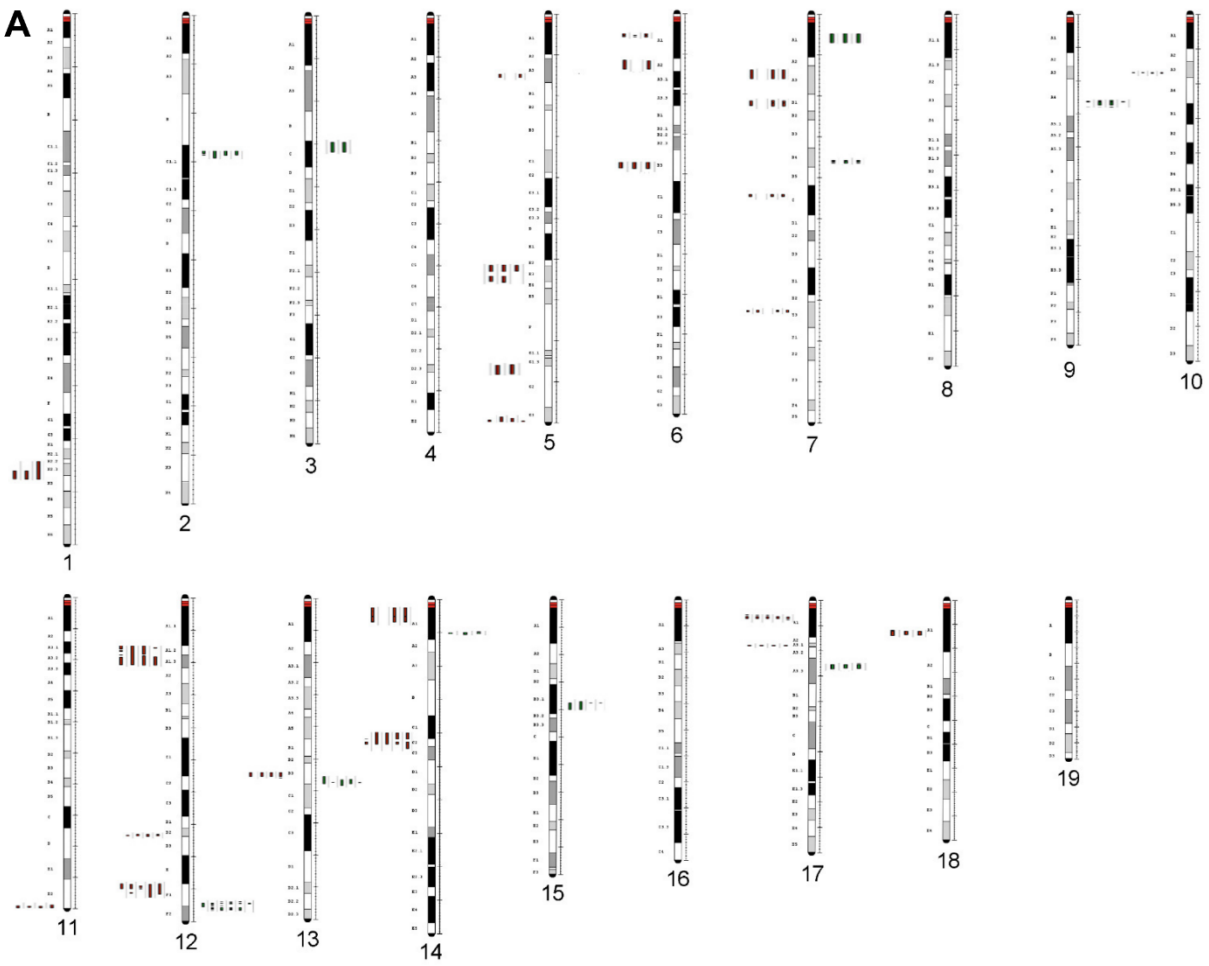
A
1
2
3
4
5
6
7
8
9
10
11
12
13
14
15
16
17
18
19

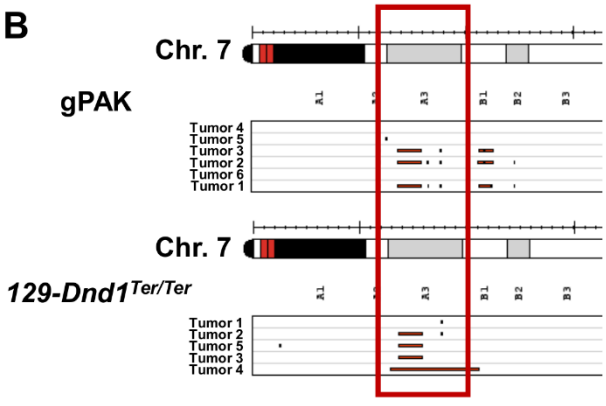
B
Chr. 7
gPAK
Tumor 4
Tumor 5
Tumor 3
Tumor 2
Tumor 6
Tumor 1
Chr. 7
129-Dnd1Ter/Ter
Tumor 1
Tumor 2
Tumor 5
Tumor 3
Tumor 4

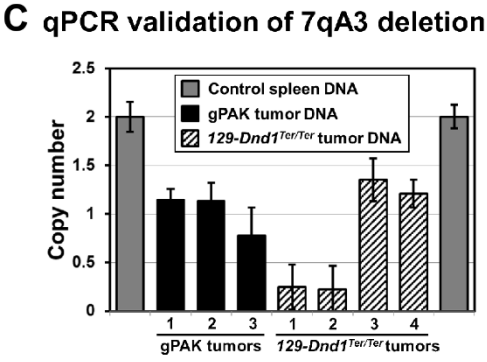
C qPCR validation of 7qA3 deletion
Control spleen DNA
gPAK tumor DNA
129-Dnd1Ter/Ter tumor DNA
Copy number
2.5
2
1.5
1
0.5
0
1 2 3 1 2 3 4
gPAK tumors
129-Dnd1Ter/Ter tumors

Supplemental Table 2.S3. Minimal common regions (MCRs) of high frequency DNA copy number aberration in *129-Dnd1*$^{Ter/Ter}$ tumors as identified via array CGH. Summary of minimal common regions (greater than 100kb) of copy number aberrations found in at least 50% of *129-Dnd1*$^{Ter/Ter}$ tumors, including chromosome band, genomic coordinates, frequency, and included genes.

		MCR coordinates						
Chromosome	Band	Start	End	Length (bases)	Frequency	Gain(+)/loss(-)	Protein-coding genes	Non-coding RNAs
4	A5	42,379,999	42,659,999	280,000	0.5	+	Gm21586, Gm10597, Gm3883, Gm2163, Gm13298, Gm10592, Gm10591, Gm2564, Ccl27b, Il11ra2	
4	A5	41,859,999	42,099,999	240,000	0.5	+	Gm21966, Gm21541, Gm29878, Gm20938, Gm21093, Gm10597, Gm21968, Gm393	
4	E1	143,099,999	144,419,999	1,320,000	0.5	+	Prdm2, Pdpn, Lrrc38, Pramel1, Pramef8, Oog4	Gm22039 snoRNA, Gm26313 misc RNA
4		112,219,999	113,939,999	1,720,000	0.5	+	Gm13043, Gm13040, BC080695, Gm13057, Gm13083, Gm13088, Gm13089, Gm13078, Gm13023, Gm13084, Gm13103, Pramef6, Gm13109, Gm13101, Pramef17, Pramel4, Gm13102, Oog3, Oog2, C87977, Pramel5, Gm13128, Gm13119, Gm13125, Pramef12, 1700012P22Rik	
6	F3	129,939,999	130,579,999	640,000	0.5	+	Klra6, Klra4, Klra8, Klra9, Klra7, Klra10, Klra13, Klra3, Klra1	Gm22555 snRNA, Gm24676 snRNA, Gm22621 snRNA, Gm24712 snRNA, Gm23552 snRNA Gm24072 snRNA
7	E1	92,099,999	94,299,999	2,200,000	0.5	+	Dlg2, Ccdc90b, Ankrd42, Pcf11, Rab30, 4632434I11Rik, Prcp, Gm9934, Gm15501	Gm22734 miRNA, Gm26944 lincRNA, Gm26981 lincRNA, Gm26862 lincRNA, Gm25860 snoRNA
7	C	67,819,999	68,139,999	320,000	0.5	+	Igf1r	
7	B5-C	60,099,999	60,979,999	880,000	0.5	+	Gm7367	
7	B1	32,419,999	34,259,999	1,840,000	0.5	+	Scgb1b29, Scgb2b15, Scgb2b17, Scgb1b19, Scgb2b20, Scgb1b21, Scgb2b24, Scgb1b24 , Scgb2b26, Scgb2b27, Scgb1b27, Scgb1b30, Wtip, Uba2, Pdcd2l, Gpi1, 4931406P16Rik, Gm12758, Gm6096	Gm24766 miRNA, Gm25817 miRNA, Gm12763 lincRNA, Gm26443 miRNA, Gm26762 lincRNA
11	B4	71,019,999	71,139,999	120,000	0.5	+	Nlrp1a	6330403K07Rik lincRNA
12	F2	115,939,999	116,779,999	840,000	0.5	+	Ighv1, Zfp386,Vipr2, Gm20658, Wdr60, Gm11027, Esyt2, Ncapg2, Ptpm2	Gm23732 snRNA, Gm23190 miRNA, Gm25112 snRNA, Gm24354 snRNA
12	F2	114,979,999	115,539,999	560,000	0.5	+	Ighv1-47, Ighv8-4, Ighv1-49, Ighv8-5, Ighv1-50, Ighv1-52, Ighv1-53, Ighv8-6, Ighv1-54, Ighv1-55, Ighv1-56, Ighv8-8, Ighv1-58, Ighv1-59, Ighv1-61, Ighv1-62-1, Ighv1-62-2, Ighv1-62-3, Ighv8-9, Ighv1-63, Ighv1-64	AC164609.1 miRNA
12	E	104,979,999	105,179,999	200,000	0.5	+	Glrx5, Tcl1b2, Tcl1b5	Scarma13 snoRNA
20	A1.1	3,019,999	4,899,999	1,880,000	0.5	-	Gm21950, Gm21364, Gm14346, Gm14345, Gm14351, Gm3701, Gm3706, Gm14347, Gm10921, Gm10922, Gm3750	
20	F5	166,419,999	166,644,267	224,268	0.5	-	Ofd1, Trappc2, Rab9, Tceanc, Egfl6	Gm15226 lincRNA

Supplemental Table 2.S4. gPAK MCRs are enriched for genes regulated by SOX2. Summary table from Enrichr analysis indicating genes from gPAK MCRs enriched for particular transcription factors, most notably SOX2.

Transcription factor	P-value	# genes from gPAK MCRs (total regulated genes)	Genes
SOX2	4.97E-18	33/188 (1878)	GM3750;4930555G01RIK;GM10666;VMN1R125;VMN1R128;VMN1R124;VMN1R143;VMN1R142;VMN1R139; VMN1R130;VMN1R129;VMN1R183;VMN1R171;VMN1R174;VMN1R175;VMN1R173;VMN1R176;GM14345; GM14347;GM14346;GM16451;VMN1R68;VMN1R69;VMN2R30;VMN2R35;VMN2R39;V1RD19;VMN2R66;DYNLT1F; DYNLT1A; DYNLT1C;DYNLT1B;PEBP4
CBEPB	7.65E-17	41/188 (3275)	NLRP5;VMN1R126;VMN1R125;VMN1R128;VMN1R127;VMN1R124;VMN1R143;VMN1R142;VMN1R139;VMN1R130; VMN1R129;VMN1R168;VMN1R181;VMN1R183;VMN1R171;VMN1R174;VMN1R175;VMN1R172;VMN1R173; VMN1R177;CYP2A22;TTC23;PEBP4;LRRC28;4930555G01RIK;CYP2G1;GM10666;GM16451;VMN2R30;VMN2R31; VMN2R33;VMN2R35;VMN2R36;VMN2R37;VMN2R39;VMN2R49;VMN2R47;VMN2R45;VMN2R46;VMN2R66;NRXN3
ETV4	1.63E-13	28/188 (1773)	CYP2G1;VMN1R128;GM4172;VMN1R183;VMN1R171;VMN1R175;VMN1R176;GM2897;GM3696;GM10406; VMN1R68;VMN2R30;VMN2R31;VMN2R32;VMN2R33;VMN2R35;VMN2R36;VMN2R39;VMN2R40;VMN2R49; VMN2R47;VMN2R48;VMN2R45;VMN2R46;GM8453;VMN2R66;NRXN3;PEBP4
POU2F1	4.95E-12	26/188 (1735)	GM14632;LRRC28;GM3750;VMN1R126;GM2897;GM14351;GM14345;GM14347;GM14346;GM3696;GM10406; VMN1R68;VMN1R69;TTC23;VMN1R70;VMN2R30;VMN2R35;VMN2R37;VMN2R49;VMN2R47;VMN2R45;V1RD19; DYNLT1F;DYNLT1C;DYNLT1B;GM10487
POU2F2	4.32E-08	21/188 (1754)	GM14632;LRRC28;GM2897;GM14351;GM14345;GM14347;GM14346;GM3696;GM10406;VMN1R69;TTC23;VMN1R70; VMN2R30;VMN2R37;VMN2R47;V1RD19;DYNLT1F;DYNLT1A;DYNLT1C;DYNLT1B;GM10487
SREBF1	8.34E-07	19/188 (1735)	GM10666;VMN1R126;VMN1R125;VMN1R127;VMN1R124;GM4172;VMN1R143;VMN1R142;VMN1R139;VMN1R130; GM5891;VMN1R68;VMN2R44;V1RD19;GM8453;DYNLT1F;DYNLT1C;DYNLT1B;SYNM
SRF	5.28E-06	18/188 (1782)	KCTD6;GM3750;VMN1R128;GM4172;VMN1R143;GM14351;GM14345;GM14347;GM14346;VMN1R68;VMN1R69; VMN2R31;VMN2R33;VMN2R52;TULP4;GM8453;D830030K20RIK;VMN2R66
TBP	4.82E-06	25/188 (3182)	VMN1R125;VMN1R128;VMN1R124;GM4172;VMN1R143;VMN1R139;VMN1R130;VMN1R171;VMN1R174; VMN1R172;GM5891;D830030K20RIK;DYNLT1F;DYNLT1C;DYNLT1B;PEBP4;4930555G01RIK;SYTL3;VMN2R30; VMN2R31;VMN2R33;VMN2R35;VMN2R47;VMN2R46;VMN2R66
NFYB	1.65E-05	17/188 (1748)	GM10666;VMN1R126;VMN1R125;VMN1R128;VMN1R127;VMN1R124;GM4172;VMN1R143;VMN1R142;VMN1R139; VMN1R130;GM5891;GM16451;VMN1R68;VMN2R44;V1RD19;GM8453
CPEB1	1.65E-05	17/188 (1748)	GM10666;VMN1R126;VMN1R125;VMN1R128;VMN1R127;VMN1R124;GM4172;VMN1R143;VMN1R142;VMN1R139; VMN1R130;GM5891;GM16451;VMN1R68;VMN2R44;V1RD19;GM8453
RBPJ	5.74E-05	16/188 (1735)	GM10666;VMN1R125;VMN1R128;VMN1R127;GM4172;VMN1R143;VMN1R142;VMN1R139;VMN1R130;VMN1R129; VMN1R181;VMN1R172;GM16451;VMN1R70;V1RD19;GM8453
NFYA	6.27E-05	16/188 (1748)	GM10666;VMN1R126;VMN1R125;VMN1R128;VMN1R127;VMN1R124;GM4172;VMN1R143;VMN1R142;VMN1R139; VMN1R130;GM5891;VMN1R68;VMN2R44;V1RD19;GM8453
FOS	1.73E-04	15/188 (1708)	ACOX2;VMN1R129;GM16451;VMN2R30;VMN2R31;VMN2R33;VMN2R36;VMN2R40;VMN2R49;VMN2R47; VMN2R48;VMN2R46;DYNLT1B;FAM107A;SYNM
CBEPA	2.44E-04	15/188 (1764)	GM14632;CYP2G1;GM10666;GM4172;VMN1R129;VMN1R174;VMN1R175;VMN1R176;VMN1R177;GM14347; GM16451;VMN1R68;VMN2R30;VMN2R46;GM10487
USF1	3.03E-04	12/188 (1219)	SYTL3;VMN2R30;VMN2R31;VMN2R32;VMN2R33;VMN2R37;VMN2R39;VMN2R44;VMN2R49;VMN2R47;VMN2R45; VMN2R46
IRF2	5.74E-04	14/188 (1706)	NLRP5;GM10666;GM4172;PXK;VMN1R129;VMN1R181;GM16451;VMN2R32;VMN2R40;V1RD19;DYNLT1F;DYNLT1C; DYNLT1B;NRXN3
GATA1	6.77E-04	14/188 (1735)	ABHD6;GM10666;VMN1R126;VMN1R127;GM4172;VMN1R142;VMN1R168;VMN1R171;VMN1R174;VMN1R175; CYP2A22;V1RD19;NRXN3;PEBP4
NR2F1	1.04E-03	10/188 (1021)	GM16451;SYTL3;GM10666;CYP2A5;VMN1R126;VMN1R128;VMN1R143;VMN1R130;VMN1R129;DYNLT1A
RORB	1.03E-03	10/188 (1020)	GM16451;SYTL3;GM10666;CYP2A5;VMN1R126;VMN1R128;VMN1R143;VMN1R130;VMN1R129;DYNLT1A
SOX10	2.56E-03	6/188 (451)	ACOX2;GM14351;GM14345;GM14347;GM14346;GM3750
STAT5B	2.01E-03	13/188 (1729)	GM3750;NLRP5;VMN1R181;VMN1R174;GM14351;GM14345;GM14346;VMN2R37;OIT1;DYNLT1A;NRXN3;PEBP4; FAM107A
JUND	2.40E-03	13/188 (1764)	FLNB;VMN1R176;VMN1R68;VMN1R69;VMN2R32;VMN2R36;VMN2R37;VMN2R40;VMN2R48;VMN2R45;DYNLT1F; DYNLT1A;DYNLT1B
SPI1	4.56E-03	12/188 (1680)	ABHD6;GM3750;SYTL3;VMN1R143;VMN1R130;CYP2A22;GM2897;GM3696;GM10406;VMN2R32;VMN2R49;PEBP4
HMGA1	1.60E-02	11/188 (1748)	KCTD6;CYP2G1;VMN1R175;VMN1R176;VMN1R69;VMN2R30;VMN2R37;VMN2R49;VMN2R47;VMN2R48;VMN2R66
	4.66E-02	3/188 (264)	TTC23;LRRC28;FAM107A

gPAK TGCTs are sensitive to chemotherapy. TGCTs in humans are exquisitely sensitive to the DNA-damaging chemotherapeutic cisplatin, which is used routinely as a frontline drug in combination with bleomycin and etoposide. To determine whether gPAK TGCTs were also sensitive to cisplatin, gPAK mice were treated intraperitoneally with either two 6 mg/kg cisplatin doses, or a full course of bleomycin/etoposide/cisplatin (BEP) at doses comparable to those used in humans. Cisplatin-treated gPAK mice lived significantly longer than untreated gPAK mice ($p=0.0192$), with a median survival of 36 days for untreated mice and 49 days for cisplatin-treated mice (Fig. 2.6A). Two cisplatin doses were not sufficient to eradicate the tumors, and both treated and untreated mice ultimately reached humane endpoint criteria; however, primary tumor volume at endpoint was significantly lower in cisplatin-treated gPAK mice than in untreated animals ($p=0.004$; Fig. 2.6B). gPAK mice were even more responsive to BEP, with several mice surviving to an arbitrary 100 day end point (median survival of 87.5 days; $p<0.001$) and primary tumor volume significantly reduced ($p=0.002$). Thus, gPAK murine TGCTs, similar to their human counterparts, can be effectively treated with chemotherapy, even in the absence of the surgical interventions that typically accompany chemotherapy in humans.

Figure 2.6. Genotoxic chemotherapeutic treatment of gPAK mice prolongs survival and selectively depletes OCT4-positive cells. A. Kaplan-Meier survival curve indicating prolonged survival of gPAK mice following two intraperitoneal doses of 6 mg/kg cisplatin, or a 4 week regiment of bleomycin, etoposide, and cisplatin (BEP). The median survival of cisplatin-treated mice was 13 days greater than in untreated mice (N=10 and 8, respectively; log-rank test; $p<0.02$) while the median survival of BEP-treated mice was 58 days longer than in untreated mice (N=5; log-rank test; $p<0.0005$). B. Primary tumor volume measured at endpoint and was significantly reduced in cisplatin-treated gPAK mice (N=9; mean +/- SEM; Student's T-Test; $p=0.007$) and BEP-treated mice (N=4; mean +/- SEM; Student's T-Test; $p<0.002$). C. Representative images of OCT4 IHC on primary TGCTs from untreated, cisplatin-treated, and BEP-treated gPAK mice (see Fig. S6 for representative SOX17 images). Scale bars represent 200 μm. D. Quantification of OCT4-positive (Student's T-Test; $p=0.02$ (cisplatin); $p<0.002$ (BEP)) and E. SOX17-positive (Student's T-Test; $p=0.098$ (cisplatin); $p=0.67$ (BEP)) cells in untreated, cisplatin-treated, and BEP-treated gPAK TGCTs, counted using Image-J.

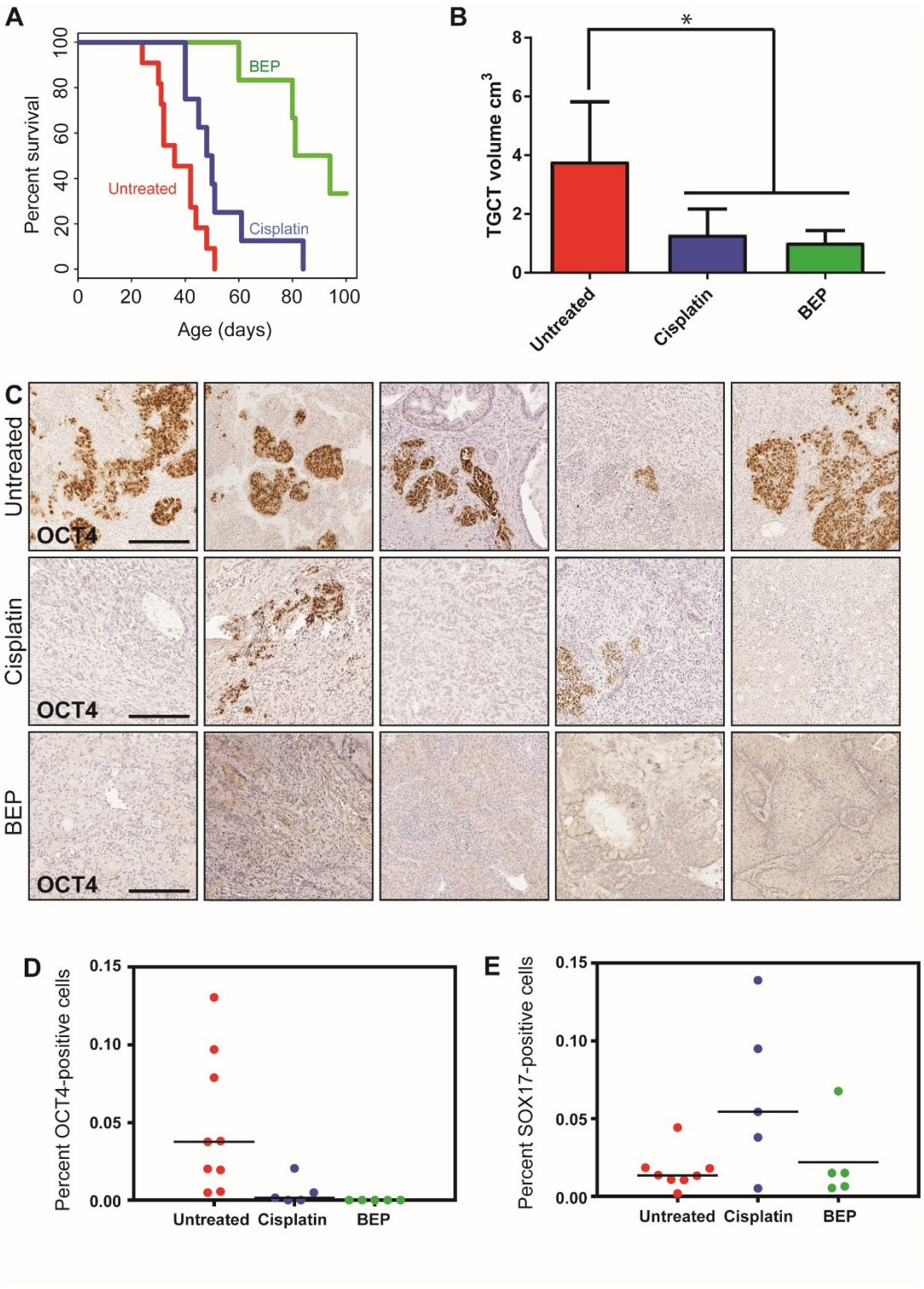
A
Percent survival
Age (days)
BEP
Untreated
Cisplatin
B
TGCT volume cm3
*
Untreated
Cisplatin
BEP
C
Untreated
Cisplatin
BEP
OCT4
D
Percent OCT4-positive cells
Untreated
Cisplatin
BEP
E
Percent SOX17-positive cells
Untreated
Cisplatin
BEP

Supplemental Figure 2.S6. SOX17-positive cells are not depleted in gPAK tumors following genotoxic treatment. Representative images of SOX17 IHC from cisplatin-treated, BEP-treated and untreated gPAK tumors from the same experiment shown in Fig. 6 (see quantification in Fig. 6E).

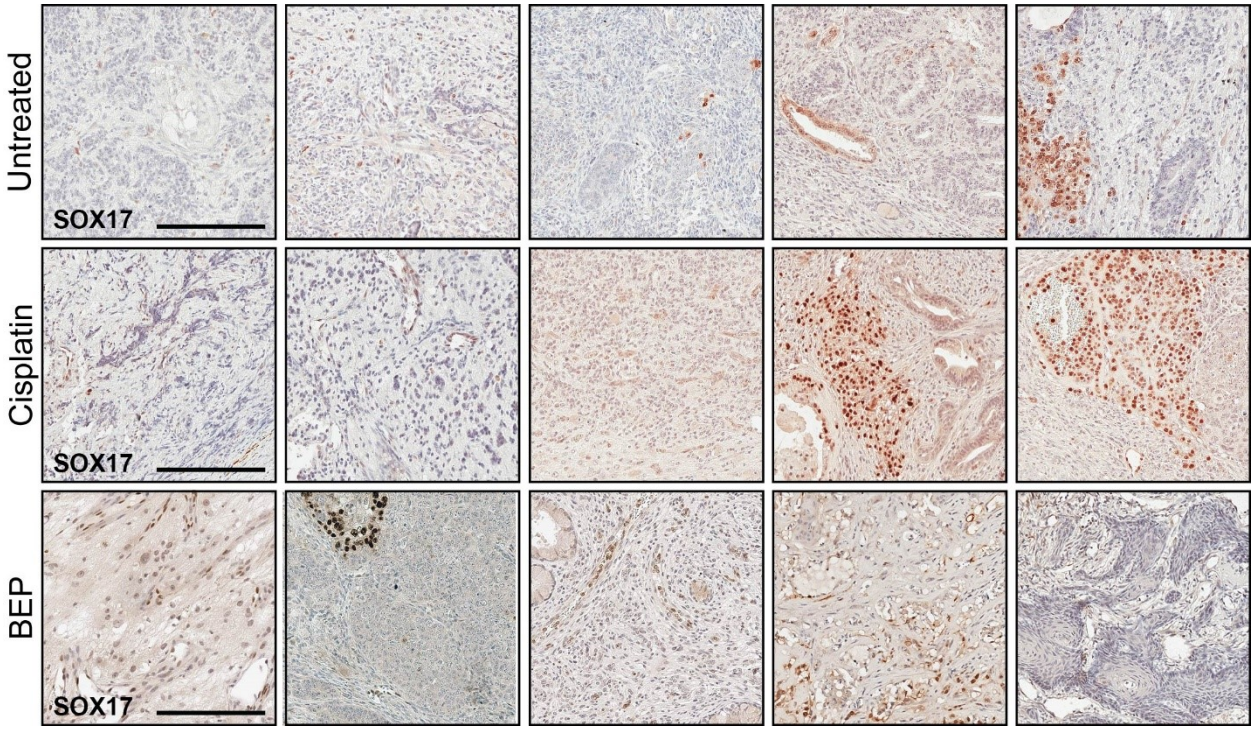

gPAK CSCs are significantly depleted following genotoxic chemotherapy. To directly test how EC cells respond to chemotherapy *in vivo,* we quantified OCT4-expressing cells in gPAK tumors collected at endpoint from mice treated with BEP or cisplatin alone. Strikingly, the percentage of OCT4-positive cells was significantly reduced in the gPAK mice treated with either cisplatin alone or BEP (Fig. 2.6C,D; p=0.02 and p=0.01 respectively). This result suggested that not only were the gPAK tumors sensitive to chemotherapy, but the OCT4-positive EC cells were more sensitive than the bulk tumor cells. To further test whether the loss of OCT4-positive cells was specific and not a consequence of loss of bulk tumor cells, we also assessed the staining pattern for SOX17, which is present in a subset of non-EC cells of the tumor. The percentage of SOX17-positive cells within gPAK TGCTs was not decreased in response to BEP or cisplatin treatment, in stark contrast to what we observed for the OCT4+ EC cells (Fig. 2.S6 and Fig. 2.6E). We conclude that TGCT chemosensitivity is specifically linked to the elevated sensitivity of EC cells to genotoxic chemotherapy. Since EC cells are the cancer stem cells of TGCTs, this selective sensitivity may explain why chemotherapy in humans is more effective against TGCTs than other somatically-derived solid cancers.

In order to understand the acute responses to chemotherapy in gPAK TGCTs, tumor-bearing gPAK mice were treated with a single dose of 6 mg/kg cisplatin and euthanized at 12 or 48 hours post-treatment. At 12 hours post-treatment, the number of apoptotic cells was increased relative to untreated gPAK TGCTs, particularly within OCT4-positive clusters (Fig. 2.7A,B). Apoptosis was reduced by 48 hours, by which time nearly all OCT4-positive cell clusters exhibited altered morphology and reduced cell number compared to untreated TGCTs (Fig. 2.7C). Importantly, this indicates that the OCT4-positive EC cells in gPAK TGCTs are sensitive to

cisplatin-induced DNA damage, which leads to rapid initiation of apoptosis and reduction in the number of CSCs.

Following chemotherapeutic treatment, it is widely accepted that surviving CSCs that are refractory to treatment can cause tumor recurrence. To determine whether the reduced amount of EC in gPAK tumors post-treatment correlated with reduced tumor-propagating activity, we compared tumor formation following transplantation of tumor cells from treated or untreated gPAK mice. Subcutaneous injection of 10,000 cells from untreated gPAK TGCTs was sufficient to produce tumors at 75% of injection sites (n=16; Fig. 2.7D and Table 2.S5). By contrast, 25,000 gPAK tumor cells transplanted 48 hours post-cisplatin treatment failed to result in tumor formation in recipient mice (n=20). Tumor-propagating activity was not completely eradicated by cisplatin treatment, as transplantation of 1 million or 100,000 cells from treated gPAK tumors was sufficient for tumor formation, though with much longer latency than observed for untreated tumor cells ($p<0.005$). Limiting dilution calculations based on these data estimated a frequency of viable CSCs of 1 in 9167 tumor cells from untreated gPAK TGCTs, which likely underestimates the true frequency of the CSCs due to EC cell death during tumor disaggregation (Table 2.S5). Notably, cisplatin-treated gPAK TGCTs contained only 1 CSC in 252,332 tumor cells, signifying a 28-fold reduction in CSC frequency following treatment. Since a single intact EC cell is sufficient to induce tumorigenesis[43], these results support the notion that the high chemosensitivity of TGCT CSCs underlies the remarkable curability of TGCTs.

Figure 2.7. Cisplatin treatment of gPAK TGCTs induces apoptosis of OCT4-positive cells and reduces tumorigenicity of transplanted tumor cells. A-C. TGCT-bearing gPAK mice were euthanized either without treatment (A), or 12 (B) or 48 (C) hours following a single intraperitoneal dose of 6 mg/kg of cisplatin. Serial sections of fixed tumors were stained with H&E, OCT4 (to identify EC) or TUNEL (to detect apoptosis) indicating a wave of apoptosis among EC cells at 12 hours post treatment. Portions of gPAK primary TGCTs, from either untreated mice, or mice euthanized 48 hours post-treatment, were digested to a single cell suspension, and the indicated number of single cells allografted into the flanks of NOD.CB17-Prkdcscid/J mice via subcutaneous injection (see Table 2.S5 for a breakdown of tumor incidence and primary tumor source). D. Kaplan-Meier tumor-free survival curve showing 25,000 post-treated cells (n=20) did not form tumors at injection sites while 75% of sites injected with 10,000 untreated cells (n=16) formed tumors that reached approximately 200 mm 3-5 weeks post-transplant (log-rank test $p<0.005$). Scale bars represent 400 μm.

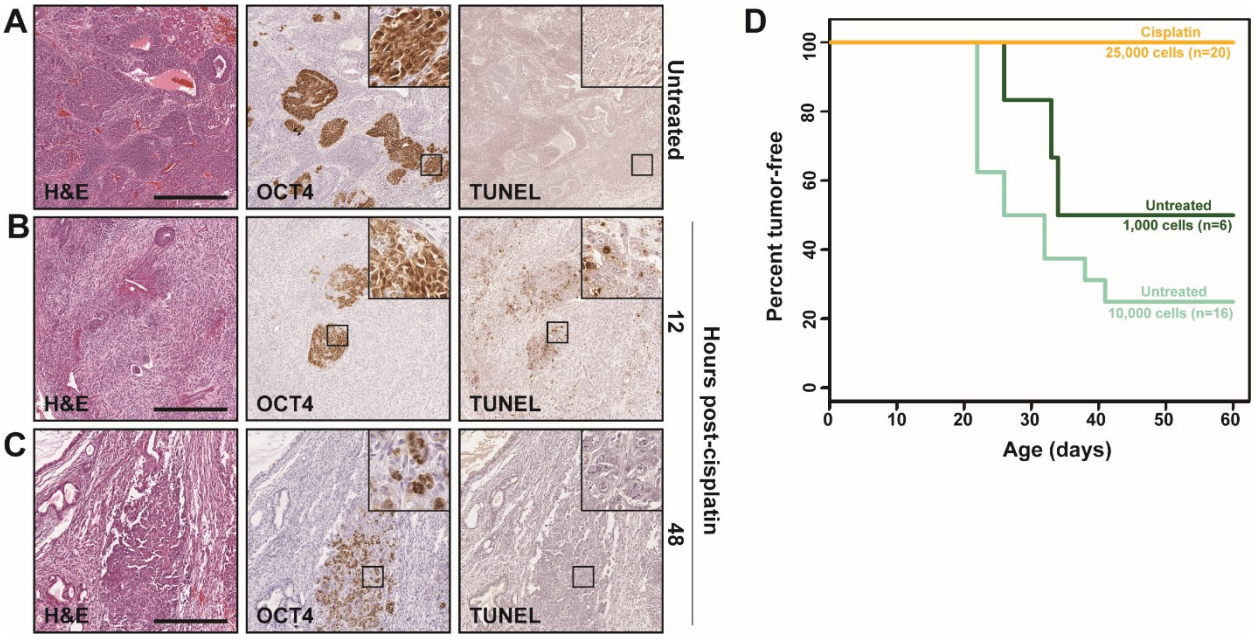
A
B
C
H&E
OCT4
TUNEL
Untreated
12
48
Hours post-cisplatin
D
Cisplatin
25,000 cells (n=20)
Untreated
1,000 cells (n=6)
Untreated
10,000 cells (n=16)
Percent tumor-free
Age (days)
0
20
40
60
80
100
0
10
20
30
40
50
60

Supplemental Table 2.S5. Tumor incidence and latency following injection of untreated or cisplatin-treated gPAK TGCT cells into recipient mice. Mice harboring primary gPAK TGCTs were either treated with 1 dose of 6 mg/kg cisplatin 48 hours before necropsy, or left untreated. gPAK primary tumors collected at necropsy were digested to a single cell suspension, and the indicated number of cells allografted into the flanks of NOD.CB17-Prkdcscid/J mice via subcutaneous injection. *indicates cells were resuspended in DMEM containing 10% FBS, LIF, and ROCKi (others were resuspended in DMEM alone) for ~45 minutes prior to transplantation. ROCK inhibition helps prevent apoptosis in EC cells induced by contact loss during disaggregation, and likely increased the number of viable CSCs transplanted, resulting in the observed 100% tumor initiation with 10,000 non-cisplatin treated TGCT cells pretreated with ROCKi.

	Primary TGCT	Number of cells injected	Injection sites	Tumors formed	Mean Latency
Untreated	A	1×10^6	3	3	19
	B	1×10^6	2	2	13
	C	1×10^6	2	2	13
	D	5×10^5	2	2	18
	E	5×10^5	2	2	17
	C	1×10^5	2	2	19.5
	F	2.5×10^4	1	1	36
	G	2.5×10^4	2	1	20
	C	1×10^4	4	4	24
	F	1×10^4	4	0	-
	F	* 1×10^4	2	2	32
	G	1×10^4	4	4	30.75
	G	* 1×10^4	2	2	22
	C	1×10^3	4	1	33
	F	1×10^3	2	0	-
	G	1×10^3	2	2	30
Cisplatin	H	1×10^6	2	2	36
	H	1×10^5	2	2	45
	I	2.5×10^4	6	0	-
	J	2.5×10^4	6	0	-
	K	2.5×10^4	6	0	-
	K	* 2.5×10^4	2	0	-

Supplemental Figure 2.S7. Schematic representation of the temporal susceptibility of germ cells to malignant transformation. Oncogenic events in germ cells during embryogenesis can cause malignant transformation and tumorigenesis, while postnatal germ cells initially hyperproliferate but then undergo apoptosis in response to the same oncogenic events. See text for details.

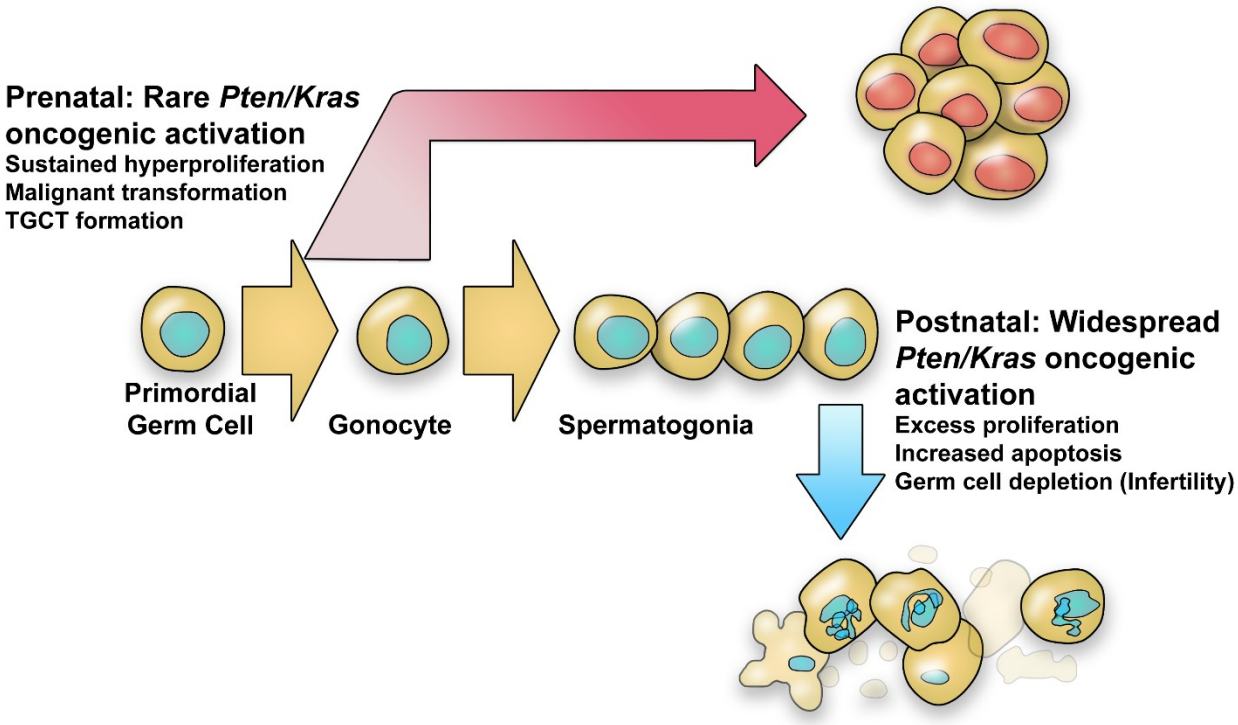

2.5 DISCUSSION

In this study, we developed a novel mouse model of malignant TGCT that, like human TGCTs, exhibits high sensitivity to the chemotherapeutic cisplatin. Using this model, we have revealed that the unusual chemosensitivity of TGCTs is associated with an inherent sensitivity of EC cells, the CSCs of TGCT, to elimination by conventional genotoxic chemotherapeutic agents. This is in contrast to most CSCs, which are refractory to treatment and often contribute to tumor recurrence and disease relapse following initial chemotherapeutic treatment[182]. This establishes a powerful system for testing the molecular mechanism underlying the chemosensitivity of these unique cancer stem cells, which we hypothesize is a direct consequence of germ cells having distinct responses to DNA damage compared to other cell types. Since there are several known determinants of cisplatin sensitivity, including DNA repair factors, studies of their roles in EC cells may reveal strategies for sensitizing other types of cancers with chemoresistant CSCs. The apparent proliferative state of gPAK CSCs may also contribute to their chemosensitivity, as quiescence may help CSCs in other tumors survive genotoxic therapies.

We observed tumors in gPAK mice as early as postnatal day 3, indicating that the tumors most likely do not arise from postnatal initiation events but rather from rare transformation of late embryonic germ cells. Consistent with this, we were able to detect *Stra8-Cre*-mediated recombination in a few small clusters of testicular germ cells at E12.5 and subsequently observed only 1-2 neoplasms per testis. It remains unknown whether the embryonic *Cre* expression observed in this model reflects the normal activity of the *Stra8* promoter or is unique to the *Stra8-Cre* transgene. However, it is worth noting that male germ cells show endogenous *Stra8* mRNA expression at E13.5[198] and a small subset of male germ cells express meiotic markers at E14.5[199],

suggesting that *Stra8* expression can occur naturally during embryonic germ cell development. Regardless, the data suggest that gPAK TGCT initiation occurs in early/mid-embryonic germ cells, a time point between PGC arrival at the gonad and the onset of G0 cell cycle arrest[200]. Notably, teratoma formation in Dnd^{Ter} mice is associated with a failure of embryonic germ cells to undergo proper mitotic arrest, suggesting that G0 arrest and downregulation of pluripotency gene expression at E12.5 to E15.5 may mark the end of the period during which germ cells are particularly susceptible to malignant transformation[201]. Interestingly, *Kras* and *Pten* targeting in postnatal germ cells initially triggered widespread overproliferation but ultimately lead to cell death and germ cell depletion. This suggests the existence of mechanisms that protect against oncogenic events in adult germ cells but fail to prevent sustained hyperproliferation at certain stages of embryogenesis. Interestingly, loss of the pro-apoptotic gene *Bax* causes testis hypercellularity soon after birth, followed by massive cell death at P25, suggesting the existence of mechanisms to eliminate excess germ cells from adult testes[202].

The gPAK model is representative of human testicular cancer, given that most human TGCTs have malignant components, and our work is consistent with the possibility that human TGCTs may arise from embryonic oncogenic insults. It is particularly striking that there seems to be a specific developmental window within which early germ cells are susceptible to oncogenic transformation (Fig. 2.S7). This mimics the case in humans, where epidemiologic data indicate that TGCT risk in men is associated with *in utero* environmental exposures[185]. Despite presumed initiation during embryogenesis, human TGCTs originating from GCNIS do not typically present until adulthood, likely due to hormone production beginning at puberty.

It is unclear why *Kras* activation or *Pten* inactivation alone is insufficient to cause germ cell tumorigenesis in the majority of cases. It has been reported previously that loss of *Pten* driven

by *Stra8-Cre* does not induce TGCTs or affect fertility[203], although in our studies we did see infrequent TGCTs as well as germ cell loss with *Pten* deletion alone. No TGCTs were observed in mice with *Stra8-Cre*-driven *Kras* activation alone even after one year. Why is *Ras* activation insufficient for oncogenic transformation in germ cells, but sufficient in other tissues? It is well documented that some mouse tissues are more susceptible to *Ras*-induced transformation than others. Mice expressing activated oncogenic *Kras* in somatic tissues, either constitutively or spontaneously, primarily develop lung cancers as well as oral, gastric, and skin papillomas and thymic lymphomas, whereas neoplastic lesions were not detected during the same time period in pancreas, liver, or small intestine[204,205]. Similarly, *Pten* inactivation leads to tumorigenesis in lung, skin, prostate epithelium, mammary epithelium, and T-cells, but rarely in the GI tract[206]. While *Pten* loss and *Kras* activation lead to some of the same downstream effects, substantial evidence indicates that these can be potent collaborating events during tumorigenesis. In mouse models of ovarian cancer, concomitant *Pten* and *Kras* alterations result in development of serous papillary adenocarcinomas[207]. Furthermore, *Pten* loss accelerates *Kras*-induced pancreatic cancer development[208], and promotes metastatic progression of *Kras*-activated melanomas[209]. Thus, *Pten* loss and *Kras* activation are functionally non-equivalent, despite their overlapping impact on key signaling pathways, and in the context of germ cells strongly synergize to promote TGCT formation.

The contrasting effects of *Pten* and *Kras* alterations in germ cells may be particularly relevant to their modulation of the germline stem cell pool. *Pten* inactivation in oocytes has been shown to promote premature activation of the entire primordial follicle pool, causing an initial surge of follicle maturation that leads to premature ovarian failure due to loss of the oocyte reserve[210]. *Ras* activation in cultured spermatogonial stem cells (SSCs), on the other hand,

promotes self-renewal rather than proliferation and differentiation[211]. Interestingly, excessive Ras-mediated self-renewal in these cultured SSCs led to development of germ cell tumors upon transplantation into murine testes. It is possible that the combined *Pten* inactivation and *Kras* activation in our model promotes premature cell division of SSC precursors concomitant with activation of excessive self-renewal signals, leading to development of germ cell-derived tumors containing OCT4-positive malignant stem cells (EC cells). Supporting this idea is the fact that *Pten* null mouse pluripotent stem cells cultured *in vitro* develop into aggressive, tumorigenic EC cells through increased survival and self-renewal caused by loss of *Nanog* repression[212].

Many open questions remain regarding TGCT biology, most notably related to the fundamental differences in the cell of origin between germ cell and somatically-derived cancers and the different molecular mechanisms governing their responses to oncogenic transformation. In stark contrast to most somatically-derived cancers, early-stage testicular germ cell cancers in our gPAK mice and in humans[92] lack the DNA damage response marker γH2AX. This fundamental difference in response to oncogene-induced DNA damage may be due to differential DDR wiring of germ cells *versus* somatic cells, with germ cells primed to apoptose in response to damage rather than risk faulty DNA repair. Alternatively, it is possible that the pre-meiotic germ cells have a dampened DDR in order to allow full DDR activation following meiotic DSB induction, which is absolutely necessary for completion of meiosis and production of functional sperm. It remains to be seen whether germ cells in fact incur as much DNA damage in response to oncogenic proliferation as do somatic cells, which would also impact DDR activation status. Interestingly, ES cells contain greater numbers of dormant origins than more differentiated cells[213], and it is conceivable that embryonic germ cells could use this or related mechanisms to protect against replication stress that normally accompanies oncogene-induced hyperproliferation. Whether the

DDR is differentially regulated depending on germ cell developmental stage also remains to be determined. For instance, whereas embryonic germ cells do not appear to mount a DDR against oncogenic events, the germ cell apoptosis and infertility associated with oncogenic events in adult gPAK germ cells could reflect a DDR triggered by replication stress associated with the widespread hyperproliferation observed at P10. Identification of what makes TGCT CSCs so sensitive to DNA-damaging chemotherapeutics may provide avenues for the development of more effective therapies for other cancers by targeting their more deadly, chemoresistant CSCs.

2.6 METHODS

Mouse strains and husbandry. Stra8-Cre transgenic mice[191] were obtained on the FVB background and then backcrossed to *129SvEv* for greater than 10 generations. *LSL-Kras^{G12D}* mice[189] were backcrossed to *129SvEv* for greater than 10 generations. *Pten$^{flox/flox}$* [214] were obtained on a mixed *B6/129/FVB* strain background. *129-Dnd1$^{Ter/Ter}$* mice[85] were maintained in the Capel laboratory at Duke University Medical Center. *Pten$^{+/flox}$* mice were crossed to *Stra8-Cre* transgenic animals to generate *Stra8-Cre*-positive *Pten$^{+/-}$* mice. *Pten^{floxlflox}* mice were crossed with *LoxP-Stop-LoxP-Kras^{G12D}* mice (referred to here as *Kras^{LSL}*) to generate *Pten$^{flox/flox}$ Kras$^{+/LSL}$* mice. In order to generate the experimental *gPAK* animals (*Stra8-Cre+ Pten$^{flox/-}$ Kras$^{+/LSL}$*), *Stra8-Cre+ Pten$^{+/-}$* mice were crossed to *Pten$^{flox/flox}$ Kras$^{+/LSL}$* mice. To generate gPAK mice with *Oct4-Gfp, Stra8-Cre+ Pten$^{+/-}$* mice were crossed with *B6;CBA-Tg(Pou5f1-EGFP)2Mnn/J*[215] and the resulting *Oct4-Gfp, Stra8-Cre+ Pten$^{+/-}$* were bred with *Pten$^{flox/flox}$ Kras$^{+/LSL}$*. In order to generate *LoxP-Stop-LoxP-LacZ* or *LoxP-Stop-LoxP-tdTomato* reporter mice, *Stra8-Cre+* mice were bred with *B6;129S4-Gt(ROSA)26Sor^{tm1Sor}/J* (Soriano 1999), or *B6;129S6-Gt(ROSA)26Sor$^{tm9(CAG-tdTomato)Hze}$/J*[216], respectively. *Oct4-gfp, LSL-Lacz, and tdTomato* mice were all used on a mixed 129SvEv/C57BL/6 background. All animals used in this study were handled in accordance with federal and institutional guidelines, under a protocol approved by the Cornell University Institutional Animal Care and Use Committee (IACUC). Mice with tumors were monitored daily and sacrificed upon reaching humane endpoint criteria.

Histology and immunohistochemistry. Tissues were fixed overnight at 4°C in Bouin's fixative or at room temperature in fresh 4% paraformaldehyde (Sigma-Aldrich) in PBS, embedded in wax,

and sectioned at 5 μm. Immunohistochemical staining for OCT4 (Abcam ab19857, 1:1000) and γH2AX (Millipore 05-636, 1:200) was done using heat-mediated antigen retrieval in EDTA, pH 8.0, while SOX17 (Neuromics GT15024, 1:500), SOX2 (Seven Hills WRAB-1236, 1:500), MVH (Abcam ab13840, 1:200), Ki67 (Vector VP-K452, 1:20), SSEA1 (Hybridoma MC-480, 1:10), and Nanog (Abcam ab80892, 1:400) staining was done using heat-mediated antigen retrieval in citrate buffer, pH 6.0. After rehydration and antigen retrieval, primary antibody was incubated overnight followed by biotinylated secondary antibody and then streptavidin HRP conjugate (Invitrogen Histostain SP) incubations at room temperature. Finally, positive cells were visualized with DAB (Invitrogen) and counterstained with 1:1 hematoxylin (Fisher CS401-1D) solution before dehydration. SOX17 immunohistochemistry was performed with anti-goat biotinylated secondary antibody (Vector BA-5000, 1:200). TUNEL assays were performed using the Apoptag kit (Millipore) as per the manufacturer's instructions.

Metaphase chromosome analysis. gPAK or *129-Dnd1*$^{Ter/Ter}$ testicular tumor cells were isolated from three primary tumors per genotype and disaggregated by treatment with 2 mg/mL Collagenase A (Roche) in serum-free DMEM with penicillin, streptomycin, and gentamycin at 37°C for approximately 1 hour prior to culturing on gelatin-coated plates in DMEM (Cellgro) supplemented with 10% fetal bovine serum (Gibco), non-essential amino acids (Cellgro), penicillin/streptomycin (Cellgro), and L-glutamine (Cellgro). Metaphase chromosome analysis was performed on low-passage cells by incubating with 10 μg/mL colcemid (Invitrogen) at 37°C for 1.5 hours, after which trypsinized cells were incubated in 0.075 M KCl hypotonization buffer at 37°C for 12 minutes and washed with prior to fixation in fresh ice-cold 3:1 methanol:acetic acid fixative. Cells were spotted on charged microscope slides (Fisher Scientific), dried, and stained for

5 minutes in fresh Giemsa stain (Harleco, Original Azure Blend) diluted 1:50 in Gurr buffer (BDH Laboratory Supplies) before imaging by standard light microscopy.

Array comparative genome hybridization (CGH). DNA was isolated from gPAK or *129-Dnd1*$^{Ter/Ter}$ testicular tumors by dounce homogenization, phenol/chloroform extraction, and ethanol precipitation. Six tumors per mouse genotype were assessed relative to one spleen DNA control sample using NimbleGen Mouse CGH 3x720k Whole Genome Tiling Arrays (Roche) and processed at the Cornell University Biotechnology Resource Center's Genomics Facility. Partial karyotype depiction of gPAK copy number aberration data (Fig. 2.S5A) was generated using waviCGH[217] via median normalization, mean pre-processing, DNA copy segmentation, probability calling, and minimal common region permutations. Small CNAs and sex chromosomes not depicted. Recurrent copy number changes listed in Tables S2 and S3 were found in at least 3 out of 6 tumors of the indicated genotype and had minimal common regions (MCRs) of 100kb or greater. Quantitative PCR validation of 7qA3 deletion in gPAK and *129-Dnd1*$^{Ter/Ter}$ tumors was performed using SYBR green detection, alpha-actin endogenous control, and primers 7delF1 (TGGTGAGTGGTCTTCGTTTC) and 7delR1 (ACAGCTGAGGAACAGGATTG). Control DNA was extracted from grossly normal spleen from the same animals. For lists of genes contained within MCRs, gene identity as protein-coding *versus* non-coding RNA was determined initially in waviCGH and reassessed using the Mouse Genome Informatics database (www.informatics.jax.org), with pseudogenes removed (Tables S2 and S3). The set of genes found in gPAK MCRs was analyzed using Panther to assess enrichment for particular gene functions[218,219] and Enrichr to determine enrichment for genes regulated by particular transcription factors[220], as listed in Supplemental Table S4.

Lineage tracing with LacZ and tdTomato reporters. For LacZ staining, embryos were collected at E13.5, 16.5, or E18.5, and young pups euthanized at postnatal day zero (P0), P3, or P6. Testes were extracted, the tunica removed, and tubules manually spread before fixation in fresh 4% paraformaldehyde in PBS with 2 mM MgCl for 30 minutes on ice. Testes were then incubated in staining solution (10mM PO_4 buffer pH7.4, 150 mM NaCl, 1 mM $MgCl_2$, 3 mM $K_4[Fe(CN)_6]$, and 3 mM $K_3[Fe(CN)_6]$, 1 mg/ml of X-gal) at 37°C for either 6 hours, or overnight for E16.5 and younger. Samples were paraffin-embedded, sectioned at 5 μm, and counterstained with nuclear fast red (Acros Organics).

For tdTomato visualization, testes from *B6;129S4-Gt(ROSA)26Sor^{tm1Sor}/J Stra8-cre*+ mice were collected at E11.5, E12.5, E18.5, postnatal day zero (P0), or P3. Testes were dissected out from animals at E18.5 or older, while E12.5 and E11.5 samples were fixed as whole embryos. All tissues were fixed in fresh 4% paraformaldehyde for 30 minutes on ice. Tissues were then washed in cold 1xPBS before being flash frozen in O.C.T. compound and cryosectioned at 20μm thicknesses. Sections were mounted on slides and covered with DAPI containing mounting medium before being analyzed for the presence of tdTomato positive cells localized to the gonads.

Sperm counts. Mature spermatozoa were isolated from the caudal epididymis as described previously[221]. Briefly, both epididymides from each mouse were minced and incubated in 1 mL warm PBS for 30 minutes, after which the sperm suspension was fixed in 10% neutral-buffered formalin and counted using a hemacytometer. Data are shown as the mean ± SEM, and values were analyzed statistically using a Tukey-Kramer test.

Chemotherapy treatments. Cisplatin (Sigma P-4394) was dissolved in 0.9% NaCl to a concentration of 1 mg/mL and stored at room temperature for up to 1 month. For survival analysis, gPAK mice were randomly selected for intraperitoneal injection of 6 mg/kg cisplatin at weaning and again one week later, or at the same time points with 0.9% NaCl for control injections. Mice were monitored until reaching one of three humane endpoints: quiet and unresponsive, have an external TGCT ulcerate or reach greater than 2.0cm^3, or were severely bloated, piloerect, and showed signs of dehydration. gPAK mice that did not develop TGCTs were excluded from the analysis. OCT4-positive cells were identified via immunohistochemical staining and quantified using ImageJ. For assessing acute responses to cisplatin, mice with detectable TGCTs were given one dose of 6 mg/kg of cisplatin intraperitoneally and euthanized 12 or 48 hours post-injection. All samples were fixed in fresh 4% paraformaldehyde for 24 hours.

For BEP treated mice, the same endpoints and cisplatin source was used, but treatment included bleomycin (Selleckchem) dissolved in 0.9% NaCl, and etoposide (Selleckchem) dissolved in 5% DMSO, with all drug prepared to 0.5mg/mL. BEP mice were treated for four weeks on a repeating 7 day cycle during which they received 1.8mg/kg cisplatin and 5.0mg/kg etoposide on days 1-5, and 1.8mg/kg bleomycin on day 2, of all four cycles. Some doses were temporarily postponed, before resumption of the treatment cycle, if drug toxicity was observed based on weight loss or severe dehydration, and wet food was given.

gPAK TGCT transplantation. gPAK testicular tumors were isolated from gPAK mice 48 hours post-cisplatin-treatment (or from untreated controls) and disaggregated with 2 mg/mL Collagenase A (Roche) in serum-free DMEM with penicillin, streptomycin, and gentamycin at 37°C for approximately 1 hour, shaking. Cells were then passed through a 4 μM filter to remove large

clumps, pelleted at 1.5 x g for 5 minutes, then resuspended in DMEM or DMEM + 10% FBS, + 1x LIF, + 10 μM ROCK inhibitor prior to injection. Approximately 30 minutes prior to injection, the desired number of cells were suspended in 100 μl PBS. Just prior to injection, 100 μL of cells were mixed with 100 μL matrigel (BP Biosciences) in a 1 mL syringe and injected subcutaneously into the flanks of NOD.CB17-Prkdc^{scid}/J mice. Mice were monitored regularly for tumor development and sacrificed upon reaching humane endpoint criteria. Tumor-free survival data was analyzed in a Kaplan-Meier plot. Limiting dilution calculations done according to[222].

2.7 ACKNOWLEDGMENTS

The authors are grateful to Drs. Peter Schweitzer and Wei Wang of the Cornell University Genomics Core Facility for aCGH analysis; Lishuang Shen and Marsha Wallace for assistance with CGH and qPCR; Drs. Robert Braun, Alexander Nikitin, and Doina Tumbar for providing mice; and Alex Nikitin and Andrew White for comments on the manuscript. This work was supported by the Cornell University Center for Vertebrate Genomics (microarray subsidy), NIH T32 HD052471 training grant support to AML, NIH T32 GM07273 training grant support to TP and LB, NIH R01 GM087500 to BC, NIH T35 AI007227 training grant support to AB, NK, and HZ, NYSTEM IDEA award C026421 to RSW, and NIH R21 CA185256 to RSW.

CHAPTER 3

CULTURED EMBRYONAL CARCINOMA CELLS RETAIN CANCER STEM CELL PROPERTIES AND EXHIBIT HYPERSENSITIVITY TO CISPLATIN

3.1 ABSTRACT

The cellular mechanisms underlying the chemosensitivity of testicular germ cell tumors (TGCTs) remains an elusive but important area of research. Although cisplatin and other genotoxic chemotherapies are used to treat a variety of late-stage cancers, TGCTs are the only solid cancer that achieves 71% five-year survival rates. Many cell culture models of human and murine malignant TGCTs exist, yet most of these cell lines have been maintained *in vitro* for decades, likely subjecting the cells to artificial selective pressures that may affect results. In this study, we isolated two new embryonal carcinoma (EC) cell lines from a novel mouse model in which TGCTs arise due to germ cell specific *Pten* inactivation alone, or in combination with oncogenic *Kras* activation. EC cells are established as TGCT cancer stem cells (CSCs) that retain the ability to self-renew as well as differentiate into teratoma tissues. Both EC cell lines retained their pluripotent phenotype and tumor-propagating abilities without notable changes. Following exposure to differentiation reagents thioridazine or retinoic acid, both EC lines exhibited loss of pluripotency and tumor propagation potential. We hypothesized that EC cells possess a unique DDR that underlies their heightened chemosensitive to genotoxic drugs like cisplatin. To test this, we treated EC cells and their differentiated counterparts with cisplatin. Both EC cell lines showed significantly reduced survival compared to their respective differentiated derivatives. Studying these EC cells along with differentiated controls will provide new insight into the basis of TGCT chemosensitivity in humans.

3.2 INTRODUCTION

Testicular germ cell tumors (TGCTs) are the most common malignancy among men 15 to 40 years of age and are increasing in prevalence in developed countries[39]. Before the advent of genotoxic chemotherapies, advanced stages of this disease had a dismal 5% five-year survival rate[71]. Now treated with a combination of bleomycin, etoposide, and cisplatin (BEP), the same advanced stage of TGCT has a 71% survival, and near 100% when detected early[71]. This success story of treatment advancement for TGCTs is historic. However, it remains unknown why these tumors respond so well to genotoxic chemotherapies while so many somatic cancers remain resistant. A better understanding of the mechanisms underlying the therapeutic response to genotoxic chemotherapies may help better treat resistant cancers.

TGCTs can be divided into two broad categories based on whether they derive from a known precursor lesion, germ cell neoplasia *in situ* (GCNIS), or not[29,30]. TGCTs derived from GCNIS comprise the majority of all germ cell tumors and tend to be highly malignant yet carry a good prognosis with BEP therapy and surgery[223]. Embryonal carcinoma (EC) is a totipotent cancer cell type found in approximately 80% of all non-seminomas. Commonly, EC cells present together with more differentiated tumor tissue lineages from all three germ layers known as a teratoma. Malignancies with both teratoma and EC components are defined as teratocarcinoma.

EC cells are the established CSC of teratocarcinoma, which is supported by data shown in Chapter 2 (Fig. 2.S1, 2.S2). CSCs are cancer cells with the ability to divide indefinitely while both self-renewing and undergoing alterations to produce the heterogeneity of a given malignancy[134]. CSCs have been identified in a variety of cancers, most notably leukemia, breast, brain, and germ

cell cancers[43,135,148,156]. Importantly, in somatic cancers, CSCs tend to be more resistant to chemotherapy[224]. This is of great clinical significance in that, despite initial positive response to treatment, viable CSCs can evade chemotherapy. In such cases, the malignancy is able to regrow and ultimately be incurable. Alternatively, targeting the CSC in combination with conventional treatments could increase survival among resistant cancers. Because EC is the CSC of teratocarcinoma, for which there is a highly efficacious treatment, understanding EC response to treatment is a key component of understanding the high cure rate among TGCTs.

Some evidence exists to suggest that EC cells have a robust DDR responsible for their hypersensitivity to genotoxic drugs. Two major apoptotic responses unique to pluripotent cells, which are lost upon differentiation, are primed BAX and a reduced or non-existent G1/S checkpoint[125,127,129]. Embryonic stem (ES) cells and induced pluripotent (iPS) cells are both known to share this hypersensitivity to DNA damage[125,126]. BAX oligomerization and localization to the mitochondrial membrane is a necessary step in apoptosis, but BAX is cytosolic and only activated upon sufficient DNA damage in the vast majority of cells. In ES and iPS cells, BAX was found already activated and stored at the golgi where it more rapidly localized to the mitochondria to induce apoptosis upon DNA damage[127]. This phenotype was lost upon differentiation[127]. Additionally, ES cells lack, or have a reduced, G1 checkpoint in mice and human-derived cells respectively.

In 1953, Leroy Stevens initated research in EC when he discovered that inbred line 129 mice had a high rate of teratoma formation[163]. Follow-up experiments showed that some of these germ cell tumors harbored EC cells and could be propagated indefinitely[80,164]. From this work, these rare tumors were categorized as malignant teratocarcinoma[164]. Kleinsmith et al. observed that when teratocarcinoma was transplanted intraperitoneally, the mouse would develop ascites

with free floating clusters of cells which appeared similar to very early embryos called embryoid bodies. Single cells were carefully isolated from embryoid bodies collected from ascites, and using glass capillary tubes, researchers transplanted single cells into 1790 mice, resulting in 43 successful engraftments of teratocarcinoma. This set of experiments provided some of the earliest evidence that single cells can function as CSCs and demonstrated that EC is functionally the CSC of teratocarcinoma[43]. Continued work with EC laid the groundwork for isolation of embryonic stem cells as well as their culture conditions[165]. The close relationship of ES and EC cells, both in a historical context and in morphology and pluripotency, supports the idea that both cells may share unique DDR as well.

Mice with germ cell specific *Pten* inactivation and simultaneous $Kras^{G12D}$ activation, referred to as gPAK mice, were introduced in Chapter 2. When treated with cisplatin, or a combination of bleomycin, cisplatin, and etoposide, tumor-bearing mice had increased survival and reduced tumor burden. Importantly, the EC component of the teratocarcinomas of treated mice was greatly reduced in comparison to the untreated tumors (Fig 1.6E). We hypothesize that a hypersensitivity of EC cells underlies the increase in survival of cisplatin treated mice within our model, and contribute to the high cure rates of TGCTs in people. To test the response of EC cells in a more controlled environment, we established two cell lines from teratocarcinomas of this novel mouse model. Both cell lines retained their tumor-propagating phenotype and pluripotency markers similar to their *in vivo* counterparts. We show that they also appear to retain a hypersensitivity to cisplatin-induced damage, and can function as a powerful reagent in elucidating the unique DDR underlying the exceptional response to genotoxic chemotherapies among TGCTs.

3.2 RESULTS

Derivation of embryonal carcinoma cell lines that retain cancer stem cell properties. Because EC cells are present in small isolated clusters, surrounded by vast amounts of heterogeneous teratoma tissues, it is difficult to study specific EC cellular responses to drugs *in vivo.* We sought to culture *in vitro* cell lines derived from our genetic model of teratocarcinomas, described in Chapter 2, to better characterize the unique mechanisms of EC cell response to genotoxic chemotherapies. Tumors collected during necropsy were mechanically disaggregated and placed in digestion media with collagenase on a shaker at 37C to generate a single cell suspension. These cells were then plated at decreasing cell concentrations, passaged upon confluency, and monitored for EC colony formation. ROCK inhibitor Y-27632 was used in initial passages as it is known to reduce disassociation-induced apoptosis in human embryonic stem cells[225]. Mouse leukemia inhibiting factor (LIF) was included in EC culture media as its ability to prevent differentiation of ES cells *in vitro* has long been characterized, and some studies show similar benefits for EC cells[226,227]. Two cell lines, EC3 and EC11, were successfully derived from primary gPAK tumors using these methods (Fig. 3.1A). Both cell lines continued consistent growth following 40 passages and formed colonies similar to those reported for ES cells and some mouse EC lines. Upon subcutaneous injection into the flanks immunocompromised mice, as few as 100 EC3 and EC11 cells were sufficient to generate tumors within two weeks, thus suggesting that they retained their CSC properties (Table 3.1). The tumors were characterized as teratocarcinomas histologically similar to primary tumors including retention of the OCT4 expressing EC cell populations (Fig. 3.1B). Retention of these CSC phenotypes suggests the *de novo* EC lines cells harbor similar pluripotency and self-renewal networks despite exposure to an artificial *in vitro* environment. The EC3 line was generated from a gPAK mouse harboring an OCT4-GFP transgene which expresses

GFP in any cell that expresses OCT4, thus allowing identification of EC cells *versus* their differentiated counterparts *in vitro* (Fig. 3.1E).

Figure 3.1 Embryonal carcinoma cells isolated from gPAK tumors retain CSC phenotype. Representative brightfield images of EC colonies appeared from heterogeneous plating of disaggregated murine teratocarcinomas (A). Upon engraftment in immunocompromised mice, cells formed teratocarcinoma similar to primary tumors, including maintenance of EC, as shown by representative sections stained with H&E and for OCT4 (B). After two weeks of exposure to $1x10^{-5}$M of Thioridazine, EC cells differentiated into a more flattened cell morphology which grew as a monolayer (C) and exhibited a reduced expression of OCT4 as evidenced by protein lysate analysis (D). EC3 cells exposed to $1x10^{-7}$M of retinoic acid for approximately two weeks also differentiated, and lost OCT4 expression as shown by loss of GFP expressed under the control of the OCT4 promoter (E).

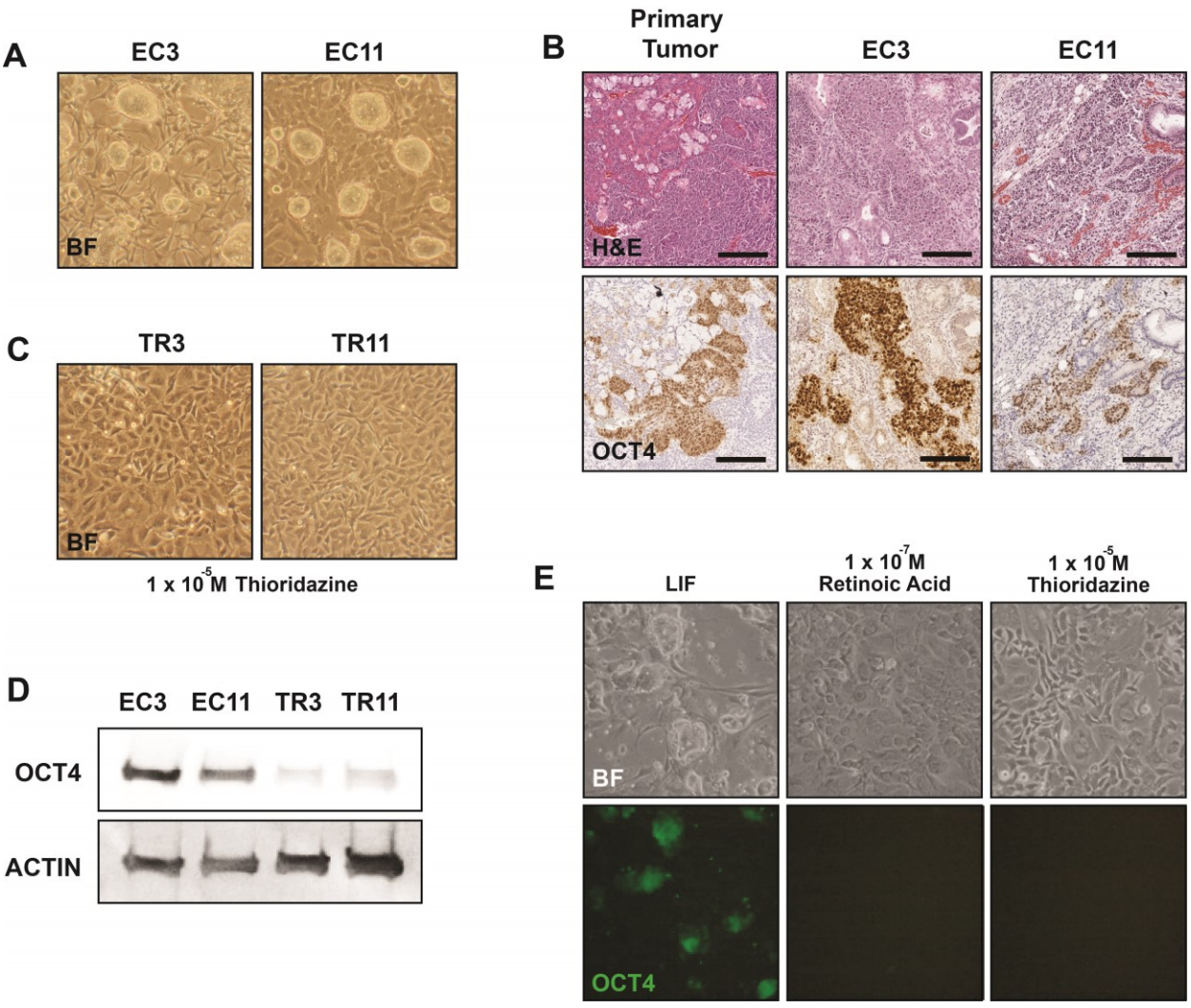
A
EC3
EC11
BF
B
Primary Tumor
EC3
EC11
H&E
OCT4
C
TR3
TR11
BF
1 x 10-5M Thioridazine
D
EC3 EC11 TR3 TR11
OCT4
ACTIN
E
LIF
1 x 10-7M Retinoic Acid
1 x 10-5M Thioridazine
BF
OCT4

Thioridazine induces EC cells to differentiate and lose pluripotency. To determine if EC cells are hypersensitive to cisplatin in the same way other pluripotent cells are, well-matched, differentiated controls derived from the pluripotent EC lines were necessary. Although very little is known about EC cell DDR, both ES, and iPS cells have been well studied. It is reasonable to expect traits found to convey ES and iPS cell genotoxin hypersensitivity will be shared by other pluripotent cells, including EC cells. Storage of primed BAX at the golgi, and a reduced or non-existent G1/S checkpoint are two major pro-apoptotic responses to DNA damage that are unique to these pluripotent cells, both of which are lost upon differentiation[125,127,129]. To generate well-matched controls, the EC cell lines were exposed to $1x10^{-5}$M of thioridazine (Fig. 3.1C). Differentiated cell lines derived from EC3 and EC11 will be referred to as TR3 and TR11 respectively. After about two weeks of constant exposure to thioridazine, the majority of cells in the culture grew as a homogeneous monolayer with very few persistent EC colonies (Fig. 3.1C). OCT4, a transcription factor necessary to maintain pluripotency, was substantially reduced in both TR cell lines (Fig. 3.1D). EC3 cells were separately exposed to $5x10^{-7}$M of retinoic acid (RA) which also induced differentiation (Referred to as RA3 cells) as evidenced by loss of EC colonies and OCT4 expression, although several persistent EC colonies remained after all differentiation attempts with RA (Fig. 3.1E). The ability to propagate tumors is another hallmark of CSCs, and as few as 100 EC3 or EC11 cells subcutaneously transplanted into immunocompromised mice were able to generate teratocarcinomas within 2 weeks (Table 3.1). However, the differentiated cell lines formed tumors at reduced frequency, and the tumors that did form did so with increased latency. Importantly, because all differentiated cell cultures had some remaining EC cells, as evidenced by the faint OCT4 band (fig. 3.1D), it is likely that the rare surviving EC cells were sufficient to propagate the tumors rather than the more differentiated cells forming tumors. This is supported

by the fact that those tumors which formed from mostly differentiated cells still contained OCT4 positive EC cells at endpoint.

EC cells exhibit greater sensitivity to cisplatin-induced damage than their respective differentiated cell lines. As described in Chapter 2, tumors that formed in gPAK mice were sensitive to genotoxic chemotherapies (Fig. 2.6A). Importantly, the EC populations within tumors were significantly reduced after treatment compared to those in untreated controls (Fig. 2.6C,D) suggesting EC cells are particularly sensitive to cisplatin compared to the more differentiated tissues that comprise the teratoma. Similarly, the lack of EC cells in post-treatment human teratocarcinomas, despite residual teratoma tissue that requires surgical resection, also suggests EC hypersensitivity compared to the differentiated teratoma components[172,173]. To test if the process of differentiation diminished chemosensitivity in the TR3 and TR11 cell lines, we tested cell survival following a 1-hour exposure to either 6ug/mL or 12ug/mL of cisplatin.

Following 6ug/mL of cisplatin, both EC3 and EC11 cells had disruption of colonies demonstrated by an increase of loosely adhered cells surrounding the colonies and significantly reduced cell survival at 24 and 48 hours post-treatment compared to differentiated controls. EC3 cells tend to grow as colonies as well as flat monolayers reminiscent of cell morphology in some human EC lines regardless of treatment status[228,229]. TR3 and TR11 showed no significant changes in cell morphology, and only a moderate loss of cell survival after 6ug/mL cisplatin. Following 12ug/mL of cisplatin, both EC cell lines showed a dramatic loss of EC colony formation, and at 48 hours very few cells remained in colony or monolayer form as evidenced by representative images and cell survival counts. The differentiated TR cells showed a slight reduction in survival at 24 hours post 12ug/mL cisplatin, while only TR11 had a large reduction in viable cells 48 hours after the

higher dose of cisplatin. While the higher dose suggests the differentiated cells don't show a survival reduction 24 hours after treatment, TR11 cells did have reduced survival at 48 hours. The 6ug/mL dose may induce apoptosis in the EC cells at a significantly higher rate at both measured timepoints, indicating a heightened sensitivity of EC cells compared to the differentiated controls which are similar to what was observed *in vivo* following cisplatin treatment (Fig. 2.6).

Table 3.1

	Number of cells injected	Injection sites	Tumors formed	Mean latency
EC3	10,000	1	1	11
	1,000	3	3	16
	100	4	3	13
	10	4	2	46
EC3-RA	1,000	2	1	21
EC3-TR	1,000	4	1	20
EC11	1000	2	2	7
	100	2	2	14
EC11-TR	1,000	4	4	20

Figure 3.2 Established EC cell lines retain hypersensitivity to chemotherapy compared to differentiated counterparts. Representative brightfield images of untreated EC3, EC11, TR3, and TC11 compared to cells 24 and 48 hours post-treatment of 6ug/mL (A) and 12ug/mL (B) of cisplatin. Quantification of percent cell survival calculated by trypan blue negative cells manually counted on a hemocytometer, normalized to untreated controls, after 6ug/mL cisplatin (C) or 12ug/mL cisplatin (D). Significantly fewer EC3 and EC11 cells survived compared to their differentiated counterparts at 24 ($p=0.045$ and $p=0.0028$ respectively, Students t-test), and 48 ($p=0.049$ and $p=0.01$ respectively, Students t-test), when treated with 6ug/mL cisplatin. At 12ug/mL, the differentiated cells also showed high sensitivity and the differences between EC and TR cells were not as significant. 24 hours post treatment (EC3 $p=0.49$ and EC11 $p=0.0023$, Students t-test), and 48 hours post treatment (EC3 $p=0.0495$ and $p=0.087$ respectively, Students t-test) at 12ug/mL.

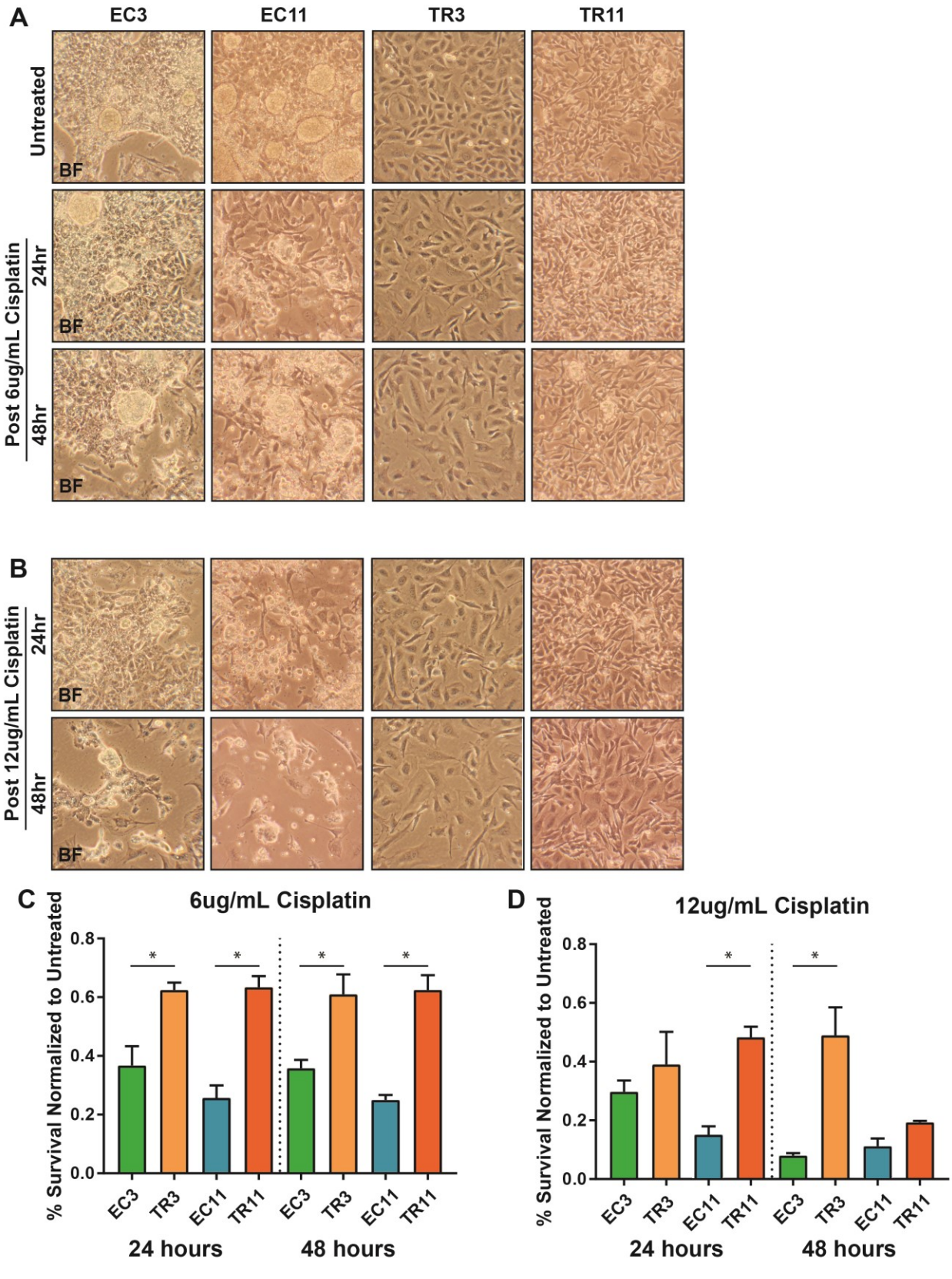
A
EC3
EC11
TR3
TR11
Untreated
Post 6ug/mL Cisplatin
24hr
48hr
BF
B
Post 12ug/mL Cisplatin
C
6ug/mL Cisplatin
% Survival Normalized to Untreated
0.0
0.2
0.4
0.6
0.8
*
EC3
TR3
EC11
TR11
24 hours
48 hours
D
12ug/mL Cisplatin

3.4 DISCUSSION

We have shown that EC cells from our novel mouse model of teratocarcinoma can be cultured while retaining their CSC and chemosensitive phenotypes (Fig. 3.1,3.2). Both cell lines grew rapidly and formed colonies, similar to ES and other EC lines. Interestingly, compared to EC11, EC3 colonies appeared less uniform, despite being derived from the same model. These differences may reflect alterations introduced during the establishment of the cultures or innate differences from the respective primary tumors, but regardless appear to be stable phenotypes of the two lines. These differences emphasize the need to isolate additional EC lines as well as caution when interpreting data from previous EC lines that have been propagated *in vitro* for decades. TERA2, NTERA2.cl.D1, and P19 are commonly used human EC cells, which exhibit differential growth and other phenotypes that may reflect their artificial environment more than differences in the original tumors[228,229]. A recent *in vitro* analysis concluded that in some established EC cell lines, reduced homologous recombination repair is responsible for their chemosensitivity[230]. Additional evidence based on *in vivo* observations and *in vitro* studies of TGCT chemosensitivity suggests the underlying mechanisms of sensitivity are an active system that is considerably more complex *in vivo*, with an interplay between DDR and pluripotency transcriptional networks[231].

Despite differences between EC3 and EC11, they both shared chemosensitivity (Fig. 3.2). This phenotype was also shared by all treated primary tumors of the gPAK model from which these cell lines were derived, suggesting the underlying mechanisms of sensitivity will also be similar (Fig. 2.6). It also needs to be determined if the EC cells surviving after 6ug/mL cisplatin remain proliferative, or senesce. Indeed, EC cells are known to have a robust P53 mediated senescence and apoptotic response to damage[169,232]. Comparing mRNA and protein level changes

following cisplatin treatment, between the EC and matched TR lines, will allow the elucidation of the underlying mechanisms of this chemosensitivity. High levels of cytosolic P21 expression were shown to be prognostic of chemoresistant EC in humans, likely avoiding apoptosis by inducing cell cycle arrest[123]. Comparing P21 expression between our chemosensitive EC lines compared to their differentiated counterparts would determine if significantly lowered P21 expression plays a role in EC sensitivity[123]. Protein and gene expression analysis will also establish if these EC cells exhibit any predicted mechanisms of chemosensitivity associated with other pluripotent cells, such as lacking G1 checkpoint or harboring primed BAX at the golgi, as is reported in mouse embryonic stem cells[127]. The rapid proliferation of EC cells compared to the relative quiescence of most somatic CSCs, may also play a role in their heightened susceptibility to DNA damaging chemotherapeutics. As discussed in Section 1.3, aside from DDR and apoptotic pathway genes, there are other determinants of chemosensitivity including the ability of cells to pump drugs out of the cell against their concentration gradient, drug detoxification, and drug target manipulation, which have yet to be explored as a basis for embryonal carcinoma chemosensitivity. We will also continue to expand this library of cell lines, making it an increasingly useful reagent for ourselves and other researchers.

3.5 METHODS

gPAK TGCT primary culture. gPAK testicular tumors were isolated from gPAK untreated and disaggregated with 2 mg/mL Collagenase A (Roche) in serum-free DMEM with penicillin, streptomycin, and gentamycin at 37°C for approximately 1 hour, shaking. Cells were then passed through a 40 μM filter to remove large clumps, pelleted at 1.5 x g for 5 minutes, then suspended in DMEM or DMEM + 10% FBS, + 1x LIF (ORF Genetics), + 10 μM ROCKi (Selleckchem) and plated with these media conditions. Both EC lines were maintained in this media without ROCKi over up to 70 passages. The media was replaced every day and cells were passaged at a 1/10 split every other day. To induce differentiation, cells were incubated with either $1x10^{-7}$M of retinoic acid (Sigma) or $5x10^{-5}$M of thioridazine (Sigma).

Transplantation of EC3 and EC11 cells. Plated cells were washed with 1X sterile PBS and then exposed to trypsin at 37C until detached from the cell culture plate. Cells per mL were calculated by hemocytometer before pelleting at 1.4g for 4.5 minutes. 10, 100, or 1000 cells were suspended in 100 μl PBS and stored on ice for transportation to mouse facilities. Just before injection, 100 μL of cells were mixed with 100 μL matrigel (BD Biosciences) in a 1 mL syringe with an 18 gauge needle and injected subcutaneously into the flanks of NOD.CB17-Prkdc^{scid}/J mice. Mice were monitored weekly for initial tumor formation and euthanized when the tumors reached approximately 2cm in diameter.

Histology and immunohistochemistry. Tissues were fixed overnight in Bouin's fixative at 4°C or in fresh 4% paraformaldehyde (Sigma-Aldrich) in PBS at room temperature, embedded in wax, and sectioned at 5 μm. Immunohistochemical staining for OCT4 (Abcam ab19857, 1:1000) was

done using heat-mediated antigen retrieval in EDTA, pH 8.0. After rehydration and antigen retrieval, primary antibody was incubated overnight followed by biotinylated secondary antibody and then streptavidin HRP conjugate (Invitrogen Histostain SP) incubations at room temperature. Finally, positive cells were visualized with DAB (Invitrogen) and counterstained with 1:1 hematoxylin (Fisher CS401-1D) solution before dehydration.

Chemotherapy treatments. Cisplatin (Sigma P-4394) was dissolved in 0.9% NaCl to a concentration of 1 mg/mL and stored at room temperature for up to 1 month. To treat cells, a master mix of media was freshly prepared of the desired working cisplatin concentration and then immediately used to replace the current media. After 1 hour of cisplatin exposure, the media was replaced by fresh cisplatin free media.

Western blot analyses of OCT4. Cells were collected in cold PBS, pelleted and resuspended in to IP lysis buffer and incubated for 30 minutes on ice, then centrifuged for 25 minutes at high speed at 4C. The lysate was then collected with the supernatant and protein concentrations were measured using Bradford reagent OD matched to a standard curve. 15ug of protein was loaded into a 12% SDS-PAGE gel, then transferred to a nitrocellulose membrane. The membrane was incubated with OCT4 (Abcam ab19857, 1:1000) overnight at 4 degrees and visualized using a Versa Doc Imaging System.

CHAPTER 4

Conclusions and future directions

The findings of this dissertation support the hypothesis that EC cells function as CSCs and that their unique response to platinum-based genotoxic drugs underlies the exceptional chemosensitivity of these malignancies. These data mostly came from experiments utilizing the novel gPAK TGCT mouse model developed by the Weiss lab, which initiated germ cell tumorigenesis by inducing germ cell specific *Pten* inactivation with simultaneous induction of constitutively active $Kras^{G12D}$ (Fig. 2.1A). The teratocarcinomas that arose within this mouse model were highly representative of human GCNIS-derived mixed TGCTs comprised of EC and teratoma components. The murine teratocarcinomas had histological similarities to the human disease, including an EC component expressing the same diagnostic pluripotent stem cell markers expressed in the human disease (Fig. 2.2A).

In humans, these malignancies are believed to initiate during embryogenesis, only presenting later in life as a result of additional changes that facilitate cancer cell growth and spread. Within the context of the gPAK model, the data showed that malignant transformation of germ cells only occurred during embryonic development (Fig. 2.3B), while the same oncogenic activation caused aberrant proliferation followed by germ cell death when induced by postnatal *Stra8-cre* expression (Fig. 2.4F, Fig 2.5A,E). The data presented also showed that EC cells functioned as the CSC of these teratocarcinomas (Fig. 2.S1, Fig. 2.S2) which support conclusions from previous studies utilizing rarely occurring spontaneous teratocarcinomas from 129 inbred mice[43]. Importantly, the teratocarcinoma in this model showed *in vivo* sensitivity to combined treatment with bleomycin, etoposide, and cisplatin administered at doses comparable to the current standard of care for human TGCTs (Fig. 2.6A). Significant sensitivity was also observed to

cisplatin when administered alone, emphasizing the pivotal role of platinum-based drugs in treatment. Sensitivity was reflected in significantly smaller primary tumors and increased survival in treated mice, but most interesting was the loss of EC cells that accompanied these responses (Fig. 2.6B,C).

The EC hypersensitivity was confirmed by comparing cell survival in response to cisplatin treatment of EC cultured cells derived from this model compared to differentiated cells also derived from the gPAK model (Fig. 3.2B,D). The data presented here are the first evidence that murine teratocarcinoma, and specifically their CSCs, respond well to genotoxic chemotherapies *in vivo*. Because EC is the established CSC of teratocarcinoma, it is very pertinent that these cells were depleted in response to treatment. The overall findings of this thesis indicate that the heightened chemosensitivity of TGCT CSC plays a major role in the overall high cure rate among patients with TGCTs.

4.1 Characterizing a relevant and reliable model of malignant testicular germ cell tumors

As referenced in the introduction, several mouse models of TGCTs exist[233]. However, these models are representative of prepubertal-teratomas in humans and make poor models of the malignant TGCTs that comprise the majority of germ cell tumors. Although 25% of gPAK mice did not develop tumors, all TGCTs that did arise in this model are malignant teratocarcinomas that included an EC component. Because of this, the tumors which formed in the gPAK model are highly representative of GCNIS derived human TGCTs. This model has proven permissive for studying bulk EC cell response to genotoxic chemotherapeutics both *in vivo* and *in vitro*, allowing for characterization of drug response timing (Fig. 3.3A-D). Additional work is still needed to understand the mechanisms by which EC cells respond to genotoxic chemotherapies as part of an

ongoing effort to elucidate potential mechanisms that confer their amazing chemosensitivity at the cellular level.

4.2 Understanding of germ cell susceptibility to oncogene-induced malignant transformation

Germ cells are among the most precious and unique cells within the adult body. While entirely dispensable to an individual's survival, viable germ cells are necessary for the survival of a species. Without their highly conserved developmental pathways, and enhanced genomic protection, germ cells would be at an increased risk of passing deleterious mutations to offspring. However, little is currently known about these protective mechanisms at most stages of development[13]. Our findings led to a model of differential response from germ cells when confronted with prenatal *versus* postnatal oncogenic activation (Fig. 2.S7). This disparate monitoring of germ cell integrity suggests that only limited developmental timepoints exist during which germ cells are susceptible to oncogene-induced malignant transformation. The isolated prenatal activation of *Stra8-cre* appears limited to around E12.5 making it the likely timepoint when gPAK tumors first initiation. This unexpected activation of *Stra8-cre* could be explained by the global reprogramming events that occur in germ cells around E12.5. Immediately following migration at E11.5, the second wave of epigenetic reprogramming results in erasure of specific histone modifications, histone variant swapping, and DNA demethylation, all of which is necessary to restore totipotency to the germ cells[234,235]. This sudden change in gene expression could allow the rare expression of *Stra8-cre* which ultimately drives the oncogene activation in the gPAK model. In mouse strains susceptible to teratoma formation, endogenous *Stra8* is also expressed around E12.5 in male mice which could allow those cells germ cells to continue proliferating rather than undergo mitotic arrest, and may be a molecular switch of malignant transformation of those germ cells[84]. We cannot determine if

the early *Stra8-cre* and *Stra8* expression is related, or if the *Stra8-cre* expression is an artifact due to the use of a partial *Stra8* promotor. This expression occurs around E13.5 and corresponds with RA production, and it is, therefore, possible that rare germ cells fail to express CYP26 sufficiently causing an inability to degrade RA, the accumulation of which would facilitate expression of *Stra8*, and *Stra8-cre*[21].

While oncogenic events in prenatal germ cells lead to malignant transformation, the same oncogenic events lead to germ cell apoptosis when they occur postnatally (Fig. 2.4,5). This change in response to oncogene activation supports the concept of an early window of susceptibility to malignant transformation hypothesis. Beyond that window, it is unclear what changes have occurred to alter susceptibility. We did not observe constitutive activation of yH2AX in early gPAK tumors, which suggests, similar to human TGCTs and contrary to human somatic cancers, there is very little activation of DDR during early tumorigenesis of gPAK TGCTs (Fig. 2.2E,F)[92]. Postnatal oncogene activation in germ cells, however, could result in increased replication stress and meiotic defects. That damage could lead to checkpoint activation similar to that of many somatic cells, ultimately inducing apoptosis due to the low tolerance for DNA damage in germ cells[88]. There is relatively little known about the germ cell response to oncogenic events at any stage of development, and these data provide some insight. The exact mechanisms that prevent malignant transformation in later germ cells are entirely unknown and represent a potentially significant research direction using this mouse model.

It is not clear why neither *Stra8-cre* mediated *Pten* inactivation nor $Kras^{G12D}$ activation alone is sufficient to cause germ cell tumorigenesis at an appreciable rate (Fig. 2.1A). While both of these oncogenic events are sufficient to induce tumorigenesis in many somatic cells, incidence varies dependent on the tissue[236]. There is evidence that the presence of *Pten* plays a major role in

facilitating mitotic arrest. Inactivation of *Pten* leads to increased iPS transformation *in vitro*, suggesting a role in transcriptional reprogramming and malignant transformation[237]. Conditional inactivation of *Pten* in earlier PGCs by *TNAP/cre* resulted in failed mitotic arrest and 100% teratoma formation in 129 inbred mice[83]. Conditional inactivation of *Pten* with *Stra8-cre* only produced tumors in 20% mice, which would likely be a higher percentage if early cre mediated excision occurred in more germ cells around E12.5. Together, this adds support to the idea that gPAK tumors only initiate around E12.5 from the sporadic *Stra8-cre* activation, and not from the more widespread activation that happens postnatally. *Pten's* role in ensuring mitotic arrest could explain why germ cells with oncogenic *Kras* activation never underwent malignant transformation. However, because all tumors in our model were teratocarcinoma, rather than teratoma, regardless of *Pten* or combined *Pten/Kras* mutations, the timing likely plays a significant role in determining the path of tumorigenesis. Furthermore, the use of both *Pten* and *Kras* alterations may sufficiently increase the chances of cellular reprogramming needed for malignant transformation within a very short window of time before mitotic arrest.

4.3 The basis of TGCT chemosensitivity and implications for CSC-targeted therapy

Our results suggest that the amazingly high survival rates achieved when treating TGCTs with platinum-based combination chemotherapy are partly due to the presence CSCs with an extremely sensitive damage response. Within this model, the CSCs are depleted upon treatments comparable to the human standard of care and the depletion occurs along with significantly increased survival and reduced tumor burden. Potentially, if tumors were surgically removed from the mice following treatment, as they are in humans, higher murine survival rates may have been achieved.

Our data suggest a rapid increase in damage following treatment that quickly induces apoptosis in EC cells (Fig. 2.7, 3.3), but many of the differentiated cells of the teratoma appear less sensitive based on their persistence *in vivo* and lack of strong apoptotic response *in vitro* (Fig. 2.6D, 3.2A-D).

These findings are similar to tumors post treatment in humans, which often have surviving teratoma tissue, devoid of EC, when it is surgically removed[172,173]. Additionally, gPAK EC cells persist if untreated, and have a relatively high expression of P53 which are both phenotypes of human EC and suggest similar self-renewal and DDR mechanisms[30]. It is important to note that seminomas comprise approximately half of all TGCTs but are homogeneous, and do not yet have an identified CSC population. However, they have a slightly better prognosis following genotoxic treatment. One potential explanation for this is that because seminoma cells express many pluripotent transcription factors and have a PGC appearance, most cells may share the same heightened apoptotic response to induced DNA damage as our data shows for EC cells. Additional work is needed to understand the mechanisms of sensitivity in our model and further validate the findings in human PDX models of EC and seminoma.

The discovery of a chemosensitive CSC within a solid cancer that is considered curable is highly relevant to the CSC field. The ultimate goal of efficiently targeting CSCs in otherwise incurable cancers is to render them curable. In our model, we have demonstrated that the standard of care treatment efficiently targets the CSC of TGCTs, which was a devastating and incurable disease before the advent of these drugs. In this context, the efficacy of TGCT treatment suggests that finding ways to eliminate CSCs in somatic cancers may result in similar success stories.

4.4 Future directions.

This dissertation work has been focused on the response to therapies known to be efficacious for treating human TGCTs. However, these drugs are toxic to all cells, and while they can cure TGCTs they also cause serious chronic illnesses, such as infertility, which has led to an interest in less toxic treatments[162,238]. Because gPAK murine TGCTs are representative of GCNIS derived human TGCTs, this model could provide an ideal system for screening alternative targeted or differentiation therapies. Differentiation therapy is already an attractive alternative for targeting chemoresistant CSCs within a variety of somatic cancers[239,240]. The goal of these therapies is to induce differentiation within the CSC population without harming normal stem cell pools. Our data shows that retinoic acid and thioridazine can be effective inducers of differentiation of EC cells *in vitro*, resulting in loss of tumor-propagating potential (Fig. 3.1A,B). Vitamin D is implicated as a potential differentiation drug for germ cell tumors as well, but the studies rely on long-term cultured EC cells[241]. Although *in vitro* screening for anticancer drugs is a powerful tool in preclinical testing, cells grown for long periods of time show deviations from *in vivo* tumors, leading to results that are not necessarily biologically relevant (Fig. 4.1). Potential alternative drugs like those mentioned could be tested *in vitro* in low passage gPAK derived EC cultures before being tested *in vivo* using the gPAK model mice. Because of this, the gPAK model holds great promise for both understanding the biological mechanisms of these tumors, and for uncovering less toxic candidate drugs for TGCT treatment.

Furthermore, we have made novel and exciting discoveries about the timing of oncogene-induced malignant transformation of germ cells. Our data clearly show that protective mechanisms prevent postnatal oncogenic events in germ cells from inducing tumorigenesis, while also showing evidence that tumorigenesis initiates at E12.5 in our model. However, this timing is only the

earliest we can describe for our model, but we can not rule out additional susceptibility between E12.5 and birth. Our results also do not show at what exact timepoint germ cells become immune to the malignant transformation from these oncogenic events. A temporally controlled, germ cell specific, *CreER* would allow separation of timing and oncogenic pathways to dissect the exact window of susceptibility. This data would help elucidate what protective mechanisms allow some oncogenic events to be dramatically more efficient at transforming germ cells than others. Currently, we have incorporated the conditional oncogenic alleles of *Pten* and *Kras* described above, with the *tdTomato* reporter, also described above. This additional tracking of early and late malignant cells will allow us to observe the earliest signs of germ cell tumorigenesis in vivo, and also determine DDR and changes in transcriptional markers relative to non-*Stra8-cre* expressing germ cells at that time. These data will provide additional insight into the timing malignant transformation susceptibility as well as a better understanding of initial malignant changes that occur in these initiating tumors, thus helping better understand their seemingly disparate path of tumorigenesis compared to most somatic cancers.

The next step for these studies is to further elucidate the mechanistic basis of the DDR following cisplatin treatment as well as other genotoxic drugs. P21 expression was shown to be prognostic of chemoresistant EC in humans, likely avoiding the apoptotic response to cisplatin-induced damage through cell cycle arrest, resulting in a refractory response to the treatment[123]. It is not yet known if cytosolic P21 levels are abnormally low in chemosensitive cells, but quantifying P21 in our EC lines compared to differentiated TR3 and TR11 cell lines will be informative. It is also not known if these EC cells will exhibit any predicted mechanisms of chemosensitivity such as lacking G1 checkpoint or harboring primed BAX at the golgi, as is reported in mouse embryonic stem cells. Elucidation of these phenotypes within the context of this model requires further

experiments to examine cell cycle checkpoint activation, lysate analysis, and response kinetics following exposure to cisplatin discussed further in Chapter 3.

Additionally, it is important to look for response pathways that have yet to be predicted as the underlying cause of chemosensitivity in TGCTs. To do this, genome-wide analysis of mRNA expression is the next immediate step of this study. Previous studies have sought to identify determinants, and the underlying mechanisms, of cisplatin-resistant cancer cells using high-throughput RNA sequencing, but no such studies exist to identify hypersensitivity of EC cells to chemotherapy[242,243]. Beyond the expected pathways of cisplatin sensitivity, this method may reveal unexpected pathways that to help unravel the crosstalk between the pluripotent transcriptional network and DDR. This unique approach could lead to a better understanding of these mechanisms and may lead to entirely novel targets for CSCs in somatic cancers.

APPENDIX

APPENDIX A. PATIENT DERIVED XENOGRAFTS OF CANINE LYMPHOMA

A.1 INTRODUCTION

Testing anti-cancer drugs within meaningful systems, and a better method for developing personalized therapies have been a growing focus of cancer research for decades[244]. Drug response screening with well-established cell lines, such the NCI-60 collection, plays a critical role in drug development as well as identifying predictive response markers and understanding the mechanisms of those responses[245]. However, cells grown under artificial conditions are known to develop mutations and gene expression changes that make them less representative of *in vivo* malignancies (Fig. 4.1). Three-dimensional culture is a growing field that seeks to combine the high-throughput power of two-dimensional culture with a more biologically relevant environment and holds great promise but does not fully represent *in vivo* systems[246]. Currently, there is great interest in the use of patient-derived xenografts (PDX) to avoid the artificially induced aberrations that can occur with in *vitro* studies, and provide a robust model for drug screening and tumor biology[247]. PDX models also provide a more representative genetic profile compared to Genetically Engineered Mouse Models (GEMMs) which usually form disease with one or two specific genetic drivers. The more realistic genetic profiles of the PDX malignancies may result in more translatable drug responses[248]. Ideally, PDX lines are established using fresh tissue from a patient malignancy that is immediately engrafted into an immune compromised mouse, introducing as few potentially selective pressures as possible in hopes of maintaining the initial tumor biology.

Following mammary cancer, lymphoma is the most common malignancy among dogs, with diffuse large B-cell lymphoma (DLBCL) (A type of Non-Hodgkin's lymphoma) being the most

common aggressive lymphoma in dogs[249,250]. DLBCL is a heterogeneous disease but can be categorized by molecular markers into two main types; activated B-cell (ABC) and germinal center B-cell (GCB) in the human disease, the latter of which carries a much better prognosis. Those same molecular markers are not diagnostic of canine DLBCL, but there are many aspects of canine DLBCL that are similar to human DLBCL which correlate to the ABC and GCB subgroups in humans suggesting possible similarities in drivers, cell of origin, and overall genetics between the DLBCL that arises in the two species[253]. Canine cancers have been proposed as a valuable model for human cancers, the study of which has benefits for both species[251,252]. Both humans and canines are treated with CHOP as frontline care for DLBCL, while humans also receive the anti-CD20 antibody rituximab (R-CHOP). Approximately 65% of Non-Hodgkin's lymphoma human patients will survive past ten years leaving an intense interest in new drugs for treating the disease in humans and canines that fail to respond. Despite a large amount of research aimed at studying these cancers, therapy response remains difficult to predict, and further research utilizing PDX models of the disease may help elucidate better predictive factors[249]. Establishing canine lymphoma PDX models will not only help find new treatments for the canine disease but due to the similarities in humans this research could also uncover new treatments for human patients as well. Here we describe results in an ongoing effort to establish the first patient-derived xenografts from separate canine lymphoma patients.

A.2 CREATION OF PDX MODELS FOR CANINE LYMPHOMA

After receiving owner consent, patients underwent removal of lymphoma tissue which was immediately processed according to the protocol described in Methods, Section A.3. Nine total patients have been enrolled in this program (Table A.1) with a detailed listing of individual engraftment attempts enumerated in Table A.3. Two successful PDX lines have been established using these methods (Figure A.1, A.4) and have been continuously propagated in mice, while viable frozen samples have been stored with support from the Cornell Biobank, along with samples for later histological, DNA, RNA, and protein investigations.

The initial engrafted PDX, referred to from here as 14298, came from a neutered male Rottweiler patient at the Cornell Animal Hospital (Table A.1). The original diagnosis was made based on flow cytometry profile, which showed no major shifts in lymphoma markers after initial passages as a PDX in mice (Table A.4, Figure A.2). One notable change in the PDX samples was increased expression of CD3 in initial and secondary passages compared to analysis of the primary tumor. CD3 is associated with T-cell development and T-cell lymphoma, but not B-cell lymphoma as this tumor was originally characterized. The implications of this increased expression are currently unclear, and we will monitor for sustained expression at higher passages. Histologically, the primary tumor and initial passages were similar large B-cell lymphoma samples (Fig. A.3).

The second engrafted PDX, referred to from here as 15810 (Table A.1), grows at approximately twice the rate of 14298, although both engrafted PDX lines still require more accurate growth rate analysis. This dog was not treated at Cornell Animal Hospital but was euthanized there, and the tumor sample was excised immediately after euthanasia. Unfortunately, because this dog was not a patient, no flow cytometry data was collected for the primary tumor, and the diagnosis of B-Cell lymphoma was made based on immunohistochemistry profile. No

substantial changes within the passaged PDX tumors were seen from flow cytometry analysis conducted by Cornell diagnostic laboratories (Table A.5, Figure A.5). One finding of note was the presence of CD5 and CD25 in first passage tumor indicating an activated phenotype, but these markers were absent from second passage tumors. Loss of CD5 after the first passage may indicate a loss of activated T-cells transferred with primary tumor tissue. As PDX mouse 15810-101 became hunched, piloerect and dehydrated necessitating euthanasia, the presence of activated CD3+ T-cells in the primary passage may support the hypothesis of graft-vs-host (GVH) disease from T-cells transferred from engraftment. Although CD3+ T-cells are not a marker for GVH, the NSG host mice are unable to produce CD3+ T-cells[254]. Alternatively, this change may represent a change in expression of tumor cells or a loss of a subpopulation of tumor cells. Histologically, the primary tumor and initial passages were similar large B-cell lymphoma samples (Fig. A.6).

The successful creation of PDX models of canine B-cell lymphoma shows the feasibility of this approach. Current efforts are directed at improving the initial success rate of engraftment from primary tumor by attempts to avoid GVH disease by titrating the initial amount of tissue injected as well as encapsulating tumors in a semi-permeable membrane to prevent the escape of T-cells that are responsible for GVH. Treating mice with T-cell targeted immunosuppressant cyclosporine is another option for reducing the risk of GVH. Using the two currently established PDX lines, we will begin trialing different therapies to identify novel and more efficacious therapies against these malignancies in the hopes of finding better treatments for canine lymphoma patients, and potentially humans.

Table A.1 List of patients from which primary tumors were collected

Collection date	Bank ID	Case ID	Breed	Sex	Tumor type
3/25/2015	13915	236436	Australian Shepherd	Neutered male	T-cell lymphoma
4/3/2015	13972	236607	Golden Retriever	Spayed female	B-cell lymphoma
6/12/2015	14298	238033	Rottweiler	Neutered male	B-cell lymphoma
7/15/2015	14691	238629	Mixed breed dog	Neutered male	B-cell lymphoma
8/4/2015	13378	234615	Golden Retriever	Neutered male	B-cell lymphoma
12/14/2015	15810	242058	Rottweiler	Neutered male	B-cell lymphoma
1/13/2016	15886	190760	Boston Terrier	Spayed female	B-cell lymphoma
2/11/2016	16016	243190	Rottweiler	Spayed female	B-cell lymphoma
8/15/2016	18785	246276	Mixed breed dog	Neutered male	Pending

Table A.2 Identifying markers used for flow cytometry analyses of primary and PDX tumors

(adapted from Tracy Stokol, et al.[255])

Antigen	Cell Population
CD14	Monocytes
CD20	B cells
CD21	B cells
CD22	B cells
CD3	T cells
CD34	Stem cell
CD4	Helper T cells, neutrophils
CD45	All leukocytes
CD5	T cells
CD8a	Cytotoxic T cells
MHCII	Lymphocytes, monocytes

Table A.3 List of PDX mice engrafted with primary or serially transplanted tumor tissue

				Date of death	
Passage	Graft date	Source	Sample ID	No tumor	Endpoint
1	3/25/2015	13915	13915-101		6/14/2015
1	3/25/2015	13915	13915-102		1/14/2015
1	3/25/2015	13915	13915-103		4/10/2015
2	5/16/2015	13915-102	13915-201	10/22/2015	
2	5/16/2015	13915-102	13915-202	10/22/2015	
2	5/16/2015	13915-102	13915-203	10/22/2015	
2	5/16/2015	13915-102	13915-204	10/22/2015	
2	5/16/2015	13915-102	13915-205	10/22/2015	
1	4/3/2015	13972	13972-101		4/27/2015
1	4/3/2015	13972	13972-102		4/30/2015
1	4/3/2015	13972	13972-103		5/5/2015
2	4/30/2015	13972-101	13972-201		6/18/2015
2	4/30/2015	13972-101	13972-202	10/21/2016	
2	4/30/2015	13972-102	13972-203	10/21/2016	
2	4/30/2015	13972-102	13972-204	10/21/2016	

Table A.3 List of PDX mice engrafted with primary or serially transplanted tumor tissue

1	6/12/2015	14298	14298-101		12/10/2015
1	6/12/2015	14298	14298-102		10/1/2015
1	6/12/2015	14298	14298-103		7/24/2015
1	6/12/2015	14298	14298-104		12/28/2015
1	6/12/2015	14298	14298-105		10/30/2015
2	7/24/2015	14298-103	14298-201	10/22/2015	
2	7/24/2015	14298-103	14298-202	10/22/2015	
2	7/24/2015	14298-103	14298-203	10/22/2015	
2	7/24/2015	14298-103	14298-204	10/22/2015	
2	10/1/2015	14298-102	14298-205		1/21/2016
2	10/1/2015	14298-102	14298-206		3/16/2016
2	10/1/2015	14298-102	14298-207		3/16/2016
2	10/1/2015	14298-102	14298-208		1/21/2016
2	10/1/2015	14298-102	14298-209		
2	10/1/2015	14298-102	14298-210		2/18/2016
2	10/1/2015	14298-102	14298-211		3/31/2016
2	10/1/2015	14298-102	14298-212		3/31/2016
2	12/10/2015	14298-101	14298-213		1/21/2016
2	12/10/2015	14298-101	14298-214		
3	1/21/2016	14298-208	14298-304		5/18/2016
3	1/21/2016	14298-208	14298-305		5/18/2016
3	1/21/2016	14298-214	14298-306		5/25/2016
3	1/21/2016	14298-214 (met)	14298-307		6/1/2018
3	1/21/2016	14298-214	14298-308		5/18/2016
3	3/16/2016	14298-207	14298-301		
3	3/16/2016	14298-207	14298-302		
3	3/16/2016	14298-206	14298-303		

Table A.3 List of PDX mice engrafted with primary or serially transplanted tumor tissue

3	3/31/2016	14298-205	14298-309	8/3/2016
3	3/31/2016	14298-211	14298-310	8/3/2016
3	3/31/2016	14298-205	14298-311	8/3/2016
3	3/31/2016	14298-218	14298-312	8/3/2016
4	5/18/2016	14298-308	14298-401	8/17/2016
4	5/18/2016	14298-308	14298-402	
4	5/25/2016	14298-306	14298-403	9/15/2016
4	5/25/2016	14298-306	14298-404	9/15/2016
4	5/25/2016	14298-306	14298-405	
4	5/25/2016	14298-306	14298-406	
4	5/25/2016	14298-306	14298-407	
4	5/25/2016	14298-309 L	14298-408	10/20/2016
4	5/25/2016	14298-309 L	14298-409	10/20/2016
5	8/17/2016	14298-401-T1	14298-501	10/20/2016
5	8/17/2016	14298-401-T1	14298-502	
5	8/17/2016	14298-401-T1	14298-503	
5	9/15/2016	14298-403	14298-504	
5	9/15/2016	14298-403	14298-505	
5	9/15/2016	14298-403	14298-506	
5	9/15/2016	14298-404	14298-507	
5	9/15/2016	14298-404	14298-508	
6	10/20/2016	14298-501-T1	14298-601	
6	10/20/2016	14298-501-T1	14298-602	
6	10/20/2016	14298-501-T1	14298-603	
6	10/20/2016	14298-501-T1	14298-604	
6	10/20/2016	14298-501-T1	14298-605	

Table A.3 List of PDX mice engrafted with primary or serially transplanted tumor tissue

1	7/15/2015	14691a	14691-101		9/7/2015
1	7/15/2015	14691a	14691-102		8/31/2015
1	7/15/2015	14691a	14691-103		8/21/2015
1	7/15/2015	14691a	14691-104		9/3/2015
1	7/16/2015	14691b	14691-105		8/10/2015
1	7/16/2015	14691b	14691-106		8/14/2015
1	7/16/2015	14691b	14691-107		8/14/2015
1	7/16/2015	14691b	14691-108		8/14/2015
2	9/7/2015	14691-101	14691-201		
2	9/7/2015	14691-101	14691-202		
2	9/7/2015	14691-101	14691-203		
2	8/14/2015	14691-106	14691-204	1/9/2016	
2	8/14/2015	14691-106	14691-205		
2	8/14/2015	14691-106	14691-206		
2	8/14/2015	14691-106	14691-207		
2	8/14/2015	14691-106	14691-208		
1	8/4/2015	13378	13378-101		
1	8/4/2015	13378	13378-102		8/31/2015
1	8/4/2015	13378	13378-103		9/2/2015
1	8/4/2015	13378	13378-104		

Table A.3 List of PDX mice engrafted with primary or serially transplanted tumor tissue

1	12/14/2015	15810	15810-101		1/25/2016
1	12/14/2015	15810	15810-102		3/9/2016
1	12/14/2015	15810	15810-103		4/22/2016
2	3/9/2016	15810-102(T3)	15810-201		4/20/2016
2	3/9/2016	15810-102(T3)	15810-202		5/10/2016
2	3/9/2016	15810-102(T3)	15810-203		6/1/2016
2	3/9/2016	15810-102(T3)	15810-204		
2	3/9/2016	15810-102(T2)	15810-205		4/20/2016
2	3/9/2016	15810-102(T4)	15810-206		4/20/2016
3	4/20/2016	15810-205	15810-301		6/15/2016
3	4/20/2016	15810-205	15810-302		6/15/2016
3	4/20/2016	15810-205	15810-303		6/8/2016
3	4/20/2016	15810-206	15810-304		6/8/2016
3	4/20/2016	15810-202	15810-305		6/8/2016
3	6/1/2016	15810-203	15810-306		7/18/2016
3	6/1/2016	15810-203	15810-307		7/18/2016
4	6/15/2016	15810-302-T1	15810-401		
4	6/15/2016	15810-301-T3	15810-402		
4	6/15/2016	15810-301-T3	15810-403		
4	6/8/2016	15810-303-T1	15810-404		7/13/2016
4	6/8/2016	15810-303-T1	15810-405		7/13/2016
4	6/8/2016	15810-303-T1	15810-406		
4	6/8/2016	15810-305-T1	15810-407		7/13/2016
4	6/8/2016	15810-305-T1	15810-408		

Table A.3 List of PDX mice engrafted with primary or serially transplanted tumor tissue

5	7/13/2016	15810-405-T1	15810-501	31-Aug
5	7/13/2016	15810-405-T1	15810-502	31-Aug
5	7/13/2016	15810-407-T1	15810-503	31-Aug
5	7/13/2016	15810-407-T1	15810-504	31-Aug
5	7/13/2016	15810-407-T1	15810-505	10/10/2016
5	7/20/2016	15810-408-T1	15810-506	
5	7/20/2016	15810-408-T1	15810-507	
5	7/20/2016	15810-406-T1	15810-508	
5	7/20/2016	15810-406-T1	15810-509	
6	8/31/2016	15810-501-Internal	15810-601	10/6/2016
6	8/31/2016	15810-501-R	15810-602	10/6/2016
6	8/31/2016	15810-503-T1	15810-603	10/6/2016
6	8/31/2016	15810-503-T1	15810-604	10/19/2016
6	8/31/2016	15810-503-T1	15810-605	10/19/2016
6	8/31/2016	15810-508-T3	15810-606	10/20/2016
6	8/31/2016	15810-508-T3	15810-607	10/27/2016
6	8/31/2016	15810-508-T3	15810-608	10/20/2016
7	10/6/2016	15810-601	15810-701	
7	10/6/2016	15810-602	15810-702	
7	10/6/2016	15810-602	15810-703	
7	10/6/2016	15810-603	15810-704	
7	10/6/2016	15810-603	15810-705	

Figure A.1 PDX transplant lineage map for patient 14298. After successful engraftment of the primary tumor, samples were collected and serially transplanted into multiple mice. Orange indicates that sample was analyzed using flow cytometry analysis, while green indicates the tissue was stored in liquid nitrogen before transplantation. PDX line from patient 14298 was serially transplanted approximately every 3 to 4 months. Tumors arising from frozen tissue had approximately one month delay before initial detection, but then appeared to grow at a similar rate compared to fresh tissue. Likely due to slow growth and soft tissue consistency, these tumors rarely interfere with mouse health, even at larger volumes.

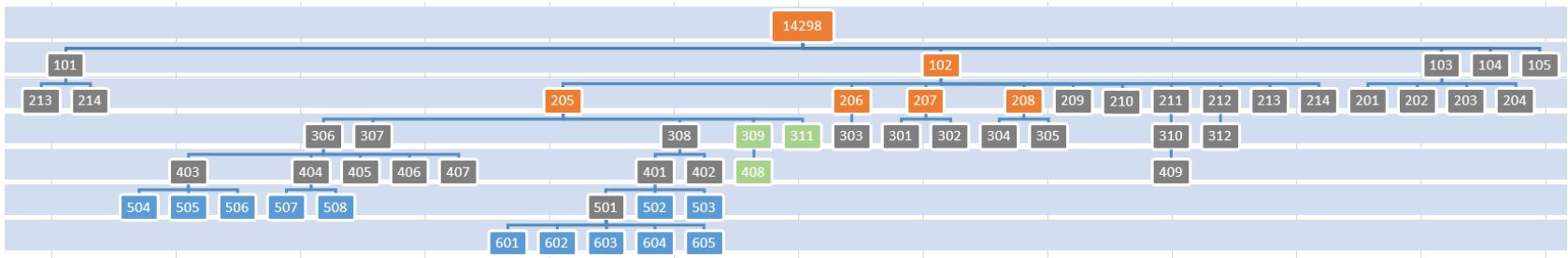
14298
101
102
103
104
105
213
214
205
206
207
208
209
210
211
212
213
214
201
202
203
204
306
307
308
309
311
303
301
302
304
305
310
312
403
404
405
406
407
401
402
408
409
504
505
506
507
508
501
502
503
601
602
603
604
605

Table A.4 Flow cytometry analysis for lymphoma markers on select PDX tumors from 14298. Flow cytometry analysis of primary canine lymphoma, compared to first, and second passages in mice. Report generated by Tracy Stokol and Nicole Belcher of the Cornell diagnostic laboratories. Tumors are relatively unchanged, except for the increased expression of CD3 with the first and second passage compared to the primary tumor. Mean Fluorescence Intensity (MFI).

Date	6/12/2015		10/2/2015		1/26/2016		1/26/2016		3/16/2016		3/16/2016	
	14298		14298-102		14298-205		14298-205		14298-206		14298-207	
Marker	%	MFI	%	MFI	%	MFI	%	MFI	%	MFI	%	MFI
CD4	0		0		Yes		Yes		Yes		Yes	
CD8	0		0		0		Weak		0		0	
MHCII	100	267	100	169	100	125	100	150	99	175	99	153
CD34	10	35	0		few		2		0.4		0.6	
CD3-conj.	0		0		weak		Weak		23	18	40	17
Unconj. CD3	ND		ND		45	41	weak		Weak		42	40
CD5	0		0		0		0		0		0	
CD45	100	991	98	239	100	271	100	375	100	382	98	375
CD21	99	108	91	55	97	121	99	239	96	77	95	137
CD22	100	189	97	37	99	64	99	75	100	66	97	83
CD14	0		0		0		0		0		0	
CD18	99	74	ND		99	60	100	62	100	70	96	43
CD25	ND		ND		93	176	97	159	99	127	99	132
CD28	ND		ND		Weak		Weak		slight		less	
CD94	ND		ND		0		0				0	
FSC	627		ND		693		700		652			
$MHCII^{+}CD34^{+}$	4		ND		2		1		0.4		0.6	

Figure A.2 Flow cytometry data showing increased CD3 from primary and 1st transplant.

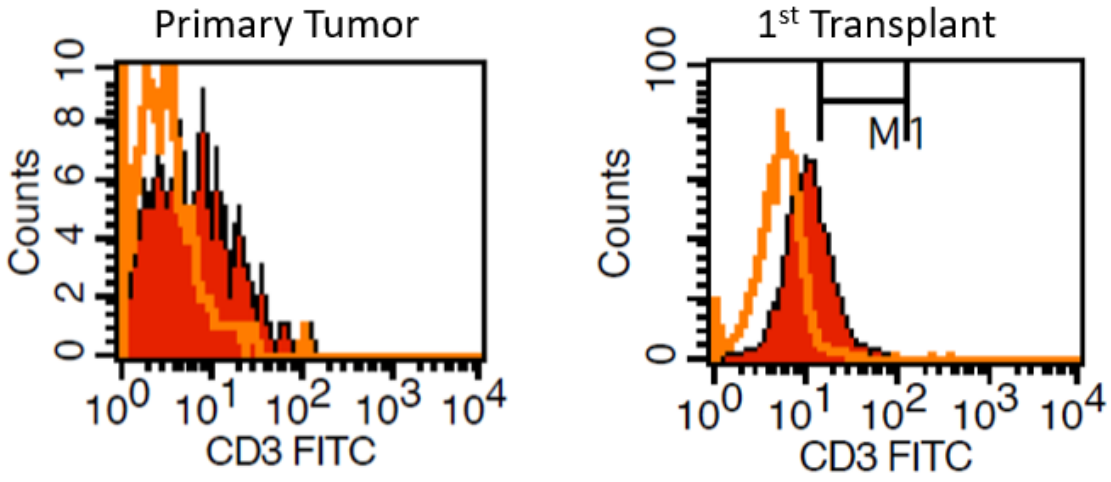

Figure A.3 First passage PDX and primary canine lymphoma are histologically similar. H&E of primary canine lymphoma 14298 (Top Left) and the subsequent serial transplants.

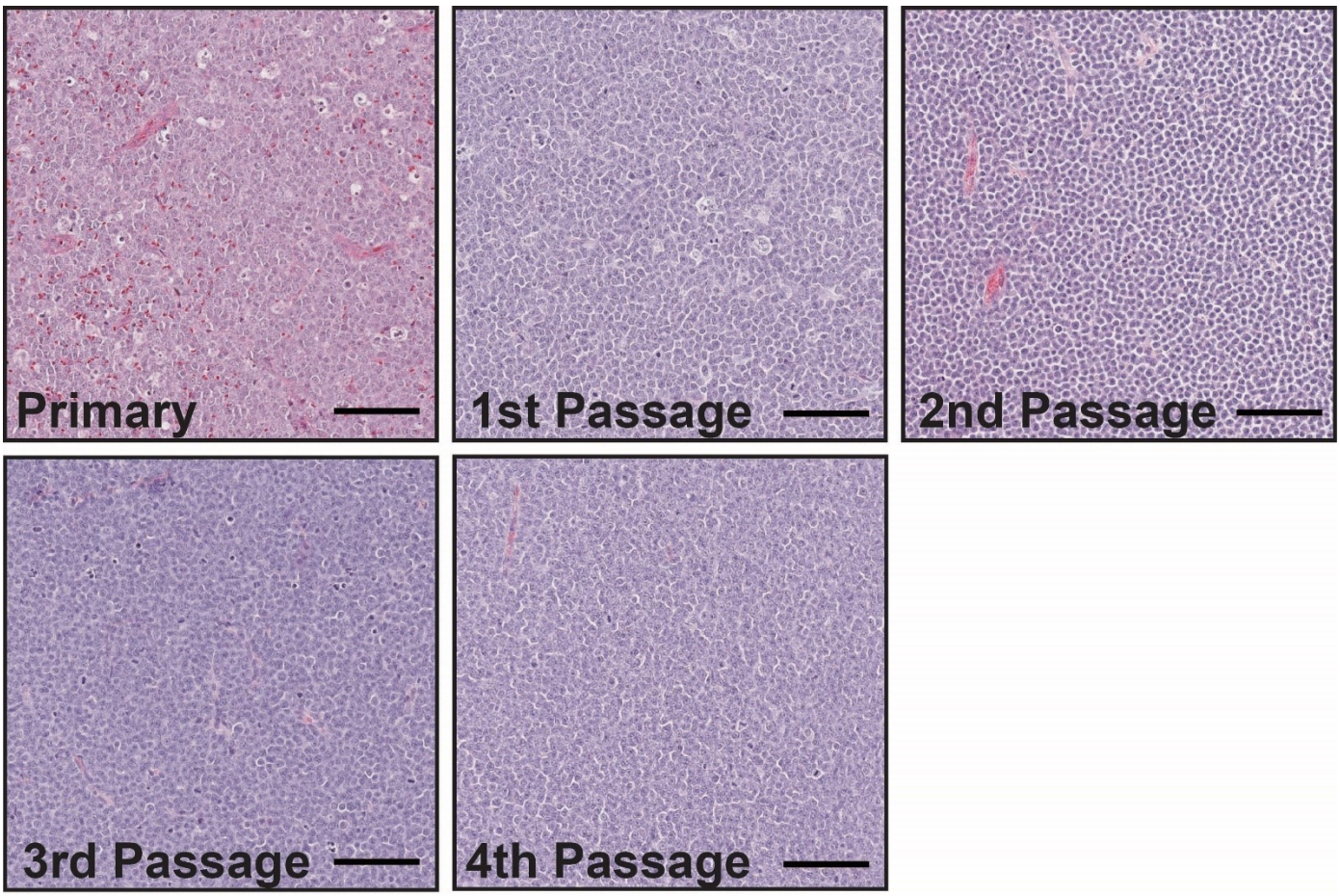

Figure A.4 PDX transplant lineage map for patient 15810. After successful engraftment of the primary tumor, samples were collected and serially transplanted into multiple mice. Orange indicates that sample was analyzed using flow cytometry analysis. PDX line from patient 15810 was serially transplanted approximately every 4 to 6 weeks. Rarely, these tumors ulcerated necessitating earlier than planned transplantation.

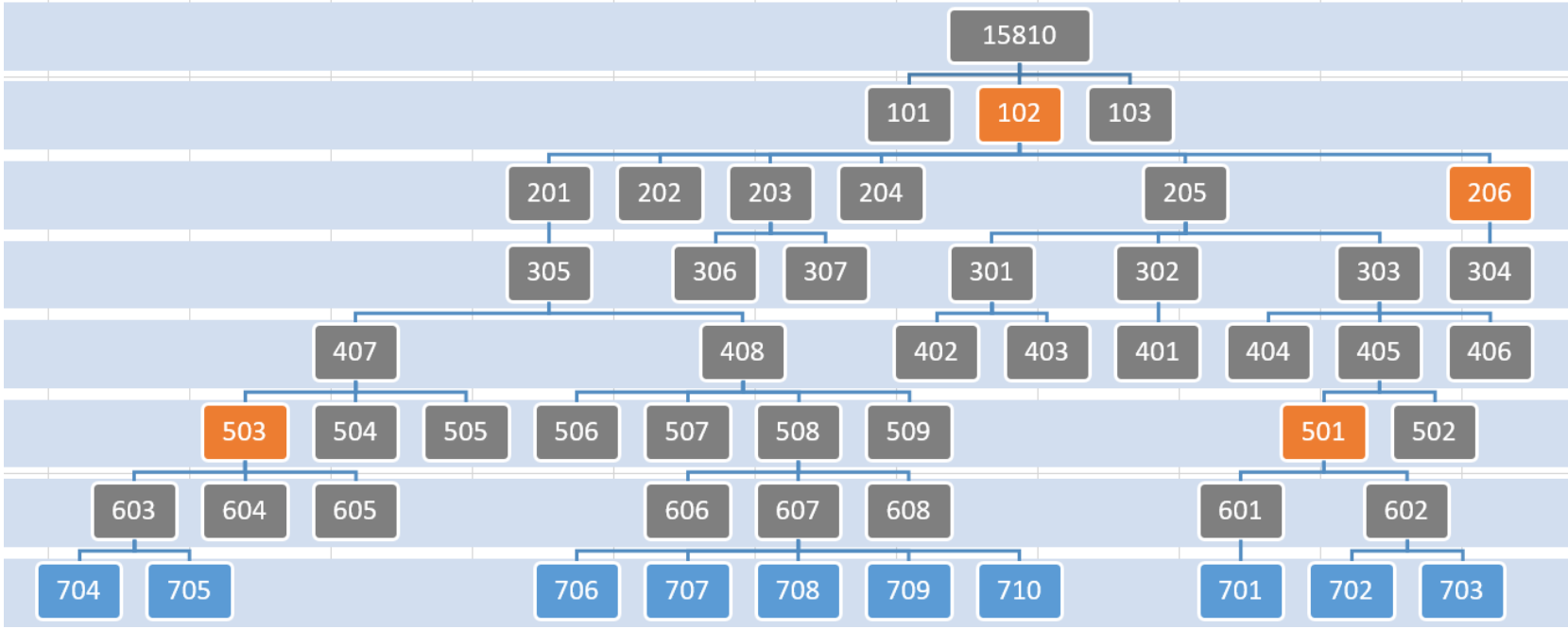
15810
101
102
103
201
202
203
204
205
206
305
306
307
301
302
303
304
407
408
402
403
401
404
405
406
503
504
505
506
507
508
509
501
502
603
604
605
606
607
608
601
602
704
705
706
707
708
709
710
701
702
703

Table A.5 Flow cytometry analysis for lymphoma markers on select PDX tumors from 15810. Flow cytometry analysis of first and second transplants of canine B-cell lymphoma. Primary lymphoma came from dog sample that was a warm body necropsy and no FACs analysis was performed on the original tumor. Loss of CD5 after the first passage is the only notable change and needs to be confirmed at higher passages. Mean Fluorescence Intensity (MFI).

Date	3/9/2016		3/9/2016		4/21/2016	
	15810-102		15810-102		15810-206	
	Suspect met		Initial site		Initial site	
Marker	%	MFI	%	MFI	%	MFI
CD4	0		0		0	
CD8	0		0			
MHCII	97	44	88	21	91	64
CD34	49	23	30	19	54	48
CD3	0		0		0	
CD5	54	28	37	10	0	
CD45	100	253	100	181	99	532
CD21	99	233	100	248	100	673
CD22	100	223	99	99	100	365
CD14	0		0			
CD18	96	58	99	70	98	87
CD25	92	113	94	129	83	128
CD28	0		0			
CD94	0		0			
FSC	634		634		758	
$CD4^+CD8^+$	ND		ND			
$MHCII^+CD34^+$	15*		7*		25*	
CD5:CD21	NA		NA		NA	
CD3:CD5	NA		NA		NA	
CD21:CD22	1:01		1:01		1:01	
CD4:CD8	NA		NA		NA	
CD18:CD45	1:01		1:01		1:01	

Figure A.5 Flow cytometry data showing increased CD3 from 1st transplant to 2nd transplant.

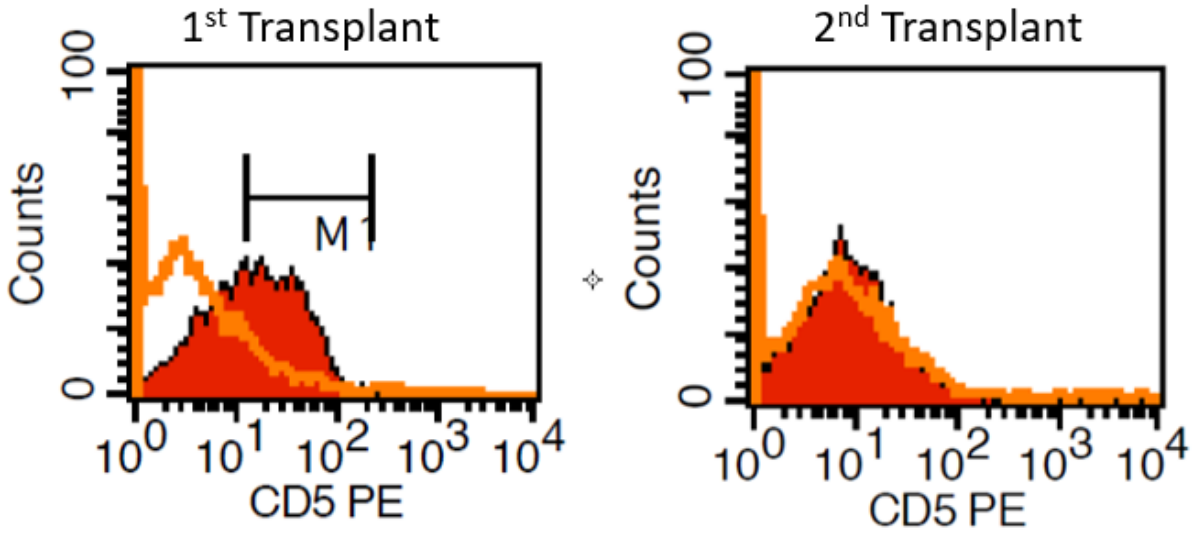

Figure A.6 First passage PDX and primary canine lymphoma are histologically similar. H&E of primary canine lymphoma 15810 (Top Left) and the subsequent serial transplants.

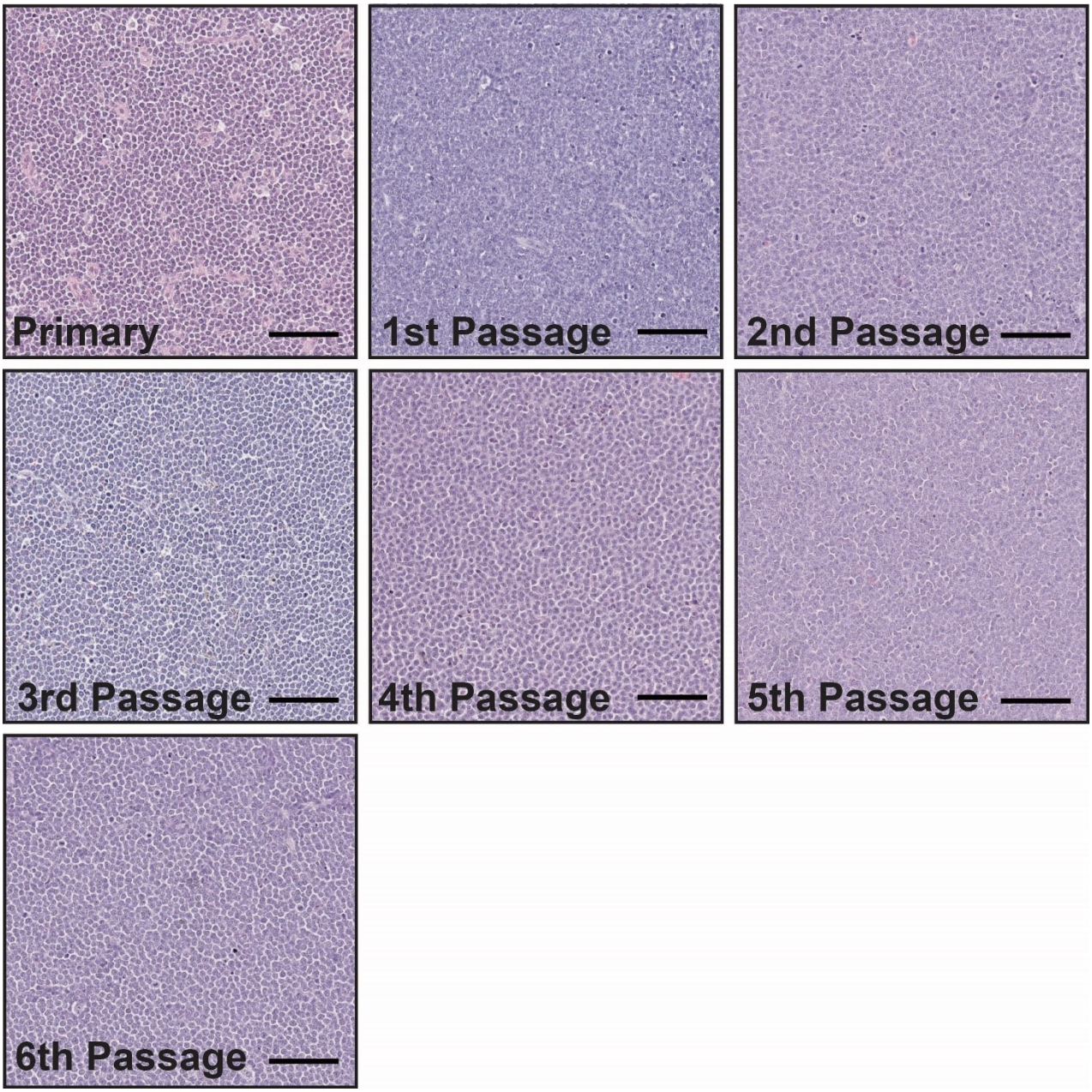

A.3 METHODS

Tissue preparation and injection. Tissue was collected into DMEM with penncillian and streptomycin and stored on ice for approximately one hour after surgery while being delivered. Once obtained, samples were minced, and approximately $2mm^3$ was placed in 1X PBS immediately before injection. NSG mice were anesthetized by isoflurane and $2mm^3$ of tumor tissue was injected into the right and left flank using an 18 gauge needle. Mice were monitored until tumor burden interfered with mobility or until mouse showed signs of dehydration or poor body condition. Tissue from mice was collected under sterile conditions, and serial transplants were performed as described above.

Histology. Fresh tissues were fixed in buffered formalin (Fisher) at room temperature for 24 hours, embedded in wax, and sectioned at 5 μm. Tissues were stained with Eosin (Fisher) and 1:1 hematoxylin (Fisher CS401-1D) solution before dehydration.

Flow cytometry. Fresh samples were prepared by gentle mechanical disaggregation and stored for up to 24 hours on ice in DMEM containing penicillin, streptomycin antibiotics, and 10% FBS. Flow analysis was performed using methods described in Tracy Stokol, et al. (2015)[255].

1. Günesdogan, U. & Surani, M. A. in *Current Topics in Developmental Biology* (ed. Wassarman, P. M.) **117,** 471–496 (Academic Press, 2016).
2. Saitou, M., Kagiwada, S. & Kurimoto, K. Epigenetic reprogramming in mouse pre-implantation development and primordial germ cells. *Development* **139,** 15–31 (2012).
3. Suwińska, A., Czołowska, R., Ożdżeński, W. & Tarkowski, A. K. Blastomeres of the mouse embryo lose totipotency after the fifth cleavage division: Expression of Cdx2 and Oct4 and developmental potential of inner and outer blastomeres of 16- and 32-cell embryos. *Dev. Biol.* **322,** 133–144 (2008).
4. Eckert, J. J. & Fleming, T. P. Tight junction biogenesis during early development. *Biochim. Biophys. Acta BBA - Biomembr.* **1778,** 717–728 (2008).
5. Marlow, F. Primordial Germ Cell Specification and Migration. *F1000Research* **4,** (2015).
6. Ohinata, Y. *et al.* A Signaling Principle for the Specification of the Germ Cell Lineage in Mice. *Cell* **137,** 571–584 (2009).
7. Aramaki, S. *et al.* A Mesodermal Factor, T, Specifies Mouse Germ Cell Fate by Directly Activating Germline Determinants. *Dev. Cell* **27,** 516–529 (2013).
8. Magnúsdóttir, E. *et al.* A tripartite transcription factor network regulates primordial germ cell specification in mice. *Nat. Cell Biol.* **15,** 905–915 (2013).
9. Hayashi, K., Ohta, H., Kurimoto, K., Aramaki, S. & Saitou, M. Reconstitution of the Mouse Germ Cell Specification Pathway in Culture by Pluripotent Stem Cells. *Cell* **146,** 519–532 (2011).
10. Irie, N. *et al.* SOX17 Is a Critical Specifier of Human Primordial Germ Cell Fate. *Cell* **160,** 253–268 (2015).
11. Kushwaha, R. *et al.* Mechanism and Role of SOX2 Repression in Seminoma: Relevance to Human Germline Specification. *Stem Cell Rep.* **6,** 772–783 (2016).
12. Boldajipour, B. & Raz, E. What Is Left Behind—Quality Control in Germ Cell Migration. *Sci. Signal.* **2007,** pe16-pe16 (2007).

13. Leitch, H. G., Tang, W. W. C. & Surani, M. A. in *Current Topics in Developmental Biology* (ed. Heard, E.) **104,** 149–187 (Academic Press, 2013).
14. Sargent, K. M., McFee, R. M., Gomes, R. S. & Cupp, A. S. Vascular endothelial growth factor A: just one of multiple mechanisms for sex-specific vascular development within the testis? *J. Endocrinol.* **227,** R31–R50 (2015).
15. Cool, J., DeFalco, T. & Capel, B. Testis formation in the fetal mouse: dynamic and complex de novo tubulogenesis. *Wiley Interdiscip. Rev. Dev. Biol.* **1,** 847–859 (2012).
16. Nel-Themaat, L. *et al.* Morphometric analysis of testis cord formation in Sox9-EGFP mice. *Dev. Dyn.* **238,** 1100–1110 (2009).
17. Tomaselli, S. *et al.* Human RSPO1 /R-spondin1 Is Expressed during Early Ovary Development and Augments β-Catenin Signaling. *PLOS ONE* **6,** e16366 (2011).
18. Liu, C.-F., Liu, C. & Yao, H. H.-C. Building Pathways for Ovary Organogenesis in the Mouse Embryo. *Curr. Top. Dev. Biol.* **90,** 263–290 (2010).
19. Dolci, S., Campolo, F. & De Felici, M. Gonadal development and germ cell tumors in mouse and humans. *Semin. Cell Dev. Biol.* **45,** 114–123 (2015).
20. Knarston, I., Ayers, K. & Sinclair, A. Molecular mechanisms associated with 46,XX disorders of sex development. *Clin. Sci.* **130,** 421–432 (2016).
21. Bowles, J. *et al.* Retinoid Signaling Determines Germ Cell Fate in Mice. *Science* **312,** 596–600 (2006).
22. Giuili, G. Murine spermatogonial stem cells: targeted transgene expression and purification in an active state. *EMBO Rep.* **3,** 753–759 (2002).
23. Anderson, E. L. *et al.* Stra8 and its inducer, retinoic acid, regulate meiotic initiation in both spermatogenesis and oogenesis in mice. *Proc. Natl. Acad. Sci.* **105,** 14976–14980 (2008).

24. Tagelenbosch, R. A. J. & de Rooij, D. G. A quantitative study of spermatogonial multiplication and stem cell renewal in the C3H/101 F1 hybrid mouse. *Mutat. Res. Mol. Mech. Mutagen.* **290,** 193–200 (1993).
25. Komeya, M. & Ogawa, T. Spermatogonial stem cells: progress and prospects. *Asian J. Androl.* **17,** 771–775 (2015).
26. Hara, K. *et al.* Mouse Spermatogenic Stem Cells Continually Interconvert between Equipotent Singly Isolated and Syncytial States. *Cell Stem Cell* **14,** 658–672 (2014).
27. Nakagawa, T., Sharma, M., Nabeshima, Y., Braun, R. E. & Yoshida, S. Functional Hierarchy and Reversibility within the Murine Spermatogenic Stem Cell Compartment. *Science* **328,** 62–67 (2010).
28. Reuter, V. E. Origins and molecular biology of testicular germ cell tumors. *Mod. Pathol.* **18,** S51–S60 (2005).
29. Moch, H., Cubilla, A. L., Humphrey, P. A., Reuter, V. E. & Ulbright, T. M. The 2016 WHO Classification of Tumours of the Urinary System and Male Genital Organs—Part A: Renal, Penile, and Testicular Tumours. *Eur. Urol.* doi:10.1016/j.eururo.2016.02.029
30. *Pathology and genetics of tumours of the urinary system and male genital organs: [... editorial and consensus conference in Lyon, France, December 14 - 18, 2002]*. (IARC Press, 2006).
31. Ghazarian, A. A., Trabert, B., Devesa, S. S. & McGlynn, K. A. Recent trends in the incidence of testicular germ cell tumors in the United States. *Andrology* **3,** 13–18 (2015).
32. Skakkebæk, N. Originally published as Volume 2, Issue 7776POSSIBLE CARCINOMA-IN-SITU OF THE TESTIS. *The Lancet* **300,** 516–517 (1972).
33. Skakkebæk, N. E. Carcinoma in situ of the testis: frequency and relationship to invasive germ cell tumours in infertile men. *Histopathology* **2,** 157–170 (1978).
34. von der Maase, H. *et al.* Carcinoma in situ of contralateral testis in patients with testicular germ cell cancer: study of 27 cases in 500 patients. *Br. Med. J. Clin. Res. Ed* **293,** 1398–1401 (1986).

35. Rajpert-De Meyts, E., Nielsen, J. E., Skakkebaek, N. E. & Almstrup, K. Diagnostic markers for germ cell neoplasms: from placental-like alkaline phosphatase to micro-RNAs. *Folia Histochem. Cytobiol.* **53,** 177–188 (2015).
36. Almstrup, K. *et al.* Carcinoma in situ testis displays permissive chromatin modifications similar to immature foetal germ cells. *Br. J. Cancer* **103,** 1269–1276 (2010).
37. Eckert, D. *et al.* Expression of BLIMP1/PRMT5and concurrent histone H2A/H4 arginine 3 dimethylation in fetal germ cells, CIS/IGCNU and germ cell tumors. *BMC Dev. Biol.* **8,** 106 (2008).
38. Berney, D. M. *et al.* Germ cell neoplasia in situ (GCNIS): evolution of the current nomenclature for testicular pre-invasive germ cell malignancy. *Histopathology* n/a-n/a (2016). doi:10.1111/his.12958
39. Chia, V. M. *et al.* International Trends in the Incidence of Testicular Cancer, 1973-2002. *Cancer Epidemiol. Biomarkers Prev.* **19,** 1151–1159 (2010).
40. Rajpert-De Meyts, E., McGlynn, K. A., Okamoto, K., Jewett, M. A. S. & Bokemeyer, C. Testicular germ cell tumours. *The Lancet* **387,** 1762–1774 (2016).
41. Horwich, A., Shipley, J. & Huddart, R. Testicular germ-cell cancer. *The Lancet* **367,** 754–765 (2006).
42. Sell, S. Stem cell origin of cancer and differentiation therapy. *Crit. Rev. Oncol. Hematol.* **51,** 1–28 (2004).
43. Kleinsmith, L. & Pierce, B. Multipotentiality of single embryonal carcinoma cells. *Cancer Res.* **24,** 1544–1551 (1964).
44. Jørgensen, A. *et al.* Pathogenesis of germ cell neoplasia in testicular dysgenesis and disorders of sex development. *Semin. Cell Dev. Biol.* **45,** 124–137 (2015).
45. Coppes, M. J., Rackley, R. & Kay, R. Primary testicular and paratesticular tumors of childhood. *Med. Pediatr. Oncol.* **22,** 329–340 (1994).
46. Waheeb, R. & Hofmann, M.-C. Human spermatogonial stem cells: a possible origin for spermatocytic seminoma. *Int. J. Androl.* **34,** e296–e305 (2011).

47. Goriely, A. *et al.* Activating mutations in FGFR3 and HRAS reveal a shared genetic origin for congenital disorders and testicular tumors. *Nat. Genet.* **41,** 1247–1252 (2009).

48. Hemminki, K., Li, X. & Czene, K. Cancer risks in first-generation immigrants to Sweden. *Int. J. Cancer* **99,** 218–228 (2002).

49. Hemminki, K. & Li, X. Familial risk in testicular cancer as a clue to a heritable and environmental aetiology. *Br. J. Cancer* **90,** 1765–1770 (2004).

50. Bussey, K. J. *et al.* Chromosome abnormalities of eighty-one pediatric germ cell tumors: Sex-, age-, site-, and histopathology-related differences—a Children's Cancer Group study. *Genes. Chromosomes Cancer* **25,** 134–146 (1999).

51. Atkin, N. B. & Baker, M. SPECIFIC CHROMOSOME CHANGE, i(12p), IN TESTICULAR TUMOURS? *The Lancet* **320,** 1349 (1982).

52. Looijenga, L. H. *et al.* Role of gain of 12p in germ cell tumour development. *Apmis* **111,** 161–170 (2003).

53. Skotheim, R. I. & Lothe, R. A. The testicular germ cell tumour genome. *APMIS* **111,** 136–151 (2003).

54. Korkola, J. E. *et al.* Down-Regulation of Stem Cell Genes, Including Those in a 200-kb Gene Cluster at 12p13.31, Is Associated with In vivo Differentiation of Human Male Germ Cell Tumors. *Cancer Res.* **66,** 820–827 (2006).

55. Almstrup, K. *et al.* Genome-wide gene expression profiling of testicular carcinoma in situ progression into overt tumours. *Br. J. Cancer* **92,** 1934–1941 (2005).

56. Roskoski Jr., R. Signaling by Kit protein-tyrosine kinase—The stem cell factor receptor. *Biochem. Biophys. Res. Commun.* **337,** 1–13 (2005).

57. Kemmer, K. *et al.* KIT Mutations Are Common in Testicular Seminomas. *Am. J. Pathol.* **164,** 305–313 (2004).

58. McIntyre, A. *et al.* Amplification and Overexpression of the KIT Gene Is Associated with Progression in the Seminoma Subtype of Testicular Germ Cell Tumors of Adolescents and Adults. *Cancer Res.* **65,** 8085–8089 (2005).

59. Rapley, E. A. *et al.* A genome-wide association study of testicular germ cell tumor. *Nat. Genet.* **41,** 807–810 (2009).

60. Park, J.-I., Strock, C. J., Ball, D. W. & Nelkin, B. D. The Ras/Raf/MEK/Extracellular Signal-Regulated Kinase Pathway Induces Autocrine-Paracrine Growth Inhibition via the Leukemia Inhibitory Factor/JAK/STAT Pathway. *Mol. Cell. Biol.* **23,** 543–554 (2003).

61. Shrestha, G. *et al.* The value of genomics in dissecting the RAS-network and in guiding therapeutics for RAS-driven cancers. *Semin. Cell Dev. Biol.* doi:10.1016/j.semcdb.2016.06.012

62. Goddard, N. C. *et al.* KIT and RAS signalling pathways in testicular germ cell tumours: new data and a review of the literature. *Int. J. Androl.* **30,** 337–349 (2007).

63. McIntyre, A. *et al.* Activating Mutations and/or Expression Levels of Tyrosine Kinase Receptors GRB7, RAS, and BRAF in Testicular Germ Cell Tumors. *Neoplasia N. Y. N* **7,** 1047–1052 (2005).

64. Alagaratnam, S., Lind, G. E., Kraggerud, S. M., Lothe, R. A. & Skotheim, R. I. The testicular germ cell tumour transcriptome. *Int. J. Androl.* **34,** e133–e151 (2011).

65. Andreassen, K. E. *et al.* Genetic variation in AKT1, PTEN and the 8q24 locus, and the risk of testicular germ cell tumor. *Hum. Reprod.* **28,** 1995–2002 (2013).

66. Di Vizio, D. *et al.* Loss of the tumor suppressor gene PTEN marks the transition from intratubular germ cell neoplasias (ITGCN) to invasive germ cell tumors. *Oncogene* **24,** 1882–1894 (2005).

67. Fisher, A. D. *et al.* Gender identity, gender assignment and reassignment in individuals with disorders of sex development: a major of dilemma. *J. Endocrinol. Invest.* 1–18 (2016). doi:10.1007/s40618-016-0482-0

68. Baxter, R. M. *et al.* Exome Sequencing for the Diagnosis of 46,XY Disorders of Sex Development. *J. Clin. Endocrinol. Metab.* **100,** E333–E344 (2014).

69. Trabert, B., Zugna, D., Richiardi, L., McGlynn, K. A. & Akre, O. Congenital malformations and testicular germ cell tumors. *Int. J. Cancer J. Int. Cancer* **133,** 1900–1904 (2013).

70. Skakkebæk, N. E., Meyts, E. R.-D. & Main, K. M. Testicular dysgenesis syndrome: an increasingly common developmental disorder with environmental aspects: Opinion. *Hum. Reprod.* **16,** 972–978 (2001).

71. Masters, J. R. W. & Köberle, B. Curing metastatic cancer: lessons from testicular germ-cell tumours. *Nat. Rev. Cancer* **3,** 517–525 (2003).

72. EINHORN, L. H. & DONOHUE, J. Cis-Diamminedichloroplatinum, Vinblastine, and Bleomycin Combination Chemotherapy in Disseminated Testicular Cancer. *J. Urol.* **168,** 2368–2372 (2002).

73. Rosenberg, B., Renshaw, E., Vancamp, L., Hartwick, J. & Drobnik, J. Platinum-Induced Filamentous Growth in Escherichia coli1. *J. Bacteriol.* **93,** 716–721 (1967).

74. Dasari, S. & Tchounwou, P. B. Cisplatin in cancer therapy: molecular mechanisms of action. *Eur. J. Pharmacol.* **0,** 364–378 (2014).

75. Yu, J., Xiao, J., Yang, Y. & Cao, B. Oxaliplatin-Based Doublets Versus Cisplatin or Carboplatin-Based Doublets in the First-Line Treatment of Advanced Nonsmall Cell Lung Cancer. *Medicine (Baltimore)* **94,** (2015).

76. Cullen, M. Surveillance or adjuvant treatments in stage 1 testis germ-cell tumours. *Ann. Oncol.* **23,** x342–x348 (2012).

77. Hande, K. R. Etoposide: four decades of development of a topoisomerase II inhibitor. *Eur. J. Cancer* **34,** 1514–1521 (1998).

78. Müller, W. E. G., Yamazaki, Z., Breter, H.-J. & Zahn, R. K. Action of Bleomycin on DNA and RNA. *Eur. J. Biochem.* **31,** 518–525 (1972).

79. Hecht, S. M. Bleomycin: New Perspectives on the Mechanism of Action [1]. *J. Nat. Prod.* **63,** 158–168 (2000).

80. Stevens, L. C. & Little, C. C. Spontaneous Testicular Teratomas in an Inbred Strain of Mice. *Proc. Natl. Acad. Sci. U. S. A.* **40,** 1080–1087 (1954).

81. Harvey, M., McArthur, M. J., Montgomery, C. A., Bradley, A. & Donehower, L. A. Genetic background alters the spectrum of tumors that develop in p53-deficient mice. *FASEB J.* **7,** 938–943 (1993).

82. Lomelí, H., Ramos-Mejía, V., Gertsenstein, M., Lobe, C. G. & Nagy, A. Targeted insertion of Cre recombinase into the TNAP gene: Excision in primordial germ cells. *genesis* **26,** 116–117 (2000).

83. Kimura, T. *et al.* Conditional loss of PTEN leads to testicular teratoma and enhances embryonic germ cell production. *Development* **130,** 1691–1700 (2003).

84. Matin, A., Collin, G. B., Asada, Y., Varnum, D. & Nadeau, J. H. Susceptibility to testicular germ-cell tumours in a 129.MOLF-Chr 19 chromosome substitution strain. *Nat. Genet.* **23,** 237–240 (1999).

85. Youngren, K. K. *et al.* The Ter mutation in the dead end gene causes germ cell loss and testicular germ cell tumours. *Nature* **435,** 360–364 (2005).

86. Abraham, R. T. Cell cycle checkpoint signaling through the ATM and ATR kinases. *Genes Dev.* **15,** 2177–2196 (2001).

87. Bouaoun, L. *et al.* TP53 Variations in Human Cancers: New Lessons from the IARC TP53 Database and Genomics Data. *Hum. Mutat.* **37,** 865–876 (2016).

88. Bartek, J., Bartkova, J. & Lukas, J. DNA damage signalling guards against activated oncogenes and tumour progression. *Oncogene* **26,** 7773–7779 (2007).

89. Wang, L., Mosel, A. J., Oakley, G. G. & Peng, A. Deficient DNA damage signaling leads to chemoresistance to cisplatin in oral cancer. *Mol. Cancer Ther.* **11,** 2401–2409 (2012).

90. Bartkova, J. *et al.* DNA damage response as a candidate anti-cancer barrier in early human tumorigenesis. *Nature* **434,** 864–870 (2005).

91. Chen, Z. *et al.* Crucial role of p53-dependent cellular senescence in suppression of Pten-deficient tumorigenesis. *Nature* **436,** 725–730 (2005).

92. Bartkova, J., Rajpert-De Meyts, E., Skakkebæk, N. E., Lukas, J. & Bartek, J. DNA damage response in human testes and testicular germ cell tumours: biology and implications for therapy. *Int. J. Androl.* **30,** 282–291 (2007).

93. Bartkova, J. *et al.* DNA damage response mediators MDC1 and 53BP1: constitutive activation and aberrant loss in breast and lung cancer, but not in testicular germ cell tumours. *Oncogene* **26,** 7414–7422 (2007).

94. Olivier, M., Hollstein, M. & Hainaut, P. TP53 Mutations in Human Cancers: Origins, Consequences, and Clinical Use. *Cold Spring Harb. Perspect. Biol.* **2,** (2010).

95. Grosse, L. *et al.* Bax assembles into large ring-like structures remodeling the mitochondrial outer membrane in apoptosis. *EMBO J.* **35,** 402–413 (2016).

96. Pandey, M. K. *et al.* Targeting Cell Survival Proteins for Cancer Cell Death. *Pharm. Basel Switz.* **9,** (2016).

97. Liu, Z. *et al.* BH4 domain of Bcl-2 as a novel target for cancer therapy. *Drug Discov. Today* **21,** 989–996 (2016).

98. Williams, M. M. & Cook, R. S. Bcl-2 family proteins in breast development and cancer: could Mcl-1 targeting overcome therapeutic resistance? *Oncotarget* **6,** 3519–3530 (2015).

99. Zhang, L.-N., Li, J.-Y. & Xu, W. A review of the role of Puma, Noxa and Bim in the tumorigenesis, therapy and drug resistance of chronic lymphocytic leukemia. *Cancer Gene Ther.* **20,** 1–7 (2013).

100. Matt, S. & Hofmann, T. G. The DNA damage-induced cell death response: a roadmap to kill cancer cells. *Cell. Mol. Life Sci.* **73,** 2829–2850 (2016).

101. Liu, J., Uematsu, H., Tsuchida, N. & Ikeda, M.-A. Association of caspase-8 mutation with chemoresistance to cisplatin in HOC313 head and neck squamous cell carcinoma cells. *Biochem. Biophys. Res. Commun.* **390,** 989–994 (2009).

102. Devarajan, E. *et al.* Down-regulation of caspase 3 in breast cancer: a possible mechanism for chemoresistance. *Oncogene* **21,** 8843–8851 (2002).

103. Martin, L. P., Hamilton, T. C. & Schilder, R. J. Platinum Resistance: The Role of DNA Repair Pathways. *Am. Assoc. Cancer Res.* **14,** 1291–1295 (2008).

104. Bertolini, F. *et al.* Prognostic and Predictive Value of Baseline and Posttreatment Molecular Marker Expression in Locally Advanced Rectal Cancer Treated With Neoadjuvant Chemoradiotherapy. *Int. J. Radiat. Oncol. • Biol. • Phys.* **68,** 1455–1461 (2007).

105. Martelli, L., Ragazzi, E., Mario, F. D., Basato, M. & Martelli, M. Cisplatin and Oxaliplatin Cytotoxic Effects in Sensitive and Cisplatin-resistant Human Cervical Tumor Cells: Time and Mode of Application Dependency. *Anticancer Res.* **29,** 3931–3937 (2009).

106. Bai, Z., Wang, Y., Zhe, H., He, J. & Hai, P. ERCC1 mRNA levels can predict the response to cisplatin-based concurrent chemoradiotherapy of locally advanced cervical squamous cell carcinoma. *Radiat. Oncol.* **7,** 221 (2012).

107. Steffensen, K. D., Waldstrøm, M. & Jakobsen, A. The Relationship of Platinum Resistance and ERCC1 Protein Expression in Epithelial Ovarian Cancer: *Int. J. Gynecol. Cancer* **19,** 820–825 (2009).

108. Konstantinopoulos, P. A., Ceccaldi, R., Shapiro, G. I. & D'Andrea, A. D. Homologous recombination deficiency: Exploiting the fundamental vulnerability of ovarian cancer. *Cancer Discov.* **5,** 1137–1154 (2015).

109. Uitto, J. The gene family of ABC transporters – novel mutations, new phenotypes. *Trends Mol. Med.* **11,** 341–343 (2005).

110. WANG, Y. & TENG, J.-S. Increased multi-drug resistance and reduced apoptosis in osteosarcoma side population cells are crucial factors for tumor recurrence. *Exp. Ther. Med.* **12,** 81–86 (2016).

111. Balaji, S. A., Udupa, N., Chamallamudi, M. R., Gupta, V. & Rangarajan, A. Role of the Drug Transporter ABCC3 in Breast Cancer Chemoresistance. *PLOS ONE* **11,** e0155013 (2016).

112. Kuan, C.-T. *et al.* MRP3: a molecular target for human glioblastoma multiforme immunotherapy. *BMC Cancer* **10,** 468 (2010).

113. Hagmann, W., Faissner, R., Schnolzer, M., Lohr, M. & Jesnowski, R. Membrane Drug Transporters and Chemoresistance in Human Pancreatic Carcinoma. *Cancers* **3,** 106–125 (2010).

114. Andersen, V. *et al.* Novel understanding of ABC transporters ABCB1/MDR/P-glycoprotein, ABCC2/MRP2, and ABCG2/BCRP in colorectal pathophysiology. *World J. Gastroenterol.* **21,** 11862–11876 (2015).

115. Moitra, K. & Moitra, K. Overcoming Multidrug Resistance in Cancer Stem Cells, Overcoming Multidrug Resistance in Cancer Stem Cells. *BioMed Res. Int. BioMed Res. Int.* **2015, 2015,** e635745 (2015).

116. Peklak-Scott, C., Smitherman, P. K., Townsend, A. J. & Morrow, C. S. Role of glutathione S-transferase P1-1 in the cellular detoxification of cisplatin. *Am. Assoc. Cancer Res.* **7,** 3247–3255 (2008).

117. Hamada, S.-I., Kamada, M., Furumoto, H., Hirao, T. & Aono, T. Expression of Glutathione S-Transferase-π in Human Ovarian Cancer as an Indicator of Resistance to Chemotherapy. *Gynecol. Oncol.* **52,** 313–319 (1994).

118. Yen, J. L. & McLeod, H. L. Should DPD analysis be required prior to prescribing fluoropyrimidines? *Eur. J. Cancer* **43,** 1011–1016 (2007).

119. Nitiss, J. L. Targeting DNA topoisomerase II in cancer chemotherapy. *Nat. Rev. Cancer* **9,** 338–350 (2009).

120. Lage, H., Helmbach, H., Dietel, M. & Schadendorf, D. Modulation of DNA topoisomerase II activity and expression in melanoma cells with acquired drug resistance. *Br. J. Cancer* **82,** 488–491 (2000).

121. Mayer, F., Honecker, F., Looijenga, L. H. J. & Bokemeyer, C. Towards an understanding of the biological basis of response to cisplatin-based chemotherapy in germ-cell tumors. *Ann. Oncol.* **14,** 825–832 (2003).

122. Houldsworth, J. *et al.* Human male germ cell tumor resistance to cisplatin is linked to TP53 gene mutation. *Oncogene* **16,** 2345–2349 (1998).

123. Koster, R. *et al.* Cytoplasmic p21 expression levels determine cisplatin resistance in human testicular cancer. *J. Clin. Invest.* **120,** 3594–3605 (2010).

124. Cárcano, F. M. *et al.* Absence of microsatellite instability and BRAF (V600E) mutation in testicular germ cell tumors. *Andrology* n/a-n/a (2016). doi:10.1111/andr.12200

125. Zhang, M., Yang, C., Liu, H. & Sun, Y. Induced Pluripotent Stem Cells Are Sensitive to DNA Damage. *Genomics Proteomics Bioinformatics* **11,** 320–326 (2013).

126. Smith, A. J. *et al.* Apoptotic Susceptibility to DNA Damage of Pluripotent Stem Cells Facilitates Pharmacologic Purging of Teratoma Risk. *Stem Cells Transl. Med.* **1,** 709–718 (2012).

127. Dumitru, R. *et al.* Human Embryonic Stem Cells Have Constitutively Active Bax at the Golgi and Are Primed to Undergo Rapid Apoptosis. *Mol. Cell* **46,** 573–583 (2012).

128. Desmarais, J. A., Unger, C., Damjanov, I., Meuth, M. & Andrews, P. Apoptosis and failure of checkpoint kinase 1 activation in human induced pluripotent stem cells under replication stress. *Stem Cell Res. Ther.* **7,** 17 (2016).

129. Hong, Y. & Stambrook, P. J. Restoration of an absent G1 arrest and protection from apoptosis in embryonic stem cells after ionizing radiation. *Proc. Natl. Acad. Sci. U. S. A.* **101,** 14443–14448 (2004).

130. Mitsui, K. *et al.* The Homeoprotein Nanog Is Required for Maintenance of Pluripotency in Mouse Epiblast and ES Cells. *Cell* **113,** 631–642 (2003).

131. Lin, T. *et al.* p53 induces differentiation of mouse embryonic stem cells by suppressing Nanog expression. *Nat. Cell Biol.* **7,** 165–171 (2005).

132. Zhang, Z.-N., Chung, S.-K., Xu, Z. & Xu, Y. Oct4 Maintains the Pluripotency of Human Embryonic Stem Cells by Inactivating p53 Through Sirt1-Mediated Deacetylation. *STEM CELLS* **32,** 157–165 (2014).

133. Mariusz Z., R., Schneider, G. & Sellers, Z. P. The embryonic rest hypothesis of cancer development – an old XIX century theory revisited. *J. Cancer Stem Cell Res.* **1,** 1 (2014).

134. Reya, T., Morrison, S. J., Clarke, M. F. & Weissman, I. L. Stem cells, cancer, and cancer stem cells. *Nature* **414,** 105–111 (2001).

135. Bonnet, D. & Dick, J. E. Human acute myeloid leukemia is organized as a hierarchy that originates from a primitive hematopoietic cell. *Nat. Med.* **3,** 730–737 (1997).

136. Das, S., Srikanth, M. & Kessler, J. A. Cancer stem cells and glioma. *Nat. Rev. Neurol.* **4,** 427–435 (2008).

137. Jordan, C. T. Cancer Stem Cells: Controversial or Just Misunderstood? *Cell Stem Cell* **4,** 203–205 (2009).

138. Quintana, E. *et al.* Phenotypic Heterogeneity among Tumorigenic Melanoma Cells from Patients that Is Reversible and Not Hierarchically Organized. *Cancer Cell* **18,** 510–523 (2010).

139. Boiko, A. D. *et al.* Human melanoma-initiating cells express neural crest nerve growth factor receptor CD271. *Nature* **466,** 133–137 (2010).

140. Döhner, H., Weisdorf, D. J. & Bloomfield, C. D. Acute Myeloid Leukemia. *N. Engl. J. Med.* **373,** 1136–1152 (2015).

141. Druker, B. J. *et al.* Five-Year Follow-up of Patients Receiving Imatinib for Chronic Myeloid Leukemia. *N. Engl. J. Med.* **355,** 2408–2417 (2006).

142. Conneally, E., Cashman, J., Petzer, A. & Eaves, C. Expansion in vitro of transplantable human cord blood stem cells demonstrated using a quantitative assay of their lympho-myeloid repopulating activity in nonobese diabetic–scid/scid mice. *Proc. Natl. Acad. Sci.* **94,** 9836–9841 (1997).

143. Elrick, L. J., Jorgensen, H. G., Mountford, J. C. & Holyoake, T. L. Punish the parent not the progeny. *Blood* **105,** 1862–1866 (2005).

144. Saito, Y. *et al.* Induction of cell cycle entry eliminates human leukemia stem cells in a mouse model of AML. *Nat. Biotechnol.* **28,** 275–280 (2010).

145. Pelosi, E., Castelli, G. & Testa, U. Targeting LSCs through membrane antigens selectively or preferentially expressed on these cells. *Blood Cells. Mol. Dis.* **55,** 336–346 (2015).

146. Sánchez-Aguilera, A. & Méndez-Ferrer, S. The hematopoietic stem-cell niche in health and leukemia. *Cell. Mol. Life Sci.* 1–12 (2016). doi:10.1007/s00018-016-2306-y

147. Nachliely, M., Sharony, E., Bolla, N. R., Kutner, A. & Danilenko, M. Prodifferentiation Activity of Novel Vitamin D2 Analogs PRI-1916 and PRI-1917 and Their Combinations with a Plant Polyphenol in Acute Myeloid Leukemia Cells. *Int. J. Mol. Sci.* **17,** 1068 (2016).

148. Al-Hajj, M., Wicha, M. S., Benito-Hernandez, A., Morrison, S. J. & Clarke, M. F. Prospective identification of tumorigenic breast cancer cells. *Proc. Natl. Acad. Sci. U. S. A.* **100,** 3983–3988 (2003).

149. Allegra, A. *et al.* The Cancer Stem Cell Hypothesis: A Guide to Potential Molecular Targets. *Cancer Invest.* **32,** 470–495 (2014).

150. Li, X. *et al.* Intrinsic Resistance of Tumorigenic Breast Cancer Cells to Chemotherapy. *J. Natl. Cancer Inst.* **100,** 672–679 (2008).

151. Shafee, N. *et al.* Cancer Stem Cells Contribute to Cisplatin Resistance in Brca1/p53–Mediated Mouse Mammary Tumors. *Cancer Res.* **68,** 3243–3250 (2008).

152. Yeboa, D. N. & Evans, S. B. Contemporary Breast Radiotherapy and Cardiac Toxicity. *Semin. Radiat. Oncol.* **26,** 71–78 (2016).

153. Diehn, M. *et al.* Association of reactive oxygen species levels and radioresistance in cancer stem cells. *Nature* **458,** 780–783 (2009).

154. McLendon, R. E. & Halperin, E. C. Is the long-term survival of patients with intracranial glioblastoma multiforme overstated? *Cancer* **98,** 1745–1748 (2003).

155. Rundle-Thiele, D., Head, R., Cosgrove, L. & Martin, J. H. Repurposing some older drugs that cross the blood–brain barrier and have potential anticancer activity to provide new treatment options for glioblastoma. *Br. J. Clin. Pharmacol.* **81,** 199–209 (2016).

156. Ignatova, T. N. *et al.* Human cortical glial tumors contain neural stem-like cells expressing astroglial and neuronal markers in vitro. *Glia* **39,** 193–206 (2002).

157. Singh, S. K. *et al.* Identification of human brain tumour initiating cells. *Nature* **432,** 396–401 (2004).

158. Suvà, M. L. *et al.* Reconstructing and Reprogramming the Tumor-Propagating Potential of Glioblastoma Stem-like Cells. *Cell* **157,** 580–594 (2014).

159. Bao, S. *et al.* Glioma stem cells promote radioresistance by preferential activation of the DNA damage response. *Nature* **444,** 756–760 (2006).

160. Beier, D. *et al.* Temozolomide Preferentially Depletes Cancer Stem Cells in Glioblastoma. *Cancer Res.* **68,** 5706–5715 (2008).

161. Liu, G. *et al.* Analysis of gene expression and chemoresistance of CD133+ cancer stem cells in glioblastoma. *Mol. Cancer* **5,** 67 (2006).

162. Zavras, N., Siristatidis, C., Siatelis, A. & Koumarianou, A. Fertility Risk Assessment and Preservation in Male and Female Prepubertal and Adolescent Cancer Patients. *Clin. Med. Insights Oncol.* **10,** 49–57 (2016).

163. Kelly, E. B. *Stem Cells*. (Greenwood Publishing Group, 2007).

164. Pierce, B., Verney, E. L. & Dixon, F. J. The Biology of Testicular Cancer. *Cancer Res.* **17,** 134–138 (1957).

165. Andrews, P. W. *et al.* Embryonic stem (ES) cells and embryonal carcinoma (EC) cells: opposite sides of the same coin. *Biochem. Soc. Trans.* **33,** 1526–1530 (2005).

166. Jacob, F. The Leeuwenhoek Lecture, 1977: Mouse Teratocarcinoma and Mouse Embryo. *Proc. R. Soc. Lond. B Biol. Sci.* **201,** 249–270 (1978).

167. Martin, G. R. Isolation of a pluripotent cell line from early mouse embryos cultured in medium conditioned by teratocarcinoma stem cells. *Proc. Natl. Acad. Sci.* **78,** 7634–7638 (1981).

168. Lin, Y. *et al.* Reciprocal Regulation of Akt and Oct4 Promotes the Self-Renewal and Survival of Embryonal Carcinoma Cells. *Mol. Cell* **48,** 627–640 (2012).

169. Jackson, T. R. *et al.* DNA damage causes TP53-dependent coupling of self-renewal and senescence pathways in embryonal carcinoma cells. *Cell Cycle* **12,** 430–441 (2013).

170. Mueller, S. *et al.* Cell-cycle progression and response of germ cell tumors to cisplatin in vitro. *Int. J. Oncol.* **29,** 471–480 (2006).

171. Li, B., Cheng, Q., Li, Z. & Chen, J. p53 inactivation by MDM2 and MDMX negative feedback loops in testicular germ cell tumors. *Cell Cycle* **9,** 1411–1420 (2010).

172. Gorbatiy, V., Spiess, P. E. & Pisters, L. L. The growing teratoma syndrome: Current review of the literature. *Indian J. Urol. IJU J. Urol. Soc. India* **25,** 186–189 (2009).

173. Sonneveld, D. J. A. *et al.* Mature teratoma identified after postchemotherapy surgery in patients with disseminated nonseminomatous testicular germ cell tumors. *Cancer* **82,** 1343–1351 (1998).

174. Nigam, M., Aschebrook-Kilfoy, B., Shikanov, S. & Eggener, S. Increasing incidence of testicular cancer in the United States and Europe between 1992 and 2009. *World J. Urol.* 1–9 (2014). doi:10.1007/s00345-014-1361-y

175. Howlader N, N. A., Krapcho M, Miller D, Bishop K, Altekruse SF, Kosary CL, Yu M, Ruhl J, Tatalovich Z, Mariotto A, Lewis DR, Chen HS, Feuer EJ, Cronin KA (eds). *SEER Cancer Statistics Review, 1975-2013, National Cancer Institute.* (2016).

176. Moch, H., Cubilla, A. L., Humphrey, P. A., Reuter, V. E. & Ulbright, T. M. The 2016 WHO Classification of Tumours of the Urinary System and Male Genital Organs-Part A: Renal, Penile, and Testicular Tumours. *Eur Urol* **70,** 93–105 (2016).

177. Chieffi, P. & Chieffi, S. Molecular biomarkers as potential targets for therapeutic strategies in human testicular germ cell tumors: An overview. *J. Cell. Physiol.* **228,** 1641–1646 (2013).

178. de Jong, J. *et al.* Diagnostic value of OCT3/4 for pre-invasive and invasive testicular germ cell tumours. *J Pathol* **206,** 242–9 (2005).

179. de Jong, J. & Looijenga, L. H. Stem cell marker OCT3/4 in tumor biology and germ cell tumor diagnostics: history and future. *Crit Rev Oncog* **12,** 171–203 (2006).

180. de Jong, J. *et al.* Differential expression of SOX17 and SOX2 in germ cells and stem cells has biological and clinical implications. *J Pathol* **215,** 21–30 (2008).

181. Hart, A. H. *et al.* The pluripotency homeobox gene NANOG is expressed in human germ cell tumors. *Cancer* **104,** 2092–8 (2005).

182. Visvader, J. E. & Lindeman, G. J. Cancer Stem Cells: Current Status and Evolving Complexities. *Cell Stem Cell* **10,** 717–728 (2012).

183. Oosterhuis, J. W., Andrews, P. W., Knowles, B. B. & Damjanov, I. Effects of cis-platinum on embryonal carcinoma cell lines in vitro. *Int J Cancer* **34,** 133–9 (1984).

184. Stevens, L. A new inbred subline of mice (129-terSv) with a high incidence of spontaneous congenital testicular teratomas. *J Natl Cancer Inst* **50,** 235–42 (1973).

185. McGlynn, K. A. & Cook, M. B. Etiologic factors in testicular germ cell tumors. *Future Oncol. Lond. Engl.* **5,** 1389–1402 (2009).

186. Heaney, J. D. & Nadeau, J. H. in *Germline Stem Cells* (eds. Hou, S. X. & Singh, S. R.) 211–231 (Humana Press, 2008).

187. Hammond, S. *et al.* Chromosome X modulates incidence of testicular germ cell tumors in Ter mice. *Mamm. Genome* **18,** 832–838 (2007).

188. Litchfield, K., Levy, M., Huddart, R. A., Shipley, J. & Turnbull, C. The genomic landscape of testicular germ cell tumours: from susceptibility to treatment. *Nat. Rev. Urol.* **advance online publication,** (2016).

189. Jackson, E. L. *et al.* Analysis of lung tumor initiation and progression using conditional expression of oncogenic K-ras. *Genes Dev.* **15,** 3243–3248 (2001).

190. Lesche, R. *et al.* Cre/loxP-mediated inactivation of the murine Pten tumor suppressor gene. *genesis* **32,** 148–149 (2002).

191. Sadate-Ngatchou, P. I., Payne, C. J., Dearth, A. T. & Braun, R. E. Cre Recombinase Activity Specific to Postnatal, Premeiotic Male Germ Cells in Transgenic Mice. *Genes. N. Y. N 2000* **46,** 738–742 (2008).

192. Nonaka, D. Differential Expression of SOX2 and SOX17 in Testicular Germ Cell Tumors. *Am. J. Clin. Pathol.* **131,** 731–736 (2009).

193. Sachlos, E. *et al.* Identification of Drugs Including a Dopamine Receptor Antagonist that Selectively Target Cancer Stem Cells. *Cell* **149,** 1284–1297 (2012).

194. Feng, C.-W., Bowles, J. & Koopman, P. Control of mammalian germ cell entry into meiosis. *Mol. Cell. Endocrinol.* **382,** 488–497 (1).

195. Fujiwara, Y. *et al.* Isolation of a DEAD-family protein gene that encodes a murine homolog of Drosophila vasa and its specific expression in germ cell lineage. *Proc Natl Acad Sci U A* **91,** 12258–62 (1994).

196. Swartzendruber, D. E., Cram, L. S. & Lehman, J. M. Microfluorometric analysis of DNA content changes in a murine teratocarcinoma. *Cancer Res.* **36,** 1894–99 (1976).

197. Barlow, J. H., Lisby, M. & Rothstein, R. Differential regulation of the cellular response to DNA double-strand breaks in G1. *Mol Cell* **30,** 73–85 (2008).

198. Heaney, J. D. *et al.* Germ cell pluripotency, premature differentiation and susceptibility to testicular teratomas in mice. *Development* **139,** 1577–1586 (2012).

199. Yao, H. H., DiNapoli, L. & Capel, B. Meiotic germ cells antagonize mesonephric cell migration and testis cord formation in mouse gonads. *Development* **130,** 5895–902 (2003).

200. Bustamante-Marin, X., Garness, J. A. & Capel, B. Testicular teratomas: an intersection of pluripotency, differentiation and cancer biology. *Int J Dev Biol* **57,** 201–10 (2013).

201. Cook, M. S., Munger, S. C., Nadeau, J. H. & Capel, B. Regulation of male germ cell cycle arrest and differentiation by DND1 is modulated by genetic background. *Development* **138,** 23–32 (2011).

202. Russell, L. D., Chiarini-Garcia, H., Korsmeyer, S. J. & Knudson, C. M. Bax-dependent spermatogonia apoptosis is required for testicular development and spermatogenesis. *Biol Reprod* **66,** 950–8 (2002).

203. Huang, Y., Mao, X., Boyce, T. & Zhu, G. Dispensable role of PTEN in mouse spermatogenesis. *Cell Biol. Int.* **35,** 905–908 (2011).

204. Guerra, C. *et al.* Tumor induction by an endogenous K-ras oncogene is highly dependent on cellular context. *Cancer Cell* **4,** 111–120 (2003).

205. Johnson, L. *et al.* Somatic activation of the K-ras oncogene causes early onset lung cancer in mice. *Nature* **410,** 1111–1116 (2001).

206. Knobbe, C. B., Lapin, V., Suzuki, A. & Mak, T. W. The roles of PTEN in development, physiology and tumorigenesis in mouse models: a tissue-by-tissue survey. *Oncogene* **27,** 5398–415 (2008).

207. Mullany, L. K. *et al.* Molecular and functional characteristics of ovarian surface epithelial cells transformed by KrasG12D and loss of Pten in a mouse model in vivo. *Oncogene* **30,** 3522–36 (2011).

208. Hill, R. *et al.* PTEN loss accelerates KrasG12D-induced pancreatic cancer development. *Cancer Res* **70,** 7114–24 (2010).

209. Nogueira, C. *et al.* Cooperative interactions of PTEN deficiency and RAS activation in melanoma metastasis. *Oncogene* **29,** 6222–32 (2010).

210. Reddy, P. *et al.* Oocyte-specific deletion of Pten causes premature activation of the primordial follicle pool. *Science* **319,** 611–3 (2008).

211. Lee, J. *et al.* Genetic reconstruction of mouse spermatogonial stem cell self-renewal in vitro by Ras-cyclin D2 activation. *Cell Stem Cell* **5,** 76–86 (2009).

212. Lindgren, A. G. *et al.* Loss of Pten causes tumor initiation following differentiation of murine pluripotent stem cells due to failed repression of Nanog. *PLoS One* **6,** e16478 (2011).

213. Ge, X. Q. *et al.* Embryonic Stem Cells License a High Level of Dormant Origins to Protect the Genome against Replication Stress. *Stem Cell Rep.* **5,** 185–94 (2015).

214. Groszer, M. *et al.* Negative Regulation of Neural Stem/Progenitor Cell Proliferation by the Pten Tumor Suppressor Gene in Vivo. *Science* **294,** 2186–2189 (2001).

215. Szabo, P. E., Hubner, K., Scholer, H. & Mann, J. R. Allele-specific expression of imprinted genes in mouse migratory primordial germ cells. *Mech Dev* **115,** 157–60 (2002).

216. Madisen, L. *et al.* A robust and high-throughput Cre reporting and characterization system for the whole mouse brain. *Nat Neurosci* **13,** 133–40 (2010).

217. Carro, A., Rico, D., Rueda, O. M., Díaz-Uriarte, R. & Pisano, D. G. waviCGH: a web application for the analysis and visualization of genomic copy number alterations. *Nucleic Acids Res.* **38,** W182–W187 (2010).

218. Thomas, P. D. *et al.* PANTHER: A Library of Protein Families and Subfamilies Indexed by Function. *Genome Res.* **13,** 2129–2141 (2003).

219. Thomas, P. D. *et al.* Applications for protein sequence–function evolution data: mRNA/protein expression analysis and coding SNP scoring tools. *Nucleic Acids Res.* **34,** W645–W650 (2006).

220. Chen, E. Y. *et al.* Enrichr: interactive and collaborative HTML5 gene list enrichment analysis tool. *BMC Bioinformatics* **14,** 128 (2013).

221. Lyndaker, A. M. *et al.* Conditional Inactivation of the DNA Damage Response Gene Hus1 in Mouse Testis Reveals Separable Roles for Components of the RAD9-RAD1-HUS1 Complex in Meiotic Chromosome Maintenance. *PLoS Genet* **9,** e1003320 (2013).

222. Hu, Y. & Smyth, G. K. ELDA: extreme limiting dilution analysis for comparing depleted and enriched populations in stem cell and other assays. *J Immunol Methods* **347,** 70–8 (2009).

223. Feldman DR, Bosl GJ, Sheinfeld J & Motzer RJ. MEdical treatment of advanced testicular cancer. *JAMA* **299,** 672–684 (2008).

224. Yang, M., Liu, P. & Huang, P. Cancer stem cells, metabolism, and therapeutic significance. *Tumor Biol.* **37,** 5735–5742 (2016).

225. Watanabe, K. *et al.* A ROCK inhibitor permits survival of dissociated human embryonic stem cells. *Nat. Biotechnol.* **25,** 681–686 (2007).

226. Smith, A. G. *et al.* Inhibition of pluripotential embryonic stem cell differentiation by purified polypeptides. *Nature* **336,** 688–690 (1988).

227. Brown, G. S., Brown, M. A., Hilton, D., Gough, N. M. & Sleigh, M. J. Inhibition of Differentiation in a Murine F9 Embryonal Carcinoma Cell Subline by Leukemia Inhibitory Factor (LIF). *Growth Factors* **7,** 41–52 (1992).

228. Przyborski, S. A., Christie, V. B., Hayman, M. W., Stewart, R. & Horrocks, G. M. Human embryonal carcinoma stem cells: models of embryonic development in humans. *Stem Cells Dev.* **13,** 400–408 (2004).

229. Liu, X. *et al.* miR-30c regulates proliferation, apoptosis and differentiation via the Shh signaling pathway in P19 cells. *Exp. Mol. Med.* **48,** e248 (2016).

230. Cavallo, F. *et al.* Reduced Proficiency in Homologous Recombination Underlies the High Sensitivity of Embryonal Carcinoma Testicular Germ Cell Tumors to Cisplatin and Poly (ADP-Ribose) Polymerase Inhibition. *PLoS ONE* **7,** e51563 (2012).

231. Voutsadakis, I. A. The chemosensitivity of testicular germ cell tumors. *Cell. Oncol.* **37,** 79–94 (2014).

232. Kerley-Hamilton, J. S., Pike, A. M., Li, N., DiRenzo, J. & Spinella, M. J. A p53-dominant transcriptional response to cisplatin in testicular germ cell tumor-derived human embyronal carcinoma. *Oncogene* **24,** 6090–6100 (2005).

233. Carouge, D. & Nadeau, J. H. Mouse models of testicular germ cell tumors. *Germ Cell Tumor* 75–106 (2012).

234. Hajkova, P. *et al.* Chromatin dynamics during epigenetic reprogramming in the mouse germ line. *Nature* **452,** 877–881 (2008).

235. Hajkova, P. *et al.* Genome-wide reprogramming in the mouse germ line entails the base excision repair pathway. *Science* **329,** (2010).

236. Parikh, N., Shuck, R. L., Nguyen, T.-A., Herron, A. & Donehower, L. A. Mouse Tissues that Undergo Neoplastic Progression after K-Ras Activation Are Distinguished by Nuclear Translocation of

phospho-Erk1/2 and Robust Tumor Suppressor Responses. *Am. Assoc. Cancer Res.* **10,** 845–855 (2012).

237. Liao, J. *et al.* Inhibition of PTEN Tumor Suppressor Promotes the Generation of Induced Pluripotent Stem Cells. *Mol. Ther.* (2013). doi:10.1038/mt.2013.60

238. McIver, S. C., Roman, S. D., Nixon, B., Loveland, K. L. & McLaughlin, E. A. The rise of testicular germ cell tumours: the search for causes, risk factors and novel therapeutic targets. *F1000Research* **2,** (2013).

239. Yang, F., Xu, J., Tang, L. & Guan, X. Breast cancer stem cell: the roles and therapeutic implications. *Cell. Mol. Life Sci.* 1–16 (2016). doi:10.1007/s00018-016-2334-7

240. Sell, S. Stem cell origin of cancer and differentiation therapy. *Crit. Rev. Oncol. Hematol.* **51,** 1–28 (2004).

241. Soprano, D. R., Teets, B. W. & Soprano, K. J. in (ed. Hormones, B.-V. &) **75,** 69–95 (Academic Press, 2007).

242. Yang, L.-X. *et al.* RNA-seq reveals determinants of sensitivity to chemotherapy drugs in esophageal carcinoma cells. *Int. J. Clin. Exp. Pathol.* **7,** 1524–1533 (2014).

243. Li, J., Wood, W. H., Becker, K. G., Weeraratna, A. T. & Morin, P. J. Gene expression response to cisplatin treatment in drug-sensitive and drug-resistant ovarian cancer cells. *Oncogene* **26,** 2860–2872 (2006).

244. Fleitas, T., Ibarrola-Villava, M., Ribas, G. & Cervantes, A. MassARRAY determination of somatic oncogenic mutations in solid tumors: Moving forward to personalized medicine. *Cancer Treat. Rev.* **49,** 57–64 (2016).

245. Niu, N. & Wang, L. In vitro human cell line models to predict clinical response to anticancer drugs. *Pharmacogenomics* **16,** 273–285 (2015).

246. Edmondson, R., Broglie, J. J., Adcock, A. F. & Yang, L. Three-Dimensional Cell Culture Systems and Their Applications in Drug Discovery and Cell-Based Biosensors. *Assay Drug Dev. Technol.* **12,** 207–218 (2014).

247. Aparicio, S., Hidalgo, M. & Kung, A. L. Examining the utility of patient-derived xenograft mouse models. *Nat. Rev. Cancer* **15,** 311–316 (2015).

248. Richmond, A. & Su, Y. Mouse xenograft models vs GEM models for human cancer therapeutics. *Dis. Model. Mech.* **1,** 78–82 (2008).

249. Aresu, L. Canine Lymphoma, More Than a Morphological Diagnosis: What We Have Learned about Diffuse Large B-Cell Lymphoma. *Comp. Clin. Med.* 77 (2016). doi:10.3389/fvets.2016.00077

250. Davis, B. W. & Ostrander, E. A. Domestic Dogs and Cancer Research: A Breed-Based Genomics Approach. *ILAR J.* **55,** 59–68 (2014).

251. Schiffman, J. D. & Breen, M. Comparative oncology: what dogs and other species can teach us about humans with cancer. *Phil Trans R Soc B* **370,** 20140231 (2015).

252. Richards, K. L. & Suter, S. E. Man's best friend: what can pet dogs teach us about non-Hodgkin's lymphoma? *Immunol. Rev.* **263,** 173–191 (2015).

253. Richards, K. L. *et al.* Gene profiling of canine B-cell lymphoma reveals germinal center and post-germinal center subtypes with different survival times, modeling human DLBCL. *Cancer Res.* **73,** 5029–5039 (2013).

254. Paz Morante, M. *et al.* Activation-associated phenotype of CD3+ T cells in acute graft-versus-host disease. *Clin. Exp. Immunol.* **145,** 36–43 (2006).

255. Stokol, T., Schaefer, D. M., Shuman, M., Belcher, N. & Dong, L. Alkaline phosphatase is a useful cytochemical marker for the diagnosis of acute myelomonocytic and monocytic leukemia in the dog. *Vet. Clin. Pathol.* **44,** 79–93 (2015).